SIMULATION OF GLUCONIC ACID PRODUCTION FROM GLUCOSE IN AN AIRLIFT BIOREACTOR

A DISSERTATION

Submitted in partial fulfilment of the
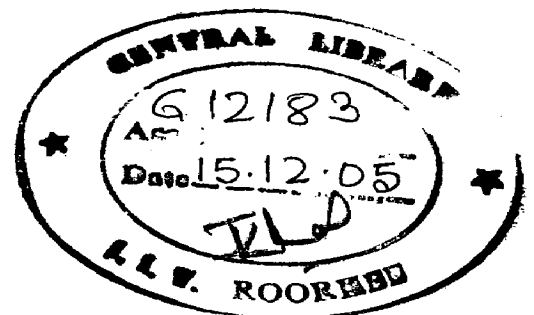*requirements for the award of the degree*
of
MASTER OF TECHNOLOGY
in
CHEMICAL ENGINEERING
(With Specialization in Computer Aided Process Plant Design)

By

MAYANI MUKESHKUMAR KHODABHAI

DEPARTMENT OF CHEMICAL ENGINEERING
INDIAN INSTITUTE OF TECHNOLOGY ROORKEE
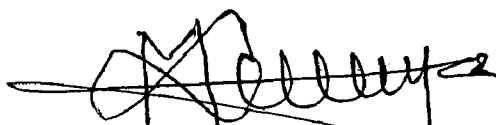ROORKEE-247 667 (INDIA)
JUNE, 2005

CANDIDATE'S DECLARATION

I hereby declare that the work, which is being presented in the dissertation entitled "SIMULATION OF GLUCONIC ACID PRODUCTION FROM GLUCOSE IN AN AIRLIFT BIOREACTOR" in partial fulfilment of the requirement for the award of the degree of Master of Technology (M. Tech.) in Chemical Engineering with specialization in Computer Aided Process Plant Design (CAPPD), submitted in the Department of Chemical Engineering of Indian Institute of Technology Roorkee, is an authentic record of my own work carried out during the period from July 2004 to June 2005 under the kind guidance of Dr. Bikash Mohanty, Professor & Head, Department of Chemical Engineering and Dr. R. P. Singh, Associate Professor, Department of Biotechnology, Indian Institute of Technology, Roorkee.

The matter presented in this dissertation has not been submitted by me for the award of any other degree of this or any other Institute / University.

Place: Roorkee

Date: June 29, 2005

(MAYANI MUKESHKUMAR KHODABHAI)

This is to certify that the above statement made by the candidate is correct to best of my knowledge.

Date: June 29, 2005

(Dr. Bikash Mohanty)

Prof. & Head,

Dept. of Chemical Engineering,

I. I. T. Roorkee, Roorkee-247 667

(Dr. R. P. Singh)

Assoc. Prof.,

Dept. of Biotechnology,

I. I. T. Roorkee, Roorkee-247 667

i

ABSTRACT

A mathematical model for the prediction of performance of a bioprocess of gluconic acid production in an airlift bioreactor (ALBR) in a batch process has been developed. The model consists of a set of simultaneous first order ordinary differential equations obtained from material balances of cell mass (X), product (P), substrate (S) and dissolved oxygen (Co) around the hypothetical well mixed stages in the bottom, riser, top and down comer sections of an ALBR. Logistic equation and contois model constitute the kinetic part of the main model and are incorporated through material balance. These equations are solved using ODE solver of MATLAB (Version 6.5). Equations similar to Leudeking-Piret, which combine growth and non-growth associated contributions are used for the representation of biomass, product, substrate and dissolved oxygen with time. The kinetic parameters of logistic equation are extracted by non-linear regression using GraphPad (Version 4.03) software.

Logistic and contois models are compared for prediction of time dependent concentration profiles of biomass, gluconic acid, glucose and dissolved oxygen (DO) in an ALBR. Validated logistic and contois models are used to predict the effect of change in initial biomass concentration (X_0) and airflow rate (Qg), respectively, when these parameters are varied from their mean values, on the performance of gluconic acid production in ALBR. An airlift bioreactor of 4.5 l working volume was designed and developed for further experimental investigation of the bioprocess.

It was concluded that the mathematical model incorporated with multi-kinetic models would be more efficient to study the overall biotechnological process. The model is simple enough to be used in design studies and it can be adapted to airlift system configurations and fermentation systems other than gluconic acid.

ACKNOWLEDGEMENT

CONTENTS

LIST OF FIGURES

LIST OF TABLES

NOMENCLATURE

Symbol	Description	Unit
A	Area of cross-section	m^2
b	Backflow parameter, ratio of the back flow rate to the net forward liquid flow rate	-
C	Concentration of the component (X, P or S)	g/l
C_o^*	Saturation oxygen concentration	g/l
C_o	Actual dissolved oxygen concentration	g/l
Kb	Form friction loss coefficient for the bottom section	-
koc	Oxygen limitation constant, Contois model	g/l
ksc	Saturation constant, Contois model	g/l
$k_L a$	Overall oxygen mass transfer coefficient	h^{-1}
M	Number of stages in bottom, riser and top section	-
$M_{Glucose}$	Molecular weight of gluconic acid	g/mol
M_o	Molecular weight of atom of oxygen	g/mol
m_O	Maintenance coefficient of oxygen mass per cell mass per h	h^{-1}
m_S	Maintenance coefficient of glucose mass per cell mass per h	h^{-1}
N	Total number of stages in the ALR	
P	Product concentration	g/l
Pe	Peclet number	-
P_g/V	Power supply for mixing in the reactor per volume	W/m^3
Q	Volumetric flow rate of liquid phase	m^3/s
Q_g	Volumetric flow rate of air	m^3/s
Q_lpm	Air supply rate in liter per min	lpm
R_C	Rate of formation of C (X, P or S)	g/l.h
R_{CO}	Rate of formation of oxygen	g/l.h
r_p	Rate of production formation	g/l.h
r_S	Rate of substrate formation	g/l.h
r_X	Rate of biomass growth rate	g/l.h

S	Substrate concentration	g/l
t	Time	h
T	Temperature	°C
X	Cell biomass concentration	g/l
Y	Yield	g/g
Ug	Superficial air velocity	m/s
Ugr	Superficial air velocity in the riser	m/s
Ugd	Superficial air velocity in the down comer	m/s
V	Volume of reactor	m^3
vlr	Superficial liquid velocity in the riser	m/s
vld	Superficial liquid velocity in the down comer	m/s
Ulr	Linear liquid velocity in the riser	m/s
Uld	Linear liquid velocity in the down comer	m/s
X	Biomass concentration	gm/l
Y	Yield	gm/gm

Subscripts

b	Bottom	-
d	Down comer	-
g	Gas phase	-
G	Glucose	-
GA	Gluconic acid	-
i	Stage no., i = 1, 2, ...M-1, M, M+1, ...N	-
l	Liquid phase	-
m	Maximum	-
o	Initial value, t = 0	-
r	Riser	-
t	Top	
x	Biomass	-

Greek letters

μ	Specific growth rate	h^{-1}

μ_m	Maximum specific growth rate	h^{-1}
ε	Gas hold up	-
ε_{gr}	Gas hold-up in the riser section	-
ε_{gd}	Gas hold-up in the down comer section	-
α	Growth-associated product formation coefficient	-
β	Non growth-associated product formation coefficient	h^{-1}
γ	Growth-associated parameter for substrate uptake; substrate mass consumed per biomass mass grown	-
λ	Non growth-associated parameter for substrate uptake; substrate mass consumed per biomass mass grown per hour	h^{-1}
η	Parameter for oxygen uptake; oxygen mass consumed per biomass mass grown	-
ψ	Parameter for oxygen uptake; oxygen mass consumed per biomass mass grown per hour	h^{-1}

GLUCONIC ACID and its salts are important materials used in pharmaceutical, food, textile, detergent, photographic, leather, biological and metal itching industries [14,37]. There are different approaches available for production of gluconic acid: Chemical, Electrochemical, Bio-electrochemical and Biochemical processes [14, 15, 27, 29, 30, 36, 41, 46, 48, 54, 58]. Fermentation is one of the dominant routes for manufacturing gluconic acid at present [8], although it suffers from many drawbacks, including those associated with process conditions required for the fermentation and microorganisms used - which has limited its commercial applicability. Further, the oxygen transfer from the gas phase into the liquid phase was found to be a limiting step for the bioconversion Markos et al. [36]. For this reason, a great attention has to be paid for the optimization of the bioreactor operation (mixing, aeration and bioreactor design) in order to enhance the oxygen transfer rate and, hence, maximizing the product at optimized condition. Microbial species such as *Aspergillus niger* [23, 27, 30, 36, 48, 54, 58, 60], *Penicillium chrysogenum* [18] and *Gluconobacter oxydans* [58] have been employed for gluconic acid production. But in the present work *Aspergillus niger* is used because it is capable of producing high activity of enzymes namely *glucose oxidase (GOD)* and *catalase*. Gluconic acid by fermentation using *Aspergillus niger* belongs to aerobic fermentations with high oxygen demand. The biotransformation of glucose to gluconic acid represents a simple dehydrogenation reaction without involvement of complex metabolic cell pathways, which is realized with a high selectivity, high rate and high yield of conversion.

1.1 GLUCONIC ACID

D-Gluconic acid (pentahydroxycaproic acid; 526-95-4) is an oxidation product of D-glucose and has stereo chemical configuration. Removal of two hydrogen atoms from D-

glucopyranose yields D-glucono-δ-lactone, which in aqueous solution is in chemical equilibrium with D-gluconic acid and with D-glucono-γ-lactone [37]. The reaction in the cell is represented by the following sequence of equations [60]:

$$\text{Glucose } (C_6 H_{12} O_6) + O_2 \xrightarrow{\quad Glucose\ oxidase \quad} \text{Gluconolactone } (C_6 H_{10} O_6) + H_2O_2 \qquad (1.1)$$

$$\text{Gluconolactone } + H_2O \xrightarrow{\quad FAD \quad} \text{Gluconic acid } (C_6 H_{12} O_7) \qquad (1.2)$$

$$H_2O_2 \xrightarrow{\quad Catalase \quad} H_2O + 0.5\ O_2 \qquad (1.3)$$
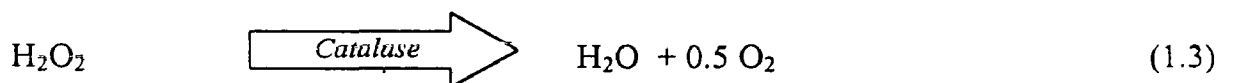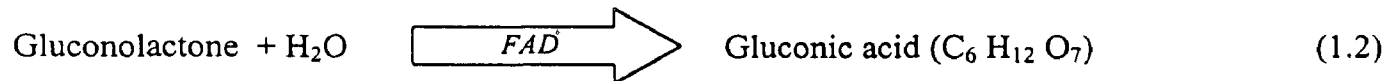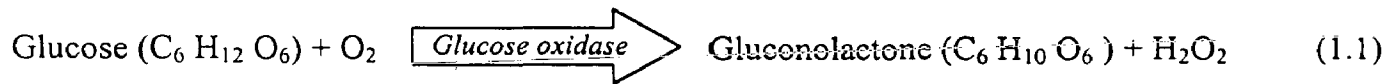
Where, *FAD* is Flavin adenine dinucleotide and *Catalase* is the enzyme to convert H_2O_2 in to water and oxygen.

The overall reaction is represented by

$$\text{Glucose } + 0.5\ O_2 \xrightarrow{\quad Glucose\ oxidase\ +\ Catalase \quad} \text{Gluconic acid} \qquad (1.4)$$
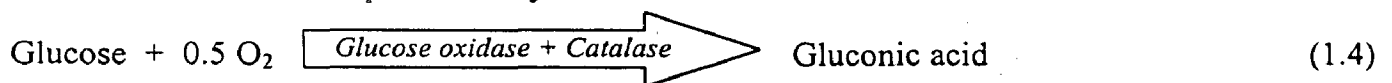
In spite of its great potential, however, gluconic acid fermentation has not received adequate attention although some work has been done. Moreover, there prevailed a lack of uniformity and reproducibility of the methods adopted in various laboratories, which may not be surprising because of the fact that very few research laboratories worked with the same strain under similar conditions.

In the present work, performance of gluconic acid production from glucose using *Aspergillus niger* in an airlift bioreactor was studied through simulation. The experimental set-up was designed and developed for further investigation. The logistic equation and contois model were compared to represent the behavior by modeling the reactor. The effect of change initial cell mass concentration and gas hold up was investigated in a 4.5 l ALBR.

2

1.2 USES OF GLUCONIC ACID AND ITS DERIVATIVES

At present, D-Gluconic acid is marketed as 50% solutions. Crystalline D-glucono-δ-lactone is commercially available in large quantities, but the γ-lactone is made only in small quantities as a specialty. Gluconic acid and its derivatives are used in the following applications:

- It is used as an additive in the food, beverage and pharmaceutical industries.

- δ-lactone is extensively used as latent acid in the preparation of pickled goods, curing fresh sausages or leavening during baking.

- The sodium gluconate has a very good sequestering action for Fe over a wide pH range. This property exploited in the use of 4% NaOH solution containing sodium gluconate used in de-rusting of ferrous metals.

- Mixtures of gelatin and sodium gluconate are used as sizing agent in paper industry.

- Textile manufacturers employ gluconate for de-sizing polyester or polyamide fabrics.

- In concrete work sodium gluconate about 0.02 – 0.2 wt% is added to produce concrete highly resistant to frost and cracking.

- Ionization of hydroxyl groups allowing use of sodium gluconate in the washing of glass bottles.

- Calcium gluconate is used to treat diseases caused by a deficiency of Ca in the body.

- Iron gluconate is often used to supply iron in cases of anemia.

- Ferrous phosphogluconate is used chemotherapeutically.

1.3 SCOPE OF WORK

D-Gluconic acid is a product of multiple-industrial significance because of its wide range of applications. The future of a majority of these applications depends mainly on commercial availability of gluconic acid and gluconates. According to the recent estimates, the annual

worldwide production of gluconic acid is more than about 60,000 tones (2004). It is not being produced on large scale in our country by fermentation process and is mostly imported nowadays. Some companies, e.g. Prathsta Industries Ltd., Secunderabad, produce calcium gluconate (Source: Chemical Weekly, September, 2004) in small amount, against large requirement, using traditional chemical process. This production processes cause not only increased cost but also have poor yield and quality. In contrast to this, fermentation process is potential and economic method. This encourages us to study and model the bioprocess to enhance the production using airlift bioreactor, which leads to develop a technology potentially economic fermentation process for large-scale production.

1.4 FERMENTATION METHODS USED FOR GLUCONIC ACID PRODUCTION

There are three different methods of fermentation, namely (i) Surface fermentation, (ii) Submerged fermentation and (iii) Solid-state fermentation, which are used for the production of gluconic acid in the laboratories and industries by fermentation route.

1.4.1 SURFACE FERMENTATION

According to Ray Psanik (1994), this method is low cost operation method. But, the problem associated to use this method is that in presence of trace metals, yellow pigment called "*asperenone*" occurs that is excreted into the medium and is difficult to remove. This phenomenon does not permit smooth operation of the process and thus limit the application of the method.

1.4.2 SUBMERGED FERMENTATION

Osterhuis et al. [42] and Heinrichs & Harmieier [21] investigated that submersed. fermentation process is best suited for high production level and it can be modified for the

continuous operation also. Blom et al. [9] developed a process, which has been used on industrial scale since years.

1.4.3 SOLID-STATE FERMENTATION

This method offers advantages such as high tolerance of *A. niger* to high concentration of glucose and metal ions over submerged conditions. But, because of few limitations including the lack of reliable method for growth characterization, no serious efforts have been made to produce gluconic acid by this process at the large scale. This method has the potential to be the most economic method in future.

Actually, the success of the technology for biological production depends on the choice of bioreactor that efficiently achieving mixing and contact of gas-liquid phases, behavior of organism under prevailing conditions and medium components. Hence, we have chosen to use the submerged fermentation process for our work.

Bioreactors such as stirred tank, bubble column and airlift are used in the literature for the submerged fermentation process in production of gluconic acid. Nakao et al. [41] and Znad et al. [60] suggested that mechanically and pneumatically stirred reactors are normally used, but the choice nowadays is given to the pneumatically agitated – Airlift reactors because of few advantages such as energy efficient operation in comparison to stirred fermenter, better for heat sensitive cultures and less prone to the leakages.

Trager et al. [53] have studied gluconic acid production and observed distinctly high dissolved oxygen in airlift bioreactor than in the stirred bioreactor, as in the former, the mass transfer is better because of the pallet growth and water like viscosity of the broth. Tripathi et al. [54] have also observed the similar results when compared stirred tank bioreactor with airlift bioreactor.

1.5 OBJECTIVES OF THE WORK

Looking at the scope for gluconic acid production by fermentation, which has tremendous potential for the country like ours. The present study for the production of gluconic acid in an airlift bioreactor has been taken up with following objectives:

(i)   To design and develop an experimental set up – concentric tube airlift bioreactor, which can be used for the production of gluconic acid from glucose.

(ii)   To develop the mathematical model for the production of gluconic acid using airlift bioreactor.

(iii)   To validate the model using the data of other investigators.

(iv)   Through simulation, to investigate the effect of variation in initial cell mass (X_0) and overall airflow rate (Qg) on the performance in an airlift bioreactor.

The review of literature and patents is the pinnacle of our dissertation topic: Simulation of gluconic acid production from glucose in an airlift bioreactor. The subject was aimed to study the performance of gluconic acid production and to identify the best operating conditions in airlift bioreactor. It was found that the production of gluconic acid is a function of reactor design, operating and kinetic parameters. Operating parameters may include pH, airflow rate, concentration of substrate(s), intermediate(s) and product(s), temperature, pressure, gas hold-up, superficial gas velocity, phase behavior, etc. Design parameters include sparger design & layout, diameter and height of internal and external cylinders, down comer design, gas disengagement space and solids contents. The objectives of this literature and patent reviews are to identify most important operating parameters that affect the kinetics and performance of gluconic acid production bioprocess. Further, it has been aimed to develop model of the system under steady state condition and hence literature review of this aspect is also important. The potential and scope of work on the subject has been realized by the following reviews systematically outlined. This chapter reviews current status on the work done for the bioprocess development on subject 'Modeling and simulation of gluconic acid production from glucose using *Aspergillus niger* in an airlift bioreactor'. The present chapter provides a brief discussion of the literature only on those aspects, which are relevant to the objectives of the dissertation work.

2.1 EXPERIMENTAL WORK

In recent years, airlift bioreactors (ALRs) have been extensively investigated as a possible alternative to stirred tank bioreactors, which are most widely used for fermentation purposes. A special property of ALR is a liquid circulation loop created by the interconnected aerating (riser)

and recirculating sections (down comer). Despite an absenting mechanical agitator, the well-defined flow pattern with high liquid velocities in line with efficient mixing and low uniformly distributed shear stresses can create an optimal environment for many productive micro-organisms. Despite these advantages of airlift bioreactors, their implementation is still limited; mainly due to an insufficient knowledge of hydrodynamics and mass transfer phenomena in the ALRs, necessary for their reliable and optimal design and operation (scale-up strategy). Most researchers dealt with systems like water or water solutions of synthetic compounds Lu et al. [28]. The intention of these works was to maximize the production of gluconic acid from glucose in internal loop airlift bioreactor and simulate the rheological behavior of *real fermentation system.*

Blom et al. [9] This paper is the first real representation of submerged fermentation process carried out in 1952 by a team of eight people. It had described pilot plant experiments in which sodium gluconate was produced directly by continuous neutralization of gluconic acid formed during submerged culture fermentation of glucose with *A. niger* in stirred fermenter. Many companies used this production technique in the 1970s.

Das & Kundu [14] A brief review of earlier work on microbial technique of gluconic production were given. It has also given information about media and other fermentation aspects.

Chisti & Moo-Young [10] Three pneumatically agitated reactors - a bubble column and two airlift devices - with identical cross section, working liquid heights and equivalent gas sparging arrangement were compared in terms of the hydrodynamic and oxygen mass transfer performance. In the study, the two airlift reactors had identical riser to down comer cross-

section area ratio of 1.0, but differed being sparged either in the central draft-tube or in risers. Study revealed that spaging air in draft tube has higher gas hold up.
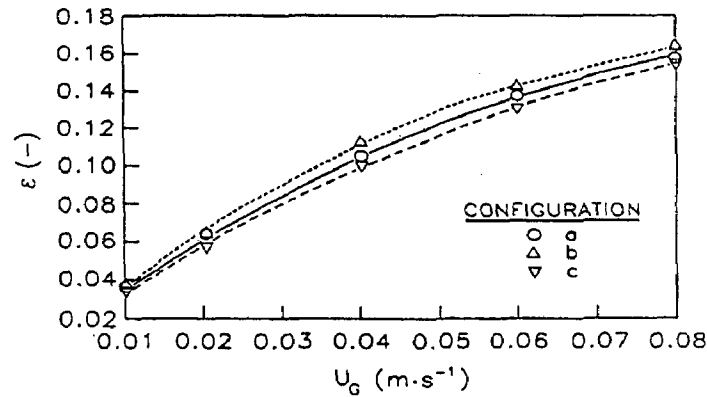
Figure: 2.1 Effect of superficial gas velocity, Ug on overall gas hold up, ε for (a) bubble column (o), (b) draft-tube sparged airlift (Δ) & (c) down comer sparged airlift reactors (∇).

The central draft-tube sparged design produce consistently higher velocities than did sparging in the peripheral down comer because of the differences in pressure drop associated with the bottoms of the two airlift reactors. Following equation is proposed for relation of riser and down comer gas hold up in the similar configuration of ALR for wide range of gas flow rate.

$$\varepsilon_d = 0.988\varepsilon_r - 0.016 \tag{2.1}$$

Nakao et al. [41] In their study, an external loop airlift bubble column (ELBC), an internal loop airlift bubble column (ILBC) and a normal bubble column (NBC) were employed to carry out the immobilized glucose oxidase (GOD) catalyzed oxidation of glucose with air to produce gluconic acid. Optimal reactor design and operating conditions were searched for kinetics and reactor characteristics. It was found that,

➤ Increase in gas hold up gives increase in productivity and lowers glucose oxidase activity. Increasing superficial gas velocity results in higher productivity. but superficial

9

gas velocity higher than 1 cm/s shows almost no increase in productivity with negligible decay of GOD activity.

➤ Initial glucose concentration higher than 10 g/l shows almost no increase in productivity, but remarkably higher activity decay.

➤ ILBC and NBC have given higher gluconic acid productivity and lower glucose oxidase activity decay due to their better mass transport than ELBC.

Tripathi et al. [51] Calcium gluconate production by *Aspergillus niger* was investigated, in shake flask, rolling shaker, airlift reactor and stirred reactor at different initial glucose concentration. They investigated that success of the technology for biological products depends on the choice of bioreactor efficiently achieving mixing and contact of liquid and gas phases. Further, found that high calcium gluconate production was achieved in airlift reactor with pellet form of cell growth at moderate specific growth rate and biomass concentration, while in stirred reactor pulpy mycelial growth was obtained and hence calcium gluconate production was poor.

Singh et al. [48] Study on bioconversion of agro-food by-products to gluconic acid using *Aspergillus niger* was done in shake flasks under surface, submerged and solid state condition. It was found that hydrogen peroxide (H_2O_2) enhances GA production. Optimum fermentation conditions have been suggested for submerged fermentation. Initial 12% glucose concentration, 1-2% inoculation level, 32 °C and pH about 5.5 are optimum for high yield. The author has also studied the production of gluconic acid under surface, submerged and solid state conditions and found that surface and solid state have given better yield then submerged fermentation but the at the large scale, it was not claimed. This directs further investigation of these fermentation methods on the larger scale with current technology.

Kulkarni et al. [27] Gluconic acid production using immobilized *Aspergillus niger* on a highly porous cellulose support was studied to obtain higher productivity. It was found that levels of dissolved oxygen and glucose concentrations during fermentation significantly affect the production and fermentation time. For efficient bioconversion, an optimum biomass on the porous cellulose support is necessary. Further, suggested that oxygen-enriched air can substitute air and reduce the fermentation period substantially.

Chisti et al., [13] Gas holdup, mixing, liquid circulation and gas–liquid oxygen transfer were characterized in a large (~1.5 m^3) draft-tube airlift bioreactor agitated with Prochem® hydrofoil impellers placed in the draft-tube in cellulose fiber slurries that resembled broths of mycelia micro fungi. The important conclusion drawn for the system of mechanically agitated draft-tube reactors that air sparging in riser zone may or may not improve the mixing performance, depending on the intensity of the mechanical agitation. At sufficiently high aeration rates (Ugr ≥ 0.04 m/s), whether mechanical agitation is used or not it has little bearing on the mixing characteristics of the reactor. This observation is of significance importance in design of energy efficient system like airlift reactors.

Markos et al. [36] The airflow rate and biomass concentration effect on the volumetric oxygen transfer coefficient (k_La) in a 10.0 l internal-loop airlift bioreactor (ILAR). A strong positive influence of the airflow rate on the rate of gluconic acid production ($r_{Glucose}$), specific rate of gluconic acid production ($k_{Glucose}$/ Cx) as well as on the volumetric oxygen mass transfer coefficient (k_La) was observed. A local maximum for biomass concentration equal to 6.68 g/l was noted. On the other hand, it was observed that the specific production rate monotonously decreased with increasing biomass concentration. The following equation was used to calculate k_La:

$$k_L a = \frac{r_{Glucose}[M_0/M_{Glucose}]}{(Co^* - Co)}$$

(2.2)

Where, $r_{Glucose}$ = Rate of gluconic acid production, g/l.min

M_0 = Mol. weight of the atom of oxygen, g/mol

$M_{Glucose}$ = Mol. weight of the giuconic acid, g/mol

Experimental results were plotted in Figure 2.2 with progress of time. Here. the pH of the medium was changed after 20 hr from 6.5 to 5.5 that does not effect too much for GA production.
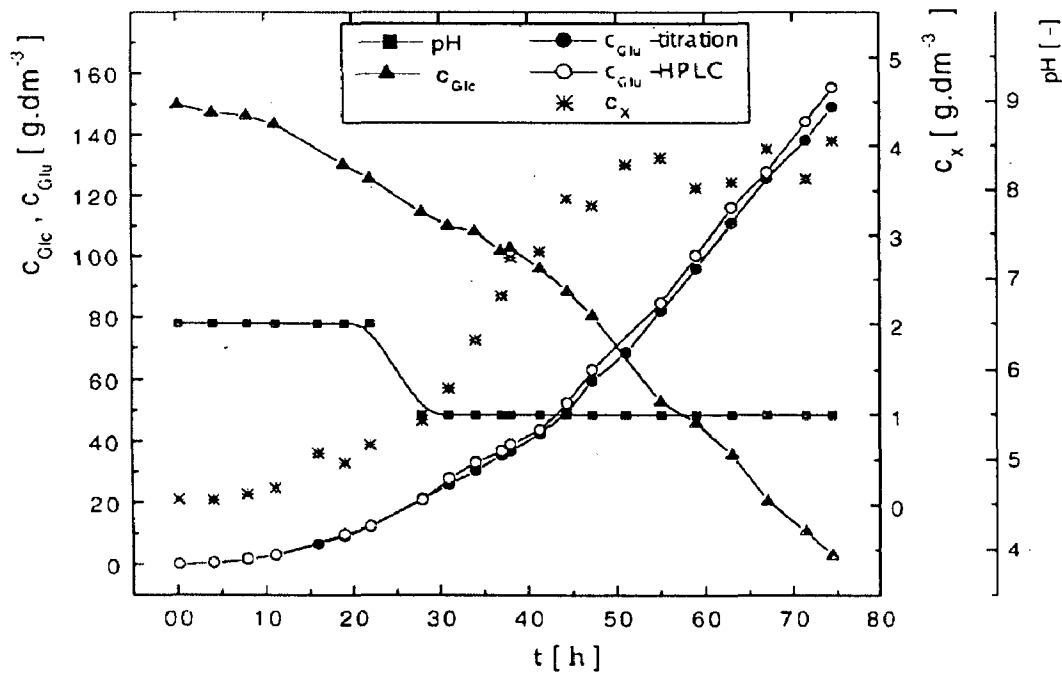
Figure: 2.2 Time dependent of values of glucose, gluconic acid and biomass concentration and pH during fermentation in a 34 l airlift reactor (Aeration rate 34.0 l/min and U_g 0.0655 m/s) [36].

Znad et al. [60] The aim of this work was to study the kinetics of gluconic acid production in 2 and 5 l stirred tank reactor using air and pure oxygen as a source of oxygen. This study involves the analysis of gluconic acid fermentation by *A. niger* under growth and

non-growth conditions. An empirical equation suggested to show the dependence of the production rate r_p on the biomass concentration Cx and oxygen flow rate Q, at constant operating conditions (30° C, 300 rpm and pH 5.5) under non-growth condition using pure oxygen was given by

$$\frac{dC_{GA}}{dt} = r_p = K_p C_x = -6.67 \times 10^{-3} + 7.87 \times 10^{-4} Q + 5.907 \times 10^{-2} C_x - 6.532 \times 10^{-4} QC_x$$
$$-5.83 \times 10^{-3} C_x^2 + 2.5 \times 10^{-4} QC_x^2 \qquad (2.3)$$

It was found that production and growth rates were higher, but substrate consumption was constant when pure oxygen was supplied. Biomass concentration had a positive effect on the production rate r_p, where as the effect of Q on r_p was positive at high biomass concentrations.

2.1.1 DIFFERENT PRODUCTION METHODOLOGIES

Literature reviews suggest that different workers have worked on the different aspects such as microorganisms used, type of reactor, operating parameters and fermentation methods used. The summary of the work for production of gluconic acid has been given in the Table 2.1.

13

Table: 2.1 Summary of different methodologies used for production of gluconic acid.

Sr No.	Research Paper	M.O. Used	Aim of the Experiment	Experimental System	Parameters Studied	Conclusion of Work
1.	Blom et al. [9] (1952)	*A.niger*	Sodium gluconate production: Fermentation with Aspergillus niger	Stirred reactor in batch fermentation	Antifoam agents, sugar concentration	Fermentation is the better method for GA production
2.	Nakao et al. [35] (1997)	*Glucose oxydase*	To study performances in three types of airlift bubble columns.	External, internal and normal loop bubbling columns. GOD immobilized on calcium alginate gel beads. Gas velocity: 0.25-4.0 cm/s 4% Pd in gel beads pH 6.0, 30 °C	Effect of Ug on k_La and k_So. Effect of operating conditions (Conc. Of G, GA, gas hold up, Ug)	Optimum operating conditions have been recommended. ILBC & NBC have given higher gluconic acid productivity and lower glucose oxidase activity decay due to their better mass transport than ELBC.
3.	Velizarov et al. [51] (1998)	Glucono-bacter oxydans (NBIMCC 1043)	To study the substrate and product inhibition situations in free GA production from G.	0.4 lit batch bioreactor (Bioflo C-30, New Brunswick) Aeration rate: 2 vvm Speed: 1000 rpm 32 °C for 8 hr Antifoam: silicon emulsion	Diff. G and GA conc., kinetic parameters and yield. Process kinetics were evaluated by comparing different inhibition models.	Substrate inhibition is linear inhibition of growth described by Tseng and Wayman[48]. Product inhibition is found non-linear inhibition kinetics fitting well with Levenspiel model[26].
4.	Tripathi et al. [47] (1999)	Aspergillus niger (NRRL - 3)	To investigate most suitable fermentation condition for calcium gluconate production.	Shake flask, rolling shaker, air-lift bioreactor (1.5 lit, 1 vvm) and stirred tank bioreactor (0.5 lit, 1 vvm, 300 rpm), 28 °C	Effect of G on biomass concentration. Spec. growth rate and calcium gluconate prod.	In all system except stirred tank, pellets were produced and calcium gluconate production was higher.

14

5.	Singh. O.V., Ph.D. Thesis [42] (2000)	Aspergillus niger (ORS-4.410)	Bioconversion of agro-food by-products to GA in surface, submerged and solid state conditions.	Shake flasks Cells immobilized on calcium alginate. 12% Glucose conc. 1-2% inoculation level 28 - 32 °C, pH 4.5 - 6.5	Various substrates (Grape must, Banana must and Molasses). Effect of regulators (H₂O₂, starch, vegetable oil) Effect of Glucose conc.	Rectified Grape must is better higher GA production. H₂O₂ enhance GA production. Surface or SSF gives better yield then submerged, but at large scale, it is not claimed.
6.	Kulkarni et al. [22] (2002)	A. niger (NCIM545)	To study and optimize fermentation conditions using A. niger immobilized on cellulose microfibrils.	Batch bioreactor with recirculation. Air (25 ml/min) mixed with pure oxygen (135 ml/min). Wowen cellulogic fabric support for A. niger- folded in spiral shape. 30 °C, pH 6.0	Initial conc. of glucose. Effect of DO and biomass conc. on the support under continuous recirculation.	Optimum biomass conc. on the cellulose support is 0.234 mg/cm². Oxygen enriched air increase productivity and reduce the fermentation time.
7.	Markos et al. [31] (2002)	A.niger (CCM 8004)	Biotransformation of G to GA by A. niger- study of mass transfer in airlift bioreactor.	10 and 34 l internal loop bioreactor pH 6.5 - during growth phase and 5.5 – during production phase (under non-growth condition)	Effect of airflow rate and biomass concentration on $k_L a$. Specific growth rate of GA production.	Increase of airflow rate (i.e. Enhancing liquid circulation velocity), intensity of mixing and mass transfer coefficient are increased. Specific prod. rate decreased with increasing biomass concentration.
9.	Lantero & Shetty, US Patent [25] (2004)	Aspergillus niger	Process for preparation of GA with concentration 25% and higher of G	10 l fermenter (Chempec, New Jersey, USA) Aeration rate: 1 vvm 30-35 °C, pH 6.0 Antifoam: 80-120 ppm.	Effect of pH, temp, initial conc. of G. Enzyme dose and quality of G tested.	Parameter effects were studied and results are available in [25].

15

2.2 PATENTS

Baker & Saret: US Patent, 1953 [6]

Objectives of this invention were to provide a highly efficient and commercially feasible process for the conversion of glucose to gluconic acid by means of enzyme glucose oxydase and also for removing glucose from solution or other aqueous media by means of the enzyme glucose oxidase. This patent had identified solutions of certain problems, which were found very crucial in successful microbial production of gluconic acid.

Lantero & Shetty: US Patent, 2004 [30]

The invention relates to the process for the production of gluconic acid from glucose wherein dissolved solid concentrations of glucose of 25 % (w/w) and higher has been used to produce spray dried and essentially pure granular gluconic acid without employing crystallization. For the various experiments, 10 l fermenter (Chempec, USA) was used. Following experiments were important in deciding the operating parameters such as pH and temperature for the submerged fermentation.

Effect of pH on conversion

Conditions: 35° C, 1 bar, aeration rate 1 vvm, pH adjusted by 50% NaOH, antifoam added, 80-120 rpm, 40% (w/w) ds. glucose.

⇒ pH between 5.0 to 6.0 gives higher conversion of glucose in short time.
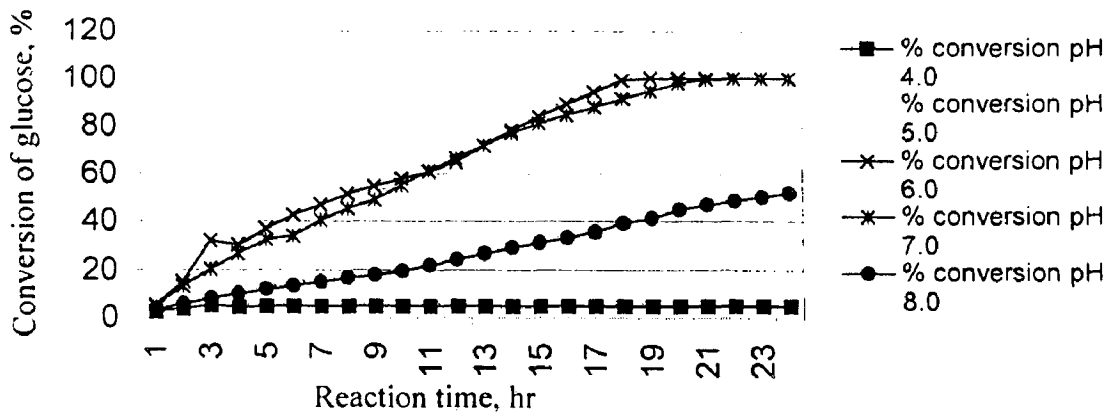
Figure: 2.3 Effect of pH on % conversion of substrate (glucose).

Effect of temperature on the conversion

Condition: 1 bar, aeration rate 1 vvm, pH adjusted by 50% NaOH, antifoam added, 80-120˙ rpm.

⇒ Temperature in between 30 °C - 35 °C gives higher conversion.
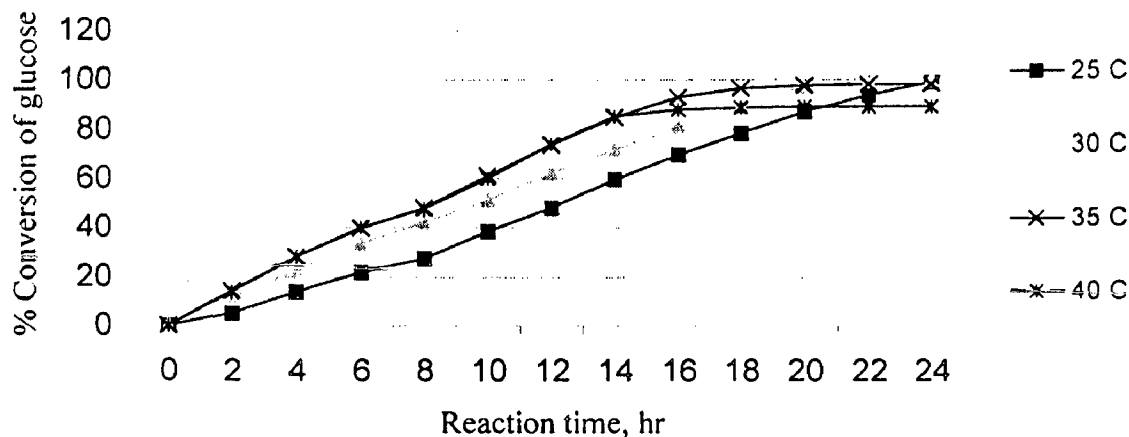
Figure: 2.4 Effect of temperature on the % conversion of substrate (glucose).

From the above experiments, it has been found that the optimum values of pH, and temperature are about 6.0, 30-32 °C respectively. The optimum value of glucose concentration is again contradictory among various findings [30,48] etc.

2.3 MATHEMATICAL MODEL

A mathematical model or process model is a set of equations whose solution, given specified input data, is the representative response of the process for a corresponding set of input. Fermentation models are normally divided into two classes: structured models (intracellular metabolic pathways are considered) and unstructured models (biomass is described by one variable). Structured model seems complicated for normal use. Unstructured models are much easier to use and have proven to accurately describe many fermentation processes [23].

17

Turner and Mills [56] They pointed out that the tanks in series or mixing cell model is more realistic and advantageous compared with the axial dispersion model. Since the growth rate of microorganism is strongly affected by temperature and the cultivation is usually exothermic. They have suggested that heat balances are also taken into account for the modeling of the airlift bioreactor for mildly exothermic bioprocess.

Kawase et al. [24] A tanks-in-series model was applied for mathematical modeling of the steady-state performance of continuous cultures in an airlift bioreactor. The objective of this study is to investigate effects of mixing in the riser and the down comer on microorganism growth in an airlift bioreactor for continuous culture processes. A mathematical model developed based on a tanks-in-series model with backflow to simulate the cultivation in airlift bioreactors. The tanks-in-series model with backflow provides non-linear algebraic equations, which are material balances of microorganism, substrate and dissolved oxygen for hypothetical well-mixed tanks or stages. They have been solved using Newton-Raphson technique. It was found that the down comer is a unique feature of airlift bioreactors and liquid mixing in the downcomer may significantly influence their productivity. Therefore, the recycle flow rate into the down comer is one of the important parameters for the optimum design and operation of airlift bioreactors. In this study, the airlift bioreactor was assumed to operate under isothermal conditions, as heat balances in the airlift bioreactor are not considered.

The simple kinetic model proposed by Monod was used in this work is given by

$$\mu = \mu_m \frac{S}{(K_s + S)} \tag{2.4}$$

Velizarov et al. [58] The aim of this study was to describe quantitatively the inhibitory effects of glucose and gluconic acid on *Gluconobacter* using a model and to establish the numerical values of parameters in models in the case of glucose to gluconic acid oxidation. The

18

biokinetic model parameters, productivities and conversion degrees on media with different glucose and gluconic acid concentrations were calculated and compared. Probable mechanisms of inhibition and possible techniques for their minimization are also discussed. The Haldane equation given by equation (2.5) is the most frequently used to depict the relationship between specific growth rate (μ) and substrate (S).

$$\mu = \frac{\mu_m S}{\left(K_s + S + S^2/K_I \right)} \tag{2.5}$$

$$\mu = \mu_m \left[\frac{S}{K_s + S} \right] \exp\left(-\frac{S}{K_I} \right) \tag{2.6}$$

In some cases, however, the equations of Aiba et al. [1] given by equation (2.6) or Tseng and Wayman [55] given by equation (2.7) for substrate inhibition kinetics afford a better representation of the experimental data.

$$\mu = \mu_m \left[\frac{S}{K_s + S} \right] - K(S - S_{crit}) \tag{2.7}$$

Equation (2.8) of Levenspiel [31] generalized the Monod equation to account for the presence of toxic products.

$$\mu = \mu_m \left[\frac{S}{K_s + S} \right] \left(1 - \frac{P}{P_{crit}} \right)^n \tag{2.8}$$

Where, P_{crit} is maximum product concentration above which no cell growth is possible and the empirical constant n is usually called toxic power. Substrate inhibition can be described by the equation of Tseng and Wayman [55], which predict linear inhibition of growth above a characteristic threshold glucose concentration.

Jian-Zhong et al. [23] The fermentation kinetics of gluconic acid by *Aspergillus niger* were studied in a 5 l stirred tank bioreactor with a working volume of 4.0 l. A mathematical

19

model was proposed using the logistic equation (2.9), which describes the inhibition of biomass on growth, was suggested to represent the behavior of gluconic acid production in stirred tank bioreactor in batch. The Luedeking–Piret equation [32] for gluconic acid production glucose consumption were used.

$$\frac{dx}{dt} = \mu_m X\left(1 - \frac{X}{X_m}\right)$$ Where, X_m = maximum cell concentration   (2.9)

The model provided a reasonable description for each parameter during the growth phase. The evaluated value of maximum specific growth rate (μ_m) is 0.22 h^{-1}. It was found that the gluconic acid formation is strongly linearly related to cell growth and is growth-associated. The author applied the same model to represent the experimental study of Takamatsu et al. (1981). Further, integrated form of cell biomass and substrate concentrations has been given, which are used in our work. X_m is taken as the experimental value for modeling.

Thibault et al. [51] This study investigates fermentation of glucose to gluconic acid by microorganism *Pseudomonas ovalis* in a batch stirred tank reactor. Their study revealed the effect of overall oxygen mass transfer coefficient on productivity, substrate and gluconic acid concentrations. The multicriteria optimization technique was capable of identifying the optimal operating conditions and/or zone, which are in an acceptable compromise when there are conflicting objectives. In this study, kinetic model and parameters proposed by Ghose et al. [19] were used.

Znad et al. [61] A tanks-in-series model was applied for mathematical modeling of the unsteady state performance of a semi batch operation in a 10.5 l internal loop airlift bioreactor for the production of gluconic acid by fermentation. A set of first order differential equations for the material balances of micro-organism, substrate, product and dissolved oxygen around the hypothetical well mixed stages in the riser and the down comer was developed and solved

simultaneously using the Athena software package. The kinetic model used considers the effect of two substrates (glucose and dissolved oxygen) on the growth rate. Both the effect of airflow rate (within the range of 9 to 45 l/min) and the height on the gluconic acid production in 10.5 l ALR were investigated. Further investigated that the shorter bioreactor shows relatively more uniform axial DO concentrations than the longer bioreactor, in which a greater variation in DO concentrations with the height was observed. It was recommended that further improvement of the model accuracy. more suitable correlations for the mass transfer coefficient and gas hold ups in a real fermentation system should be taken into account in the model. Further, a heat effect has not been considered in the model and also the kinetic were adjusted which was used previously for stirred bioreactor operation.

Mitchell et al. [40] Various microbial kinetic profiles have been reported. including exponential, logistic and fast accelerating/slow deceleration. The typical forms of these curves are given in the following figure.
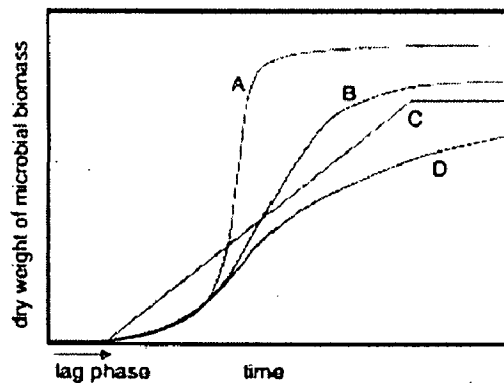
Figure: 2.5 Various empirical kinetic profiles in microbial systems: (A) exponential; (B). logistic: (c) linear and (D) fast-acceleration/slow-deceleration.

Further, the effect of environmental conditions such as pH and temperature on growth has been described within the bioreactor as given by the equations (2.10) and (2.11).

$$\mu = \frac{2.694 \times 10^{11} e^{(-70225/8.314T)}}{1 + 1.3 \times 10^{47} e^{(-283356/8.314T)}} \qquad (2.10)$$

and
$$X_m = -127.08 + 7.95(T - 273) - 0.016(T - 273)^2$$
$$- 4.03 \times 10^{-3}(T - 273)^3 + 4.73 \times 10^{-5}(T - 273)^4 \qquad (2.11)$$

Where, T is the absolute temperature (°K).

Mayani et al. [62] The authors have studied the behavior of fermentation process for gluconic acid production in batch operation through model using two substrate kinetic models. Well known Monod model and Contois model behaviors revealed that the representation of biomass and dissolved oxygen concentration are very poor by Monod model, while Contois model represent them with better accuracy. In this paper, the study was carried for the batch bioreactor without consideration of any hydrodynamic effect in the model equations.

Kinetic model proposed by Contois equation (2.12) was used for simulation with adjusted kinetic parameters of batch reactor.

$$\frac{dX}{dt} = \mu X = \mu_m \frac{S}{(ks'X + S)} \frac{Co}{(ko'X + Co)} X \qquad (2.12)$$

In the Contois kinetics, an influence of the biomass concentration is included. i.e. at high biomass concentration; there is an inhibition of cell growth. It is likely that the biomass concentration as such inhibits cell growth but there may well be an indirect effect. e.g. the formation of inhibitory compound may give a very viscous medium and that result in mass transfer problems.

The different expressions clearly demonstrate the empirical nature of these kinetic models and it is therefore futile to discuss which model is to be preferred, since they are all simply data fitters and one should simply choose the model that gives the best description of the system being studied.

22

2.3.1 COMPARISON OF MODELS

Axial dispersion models and a tanks-in-series models have been applied to describe mixing in bioreactors as given in the Table 2.2. In spite of the applicability and flexibility of tanks-in-series model, only few investigations concerning modeling have been published for simulation of fermentation systems including imperfect mixing in an airlift bioreactor.

Table: 2.2 Mixing models of process in tower type bioreactors.

Authors	Reactor	Kinetic model	Operation	Reactor model
Prokop et al. [44]	Airlift	Oxygen transfer	Continuous	Tanks-in-series with back flow
Erickson et al. [16]	Bubble	Monod	Continuous	Tanks-in-series with back flow
Ho et al. [22]	Airlift	Oxygen transfer	Cont. and batch	Tanks-in-series with back flow
Merchuk et al. [38]	Airlift	Monod	Continuous	Axial dispersion
Adler et al. [2]	Airlift	Monod	Continuous	Axial dispersion
Luttman et al. [34]	Airlift	Monod	Batch	Axial dispersion
Andre et al. [3]	Airlift	Oxygen transfer	Cont.and batch	Tanks-in-series
Pigache et al. [43]	Airlift	Oxygen transfer	Continuous	Tanks-in-series

Prokop et al. [44] and Erickson et al. [16] examined the performance of a multistage tower fermenter using a tanks-in-series model with back flow. In their studies bubble column bioreactors were considered rather than airlift bioreactors and oxygen mass transfer was not taken into account. Ho et al. [22], Andre et al. [3], Pigache et al. [43] applied tanks-in-series models but they did not discuss cultivation of microorganisms in the bioreactors. Turner and Mills [56] pointed out that the tanks in series or mixing cell model is more realistic and

advantageous compared with the axial dispersion model. Since the growth rate of microorganism is strongly affected by temperature and the cultivation process is usually mild exothermic, heat balance should be taken into account for the modeling of the airlift bioreactor. This aspect is proposed to study on the airlift bioreactor in the future work.

Brief summary of the mathematical model carried for the real system of gluconic acid production process is given in the Table 2.2. This table enables the information such as microorganism used, the aim of the experiment, the system of experiment, parameters and the general conclusion drawn of the work.

Table: 2.3 Mathematical models of the fermentation processes for the production of gluconic acid.

Sr No.	Research Paper	Micro-organism Used	Aim of the Experiment	Experimental System	Parameters Studied	Conclusion of Work
1.	Jian-Zhong et al. [19] (2002)	A.niger (ZBY-7)	Mathematical modeling for fermentation kinetics of GA production.	5 l stirred tank bioreactor. (Biostate. B. B. Biotech, Germany) Aeration rate: 0.9 vvm, Speed: 756 rpm, pH 6.0, 32 °C	Microbial growth, product formation and substrate uptake rate. Model parameters determined.	Kinetic model is developed and validated within ± 10 % error.
2.	Znad et al. [54] (2004)	Aspergillus niger (CCM 8004)	Modeling and simulation of fermentation process.	10.5 l internal-loop airlift bioreactor. Inoculum was prepared in a shake flask for 48 hr. Bioreactor inoculated with 2% volume. 15.36 lpm airflow in riser, 30 °C, pH 6.0	Effect of Ug on growth, biomass conc., $k_L a$ and GA production. Effect of riser height on DO. Model parameters were estimated.	Optimum air flow rate range is 9 - 45 l/min. Shorter bioreactor shows more uniform axial DO conc.
3.	Mayani et al. [62] (2005)	Aspergillus niger (CCM 8004)	Modeling of a bioprocess of GA production from D-glucose: comparison of monod and contois models	5.0 l stirred tank bioreactor	Comparison of two substrate models of monod and contois to representation of biomass, product. substrate and DO	Contois model is better than monod to study the behavior of bioprocess of GA production

2.4 INDUSTRIAL PRODUCTION PRACTICES

Hlasiwets and Haberman had identified Gluconic acid (GA) for the first time in 1870. In 1922 Molliard showed that GA was produced by strain of *Sterimatocystis nigra* (probably *Aspergillus niger*) on a sucrose medium. Bernhauer (1928) selected a strain of *Aspergillus niger* which under specified condition produced only gluconic acid. In 1929, May et al. studied the *Pluteum purpurogenum* fermentation on the pilot plant scale using aluminum pans and obtained a 57% yield of gluconic acid in 11 days. Curri *et al.* (1931) patented the first time use of stirred aerator fermenter and 90% yield of calcium gluconate was obtained from a glucose medium (200 kg/m^3) in 48 to 60 hours using *A. niger* Milsom et al. [37]

In 1952, a process of GA production by fermentation using *A. niger* described by Blom et al. [9] is essentially used by most manufacturers in the 1980s and 1990s. Nyeste *et al.* (1980) have modeled and optimized gluconic acid fermentation using *Acetobactor suboxydans* and Oosterhuis et al. [42] have investigated the effect of physical parameters on the fermentation with *Acetobactor suboxydans*. However, the processes in use in the 1990s employ either *A. niger* or *Acetobacter (Gluconobacter) suboxydans* in submerged culture.

2.4.1 FERMENTATION PROCESS

➢ *Aspergillus niger* **Process Media:**

The carbohydrate source of gluconate production is glucose either in the form of glucose monohydrate crystals (Blom *et al.*, 1952) or dextrose syrup (Hatcher, 1972). Sources of nitrogen (ammonium salts, urea, corn steep liquor), phosphate, potassium and magnesium must be provided for growth of the mold. Optimal pH is maintained by online addition of NaOH solution for sodium salt and CaCO$_3$ solution for calcium salt.

➢ *Aspergillus niger* **Process Details:**

A suitable process layout of a plant for sodium gluconate or gluconic acid production is shown in figure 2.5. The prepared medium as shown is sterilized using plate heat exchanger but sterilization in the fermenter is a possible variant, although excessive darkening of

medium can occur. Wherever the medium is sterilized outside the fermenter, the latter must be steam sterilized separately.

The first fermentation stage is the growth of the vegetative inoculum. Strain of *A. niger* prepared from a culture grown on a solid medium is introduced into the inoculum fermenter. The initial pH of the inoculum-medium is adjusted to about 6.5 with NaOH. Both the inoculum and production fermenter are stirred, baffled, stainless steel tanks, sparged with air from the base and provided with a means of cooling. After a period, the inoculum is transferred to the product fermenter at the rate of about 1 part inoculum to 10 parts production medium. The correct time for this transfer may be judged by the amount of mycelial growth or by the rate of increase of glucose oxydase activity in the mycelial cells (Hatcher, 1972). Observing the rate of addition of NaOH solution may follow the progress of gluconic acid production. The fermentation period can be as short as 19 hours Blom et al. [9].

In order to promote the formation of gluconate, the production medium may contain 220 kg glucose/m^3 is maintained at pH of between 6.0 and 7.0 by addition of NaOH solution. The alkali addition is controlled with the aid of a sterilizable pH electrode installed in the fermenter. During the fermentation, which is conducted at 30 to 33 °C, the broth is agitated and sparged· with air at the rate of up to 1.5 volumes of air per medium volume per minute (vvm).

As a variant of this process, the mycelium may be re-used up to twice or more. A further variant, it is desirable that the broth at the end of the fermentation should have as high a product concentration as possible to save on evaporation costs. In order to achieve this, glucose is added in stages. For instance the initial glucose concentration might be 270 kg/m^3 and subsequently additions of 300, 80 and 90 kg/m^3 may be made. It is apparently not necessary to sterilize the later additions of glucose. Typically 97 to 99 % yield of product expressed as gluconic acid are obtained in 60 to 70 hours.

2.4.2 RECOVERY PROCESS

Fermentation the broth containing gluconic acid, calcium gluconate and sodium gluconate is treated as follows as required. There are three ways of treating fermented liquor.

(1) If a technical grade of sodium gluconate, e.g. of 98 % purity is required, the liquor may be directly spray dried. If the glucose is added in stages in which have been unsterilized the fermented liquor will be much lighter in color.

(2) If a pure grade of sodium gluconate is required, the liquor after concentration may be transferred to a crystallizer and the crystals so obtained separated in a centrifuge. The mother liquor may be re-circulated to an earlier stage of the process.

(3) If 50 % gluconic acid solution is required the evaporated liquor may be passed through a cation exchanger in the hydrogen from to remove the sodium ions.

2.5 OPERATING PARAMETERS

To determine a suitable set of input operating parameters that provides an optimal set of output parameters is a major challenge, primarily due to the existence of multiple substrate, varieties of microorganisms and different design of experimental set ups. The purpose of this section is to search a suitable set of operating parameters. This task is constrained by a lake of uniformity of suitable data. The different workers proposed varying operating parameters for the submerged fermentation process, which is used in the present work. This proposed operating parameters may be used as the starting information for the bioprocess development.

2.5.1 AERATION RATE

Low solubility of oxygen in an aqueous media and the poor transport properties make the oxygen supply a rate-limiting factor. The airflow should be such that it maintains the maximum oxygen concentration in the solution. The optimum range of airflow rate proposed by Znad et al. [61] is 15 l/min in 10.5 l internal loop airlift bioreactor at 57 h of batch time beyond which the process will not be economical. Some workers, for example, Das & Kundu [14], Tripathi et al.

[54], Jian-Zhong et al. [23], Lantero & Shetty [30] and Markos et al. [36] suggested about 1.0-1.5 vol air/vol solution per min (vvm) of air flow rate as optimum. This is equivalent to 4.5 – 6.75 lpm in a4.5 l reactor.

2.5.2 TEMPERATURE AND PRESSURE

Most of the above workers carried out experiments about 30° C - 32° C as shown in Table 2.1. Lantero et al. [30] studied the effect of temperature and found that optimum temperature is 30° C. pH should be maintained 6.5 during the growth phase and at 5.5 during the production phase by addition of NaOH used by Markos et al. [36].

Further, the inoculation level found by Singh [48], Markos et al. [36] is 2%. Antifoam addition, if required, would be about 80 – 120 ppm. Higher pressure increases the oxygen solubility, but operating cost goes up. So the reactor should be operated at the pressure slightly above the atmospheric pressure.

2.5.3 GLUCOSE CONCENTRATION

It was found by Markos et al. [36] that glucose concentration higher than 6.68 g/l, formed higher biomass, which negatively effects the formation of gluconic acid. This parameter is very conflicting as different workers proposed different values by Gutierrej-Rojas et al. [20] (30 gm/l), Singh et al. [48] (12% w/w), Lantero et al [30] (30% w/w), Markos et al. [36] (150 g/l). Zhong et al. [23] (100 g/l) and Znad et al. [61] (200 g/l). Higher the concentration will reduce the inhibition effect of product in the solution during the fermentation of glucose.

2.5.4 SUPERFICIAL GAS VELOCITY AND OXYGEN MASS TRANSFER COEFFICIENT

The oxygen dissolved from the liquid is used only for biotransformation of glucose to gluconic acid. Thus the oxygen transport characteristic of oxygen from gas phase to the liquid phase is influence the gluconic acid production. A higher airflow rate supports a higher supply

of oxygen into the bioreactor and increases the gas hold up, enhance bulk mixing and improve DO and mass transfer. Thus, the optimum value of this parameter is of prime importance.

Znad et al. [61] indicated riser superficial gas velocity as 0.0667 m/s (equivalent to 15 l/m) in 10.5 l airlift fermenter beyond which the process may not be economic.
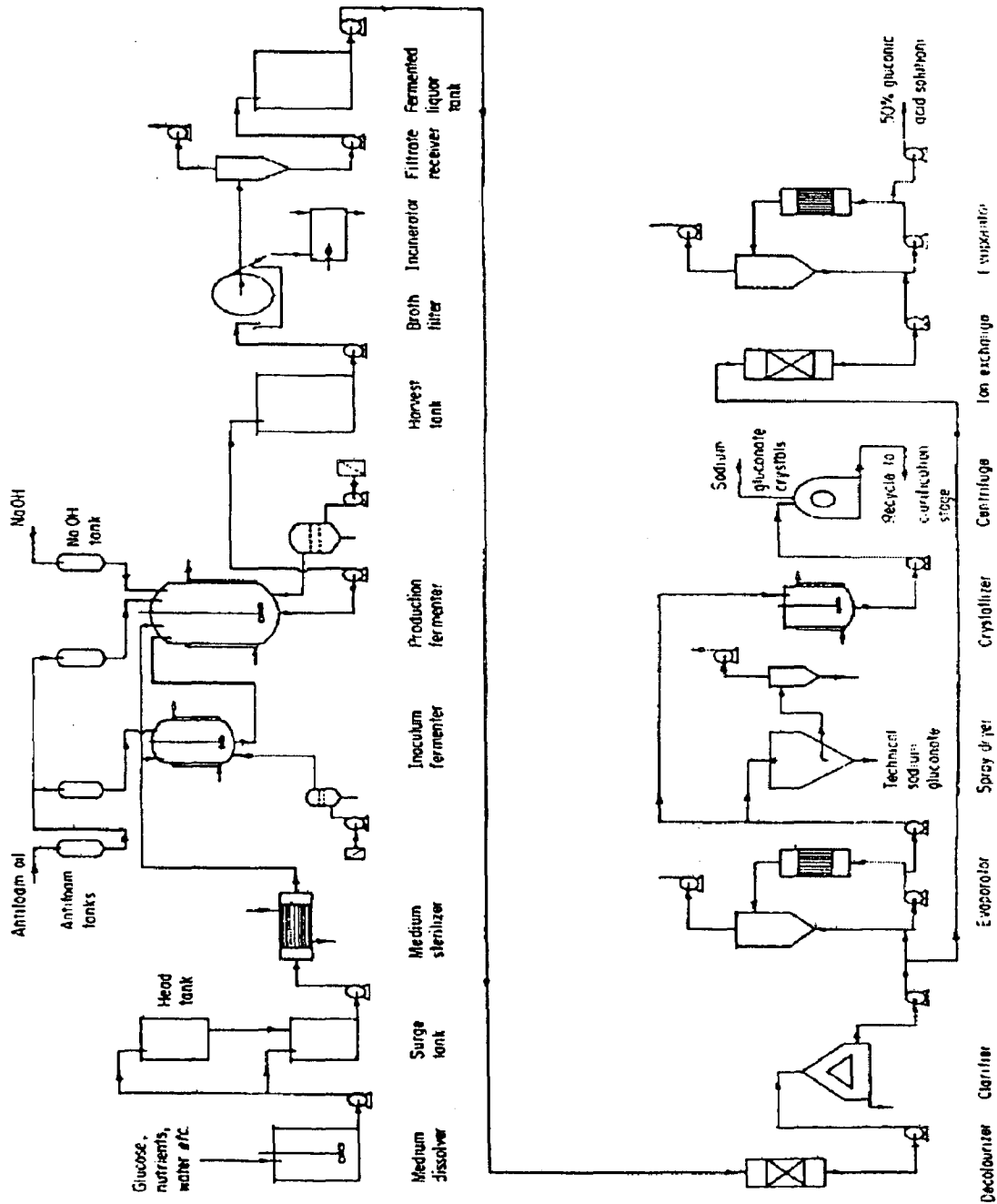
Figure: 2.6 Process layout of gluconic acid production by submerged fermentation. Milsom et al. [37]

3.1 INTRODUCTION

Most industrial bioreactors are still conventional stirred tanks. As an alternatives to then, recently, airlift bioreactors have received increased attention. Due to their simple construction and less shear stress to shear-sensitive cells compared with stirred tanks, these have found potential applications in biotechnology industries. However, accurate description of the performance of an airlift bioreactors is still difficult. Further, the airlift reactor is a promising reactor for two and three phase reactions due to its advantages of high fluid circulation, heat and mass transfer, short mixing time, low shear stress and low energy consumption. Airlift reactors have been widely applied in chemical engineering, biochemical fermentation and biological wastewater treatment processes. In order to design such a bioreactor with confidence, further information is required on the relationship between its performances and hydrodynamic, heat and mass transfer characteristics, etc.

In the present Chapter, design, hydrodynamic & separator details of fabricated concentric tube airlift reactor have been given. For further investigation of various characteristic of ALBR, necessary considerations in the design were discussed.

3.1.1 SELECTION OF ALBR

Airlift bioreactors can be used for growing both plant and animal cells. Selection of airlift reactor relies on the following advantages and disadvantages.

Advantages include:

❑ Simple construction with no moving parts or agitator, less risk of contamination and easier sterilization.

❑ Lower shear rate and large specific interfacial contact area with low energy input.

❏ Well-controlled flow and efficient mixing.

□ Satisfy a high level of oxygen demand, especially in the large scale, where a high liquid level creates high partial pressure of oxygen.

□ Uniformly distributed shear stresses can create an optimal environment for many productive microorganisms.

□ When compared with bubble column, ALRs have increased heat and mass transfer capacity & less energy consumption for mixing.

Disadvantages include:

□ Greater air throughput and higher pressures needed, particularly for large-scale operation.

□ Inherently impossible to maintain consistent levels of substrate, nutrients and oxygen with the organisms circulating through the bioreactor and conditions changing.

□ Inefficient gas/liquid separation when foaming occurs.

3.2   DESIGN DETAILS OF AIRLIFT BIOREACTOR

An airlift reactor consists of four distinct sections: riser, down comer, top and bottom sections. Each section of ALR exhibits different hydrodynamic and mixing behavior. Airlift reactors have no moving parts and mixing is caused pneumatically. Gas-liquid circulation is caused by the gradient in density between riser and down comer because the gas hold-up is different in riser and down comer.

The design of the airlift reactor is based on the scale-down of that given in [61] and consideration of certain other aspects given in section 3.2.1. For the scale down, overall mass transfer coefficient (k_La) and gassed power per unit volume (P_g/V) were kept almost constant [7]. The main specifications of the reactor are:

Draft tube (Riser tube):	ID = 0.042 m, Height = 100 cm
Airlift reactor tube (Down comer):	ID = 0.0725 m, Height = 1.032 m
Separator:	ID = 0.2 m, Height = 0.18 m

Table 3.1 Comparison of present reactor after scale down and the reactor used in [61].

Sr. No.	Design parameter	Present work, 4.5 l	10.5 l Znad *et al.* [61]
1.	k_La (h^{-1})	106.4915	103.2304
2.	P_g/V (W/m^3)	362.3637	350.3823
3.	Air flow rate (lpm)	7.8	15.36

3.2.1 DESIGN CONSIDERATIONS

Following design considerations were implemented in the present ALR:

❏ Sparging of air in the draft tube is more efficient and productive since it has high gas hold up [12]. Further, Ugr above 0.04 m/s did not improve mixing to a greater extent [13].

❏ The glass tubes are used to visualize the entire operation of mixing in the riser and down comer sections.

❏ Higher height to diameter ratio was used in order to increase the oxygen residence time and thus solubility caused by higher hydrostatic pressure in ALR.

❏ Expanded top zone allows easy release of air and less entrainment of fluid particles.

❏ Provision for sample withdrawal was made at the bottom, to avoid contamination.

❏ The air supply tube introduced from top to avoid chocking or backflow in the air supply line, which may happen during operation due to sudden power failure.

❏ For the study of sparging in down comer, provision has been made to sparge air in down comer with a new sparger.

❏ Sight glass and light glass has been provided to visualize the liquid level in the gas-liquid separator.

3.2.2 GAS – LIQUID SEPARATOR DESIGN

The terminal settling velocity of liquid particles (u_t):

The separator design should allow the gas to escape without entrainment of liquid particles. The settling velocity of liquid particles is given by

$$u_t = 0.15\sqrt{(\rho_l - \rho_g)/\rho_g} \qquad (3.1)$$

Where, u_t = Terminal settling velocity of liquid particles, m/s

ρ_l = Density of liquid, kg/m^3

ρ_g = Density of gas, kg/m^3

The minimum allowable separator diameter ($D_{s,\,min}$):

This diameter allows gas velocity to reduce to such a level that the liquid particles will be able to settle.

$$D_{s,min} = \sqrt{4Q_g/\pi u_s} \qquad (3.2)$$

Where, Q_g = Volumetric flow rate of gas, m^3/s

u_s = 0.15*u_t for separator without a demister pad, m/s

Here, u_t comes out to be 4.855 m/s and using Q_g = 1.3*10^{-4} m^3/s, $D_{s,\,min}$ was found to be 0.01322 m. The actual value was taken as 0.2 m, which is larger than required. Hence, our design is suitable and there is no chance of liquid that carried away with air.

3.2.3   3D MODEL AND CONSTRUCTION DETAILS

3D model of concentric tube airlift bioreactor with actual dimensions has been developed in AutoCAD 2000 and is presented in the Figure 3.1 with important dimensions. Upper and lower parts of reactor were made up of SS 304, whereas middle parts including riser and down comer sections were made of glass for visualization of mixing. Entire stand was made from SS 304 and glass bottles are placed at the top for addition of base, acid or antifoam, etc. The working volume of the reactor is 4.5 l.

3.2.4   EXPERIMENTAL SET-UP DETAILS

The overall size of the experimental set-up made of SS and glass is about 2 m x 1 m. The system is closed and designed such that it can be sterilized *in situ* using steam at about 121 °C

for 15 min after replacing sensors and probes by blinds. Sparger can also be removed for cleaning purpose and replaced by another one to sparge in down comer. Water-cooling is provided to maintain the temperature of the system by manually controlling the flow rate. The size of the air filters provided at the inlet and outlet has pore size of 0.2 micrometer, which prevents entry of any microbes present in the atmospheric air.
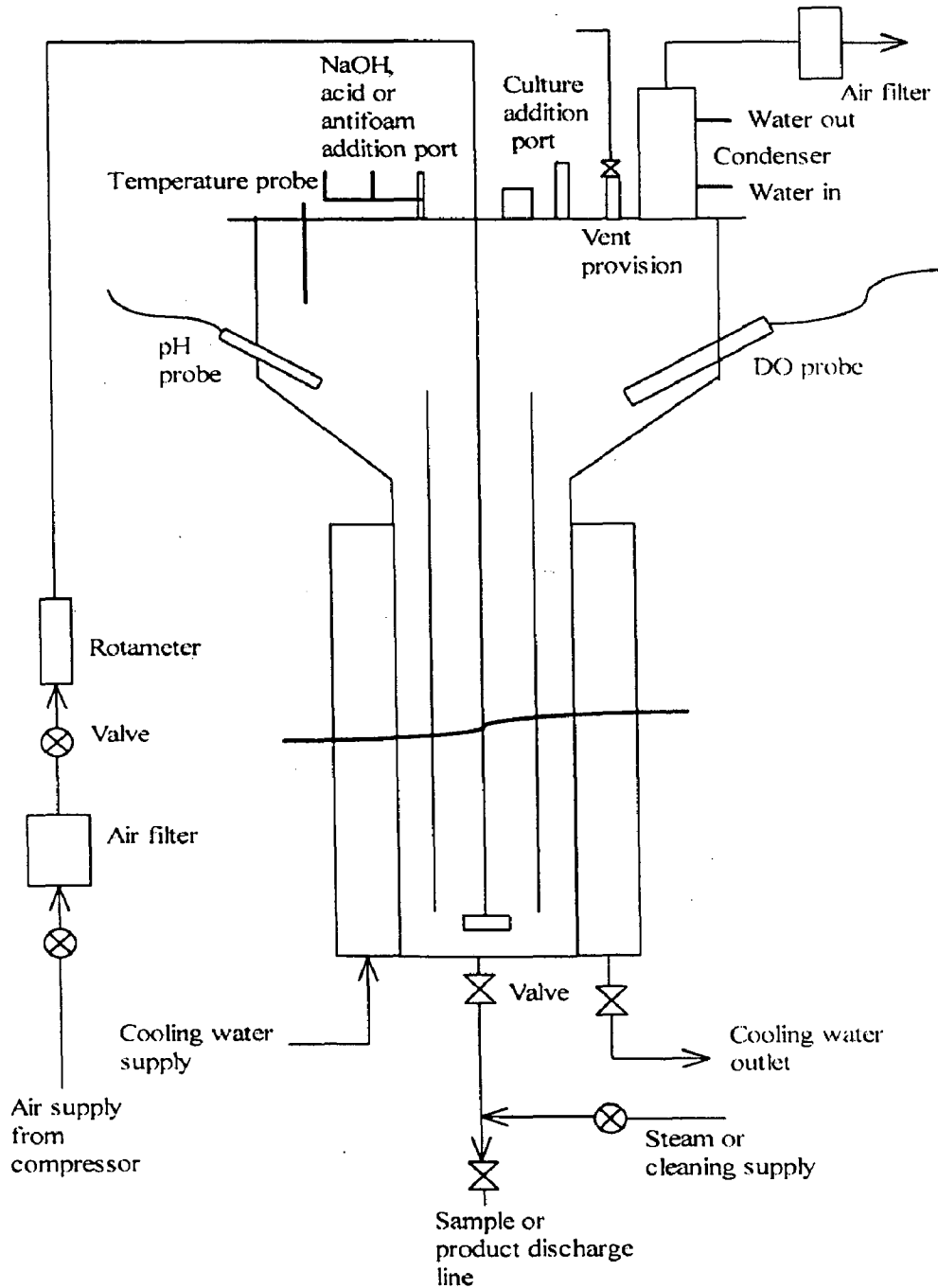
Figure: 3.1 Schematic diagram of experimental set-up with air supply and system accessories.

35
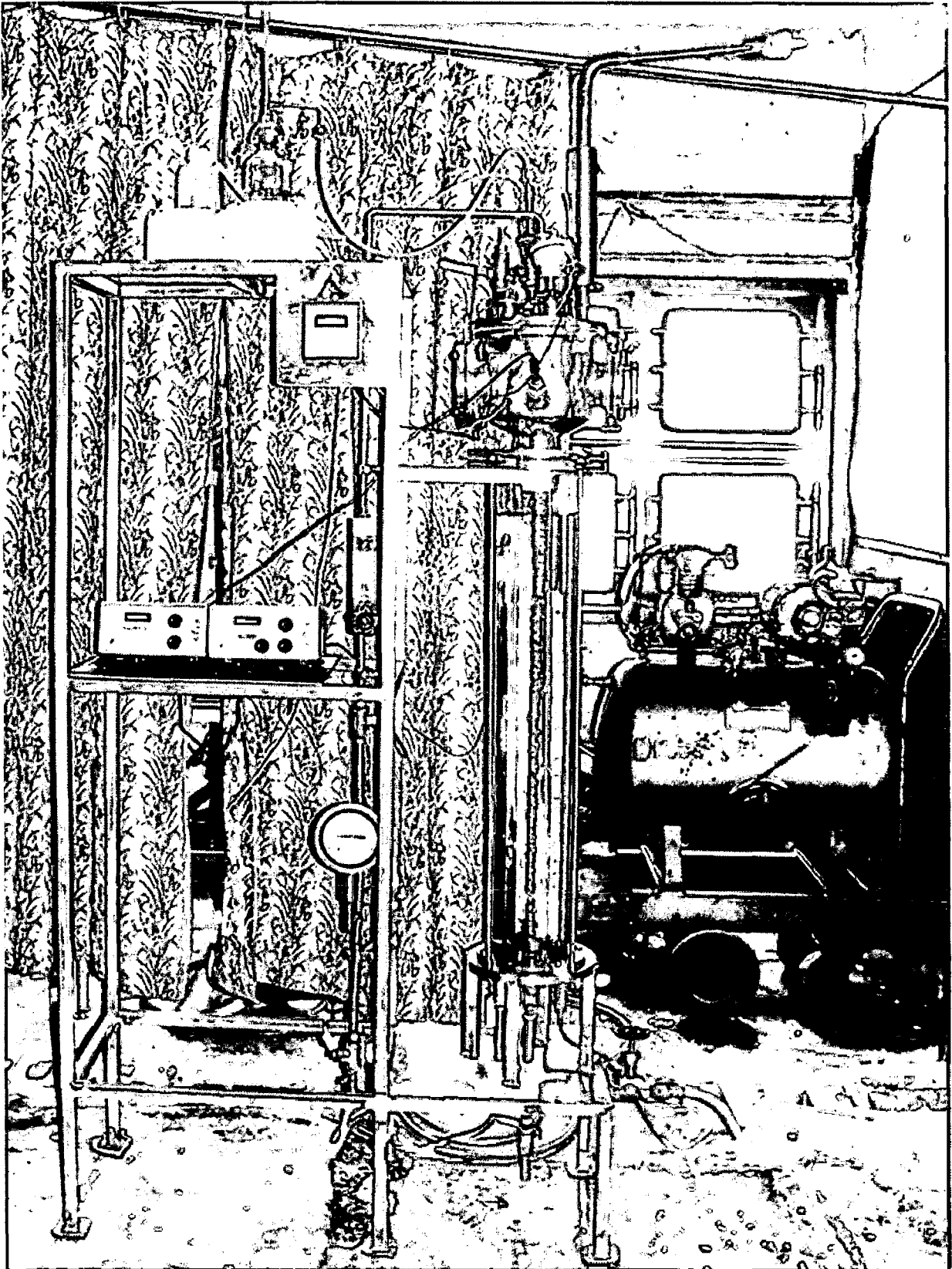
Figure: 3.2 Overview of the experimental set-up of the airlift bioreactor system.
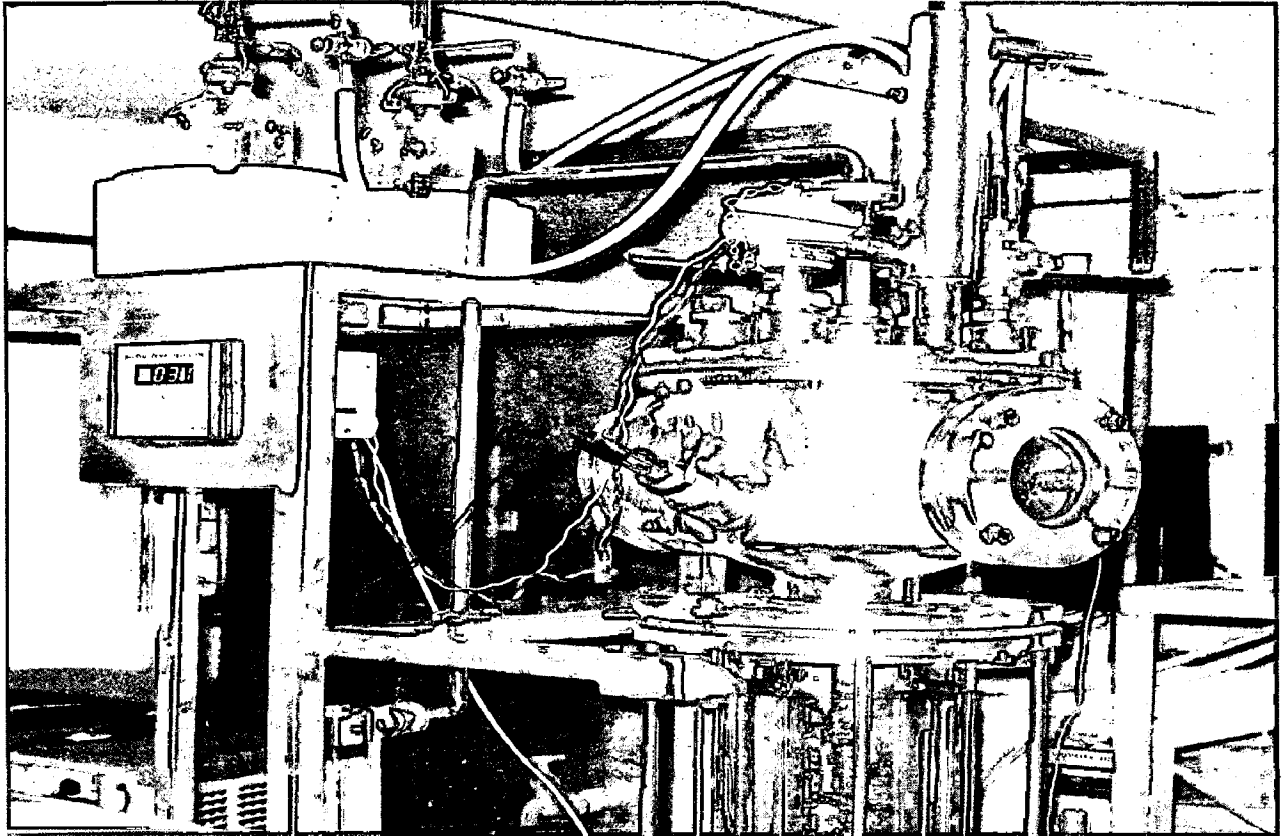
(a)
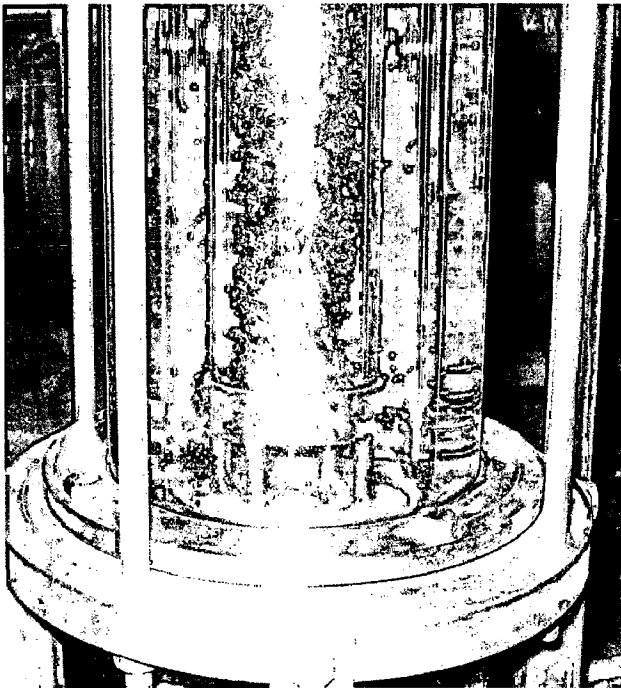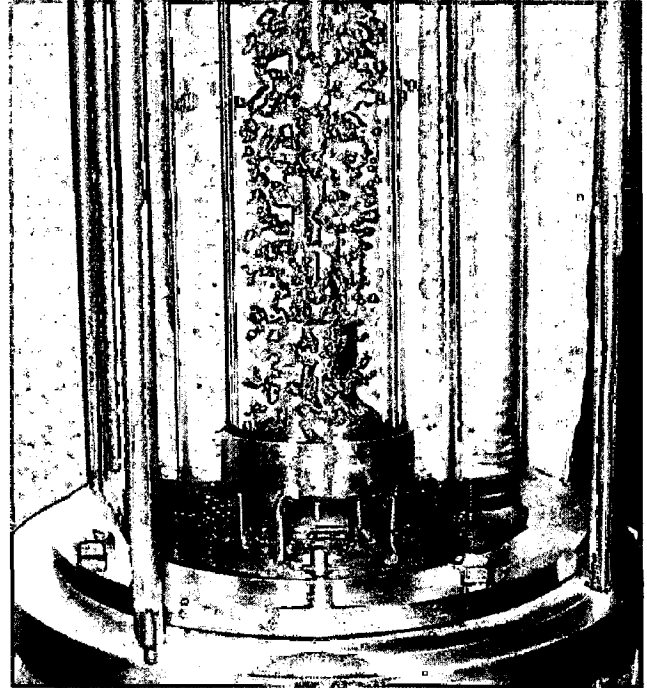
(b)   (c)

Figure: 3.3 Details of sparged airlift reactor, (a) Separator and sensor parts, (b) Sparging at 10 lpm and (c) sparging at 7 lpm of air.
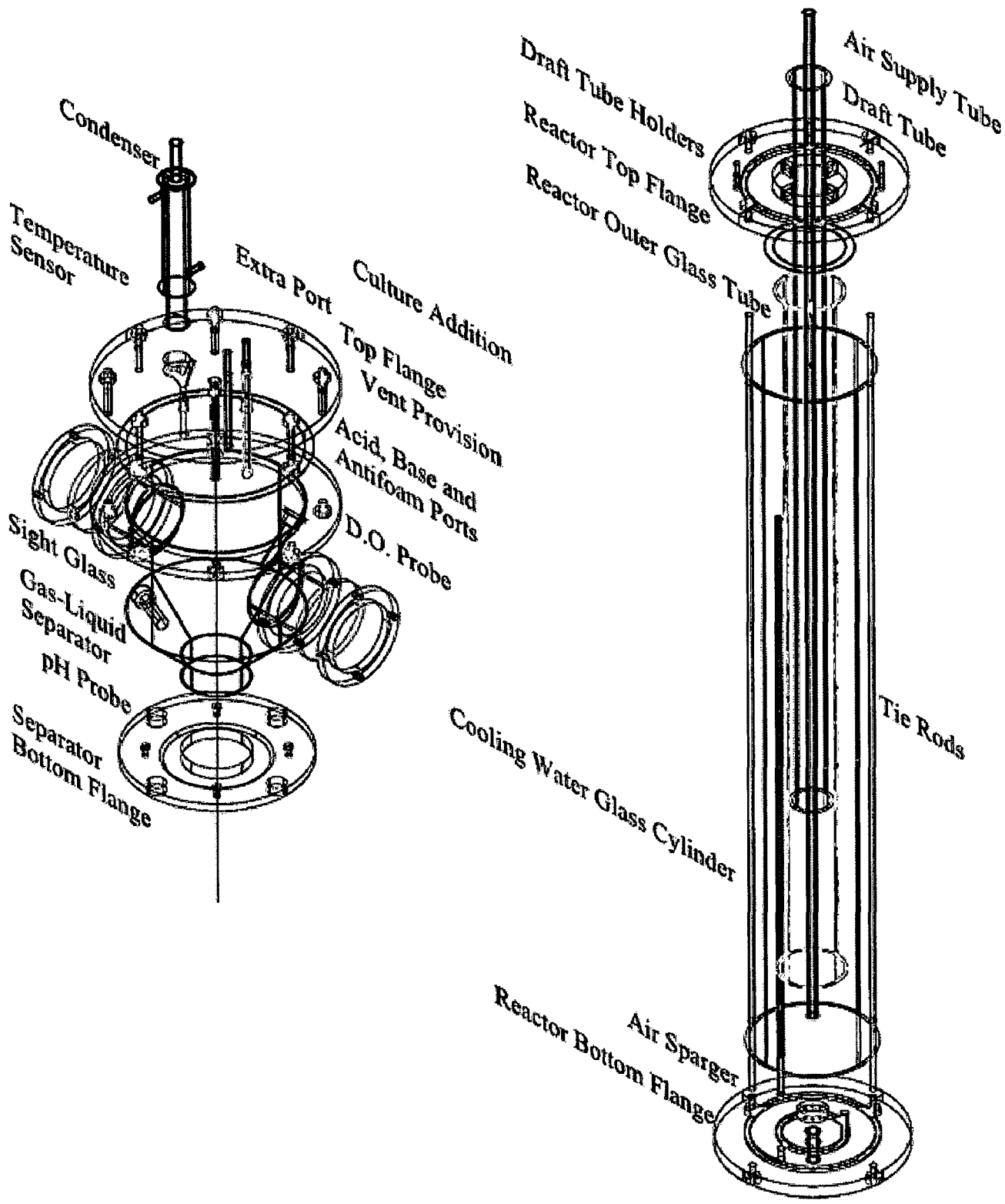
Figure: 3.4 3D model view of an airlift bioreactor with important parts.

3.3 PROPOSED EXPERIMENTAL PROCEDURES

The proposed experimental methods are presented in the present section for media preparation and for determination of the concentration of the substances.

3.3.1 PROPOSED MEDIA PREPARATION

The microorganism *Aspergillus niger* ORS-4.410 with a high activity of glucose oxidase and catalase was used. The mycelium grew in a pellet form. The inoculum was prepared in shake flasks for 48 h. The bioreactor was inoculated with 2% of volume. The reactor temperature was kept at 30 °C. Air flow rate of 8 lpm (at 273 °K and 1.2 atmosphere pressure was used in ALR. All media were sterilized at 121 °C for 30 min. pH was maintained at 6.5 during the growth phase and at 5.5 (maximal GOD activity) during the production phase by the addition of 12 M sodium hydroxide. Peanut oil used as antifoam agent.

A proposed medium with a following contents was given in [61]:

Glucose	: 200.0 g/l	$MgSO_4 \cdot 7H_2O$	: 0.25 g/l
$(NH_4)_2SO_4$	: 0.59 g/l	$Ca(NO_3) \cdot 4H_2O$	: 1.0 ml/l
KCl	: 0.25 g/l	50% corn-steep liquor	: 1.5 ml/l
KH_2PO_4	: 0.25 g/l		

3.3.2 PROPOSED ANALYTICAL METHODS

The dry weights of mycelium were obtained after filtration of broth samples through pre-weighed filter discs. The harvested biomass was then washed with de-ionized water, dried for 8 h at 105 °C, cooled in a desiccator and weighed.

The concentration of gluconic acid was calculated by noting the amount of NaOH used to keep the pH value of liquid in the fermenter at 6.5 during the growth phase and 5.5 during the production phase. The amount of by-product acids, e.g. citric acid, was assumed to be negligible compared with that of gluconic acid [23]. The other method of determination of glucose and gluconic acid concentration is by HPLC analysis of the filtrate. Density of the broth was measured by gravimetric method.

4.1 INTRODUCTION

A model generally describes relationships between principal state variables and explains quantitatively the behavior of a system. The model can provide useful suggestions for the analysis, design and operation of a fermenter [23]. Mathematical models can be of fundamental, empirical. analog or probabilistic type. Fundamental models make use of basic science of axioms of the model, while empirical models uses set of inputs to a process for getting set of outputs and require fundamental model.

Mixing in airlift bioreactors is usually imperfect and mathematical models for airlift bioreactors cannot be described by either perfect mixing (continuous stirred tank reactors: CSTR) or plug flow (plug flow reactors: PFR) [35, 36]. The mixing model used in most of the previous investigations dealing with airlift bioreactors is an axial dispersion models [2.39]. It should be noted that the ADM could describe satisfactorily only mixing, which slightly deviates from the plug flow [59].

In this work a mathematical model based on a tanks in series with back flow was developed and simulated for a bioprocess in an airlift bioreactor under steady state condition.

4.2 ASSUMPTIONS

Following assumptions have been made for the development of a mathematical model.

(1) Constant temperature and constant air flow rate.

(2) Reaction occurs in the liquid phase.

(3) There are no radial gradients in liquid and gas phase.

(4) The gas hold-up in the top and bottom sections are equal to the gas hold up in the riser.

(5) Saturated concentration of oxygen in liquid phase is uniform in the reactor. Change in oxygen concentration in the gaseous phase flowing through the reactor is negligible, so

40

the material balance of oxygen in the gaseous phase can be neglected Klein et al. [25].

The effect of hydrostatic pressure effect is also neglected.

(6) The gas hold-up and mass transfer coefficients almost constant along the riser and down comer.

(7) The back mixing in the down comer is neglected, i.e. b = 0.

(8) Concentration of cell mass was measured on dry basis [61].

(9) During the multiplication process of the viable cell, no toxic compound was produced which has adverse effect on cell growth and product formation.

4.3 FORMULATION OF MODEL

The airlift bioreactor is composed of a column, which is divided into the region containing the gas-liquid up flow (the riser) and the region containing the gas-liquid down flow (the down comer).
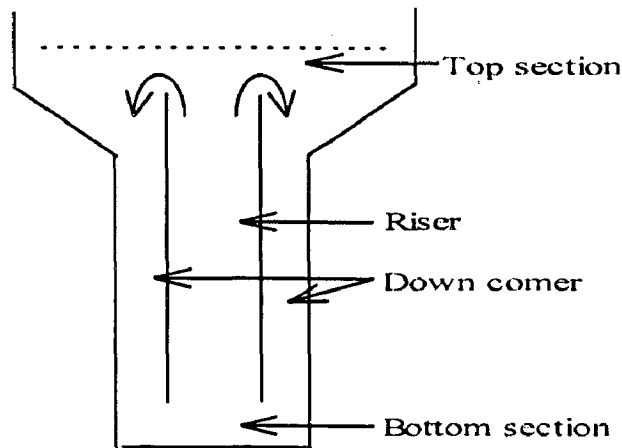
Figure: 4.1 Concentric tube airlift bioreactor.

In this work, the mixing characteristics are described by a tanks-in-series model, the flow in the airlift bioreactor is considered as flow through a series of equal sized, well-mixed stirred stages or tanks and the parameter describing non-ideal flow is the number of stages. The mixing characteristics of the riser, down comer, top and bottom sections in airlift bioreactors are different [57]. Introducing back flow can do an extension for the incorporation of micro-mixing

effects into the model. The model is represented schematically in Fig. 4.1. The bottom section $(i = 1)$ is treated as a well-mixed stage. The riser and the top sections $(i = 2, ..., M)$ are described as tanks-in-series with back flow. Since the flow in the down comer $(j = M + 1, ..., N)$ is relatively well defined, the back flow in the down comer is neglected.

At the top section, most of gas bubbles passing upward in the riser disengage and only the rest is entrained downward by liquid re-circulation into the down comer. On the other hand, the flow in the down comer is almost single-phase and relatively well defined. Therefore, the back mixing in the down comer is neglected. The riser, including the top and bottom sections, is divided into (M) hypothetical well-mixed stages. In other words, the $(M - 2)$ stages with back flow are used to characterize mixing in the riser. Consequently, mixing in the down comer is represented by $(N - M)$ stages without back flow. The stages in the riser are numbered upwards and those in the down comer are numbered downwards.
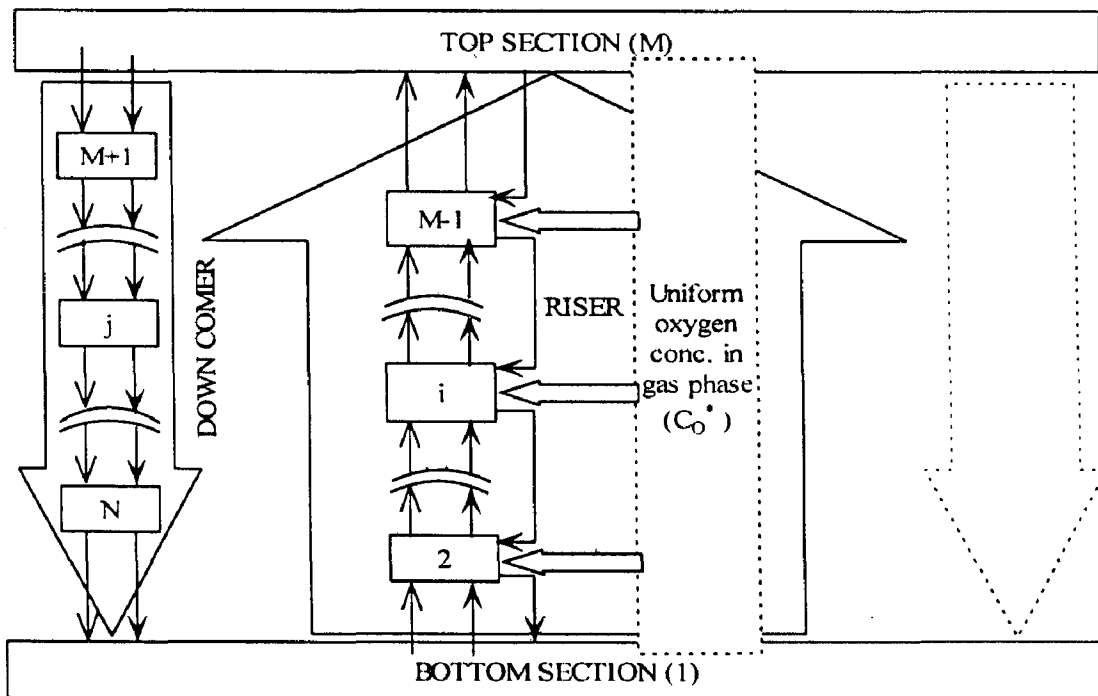
Figure: 4.2 Different sections (riser, bottom, top and down comer) and corresponding stages (i = 1 to N) of an airlift bioreactor.

42

Table: 4.1 Distribution of stages among sections in an ALBR.

Characteristic part	Section of ALR	Stages	Total stages
I	Bottom	$i = 1$	1
	Riser	$i = 2, \ldots\ldots, M\text{-}1$	2 to 21
	Top	$i = M$	22
II	Down comer	$i = M+1, \ldots\ldots\ldots, N$	22 to 44

4.4 SET OF EQUATIONS

Material balances of the biomass (X), product (P), substrate (S) and dissolved oxygen (Co) in hypothetical well-mixed tanks or stages can be written as follows. The unsteady state material balances of these components with back flow (b) provide four simultaneous first order ordinary differential equations in each stage. 'C' is referred as component either of X, P or S.

4.4.1 BOTTOM SECTION [i =1]:

For C = Substrate (S), microorganisms (X) & Product (P):

Material balance in bottom section-1 can be written as

Rate of change in C in sec.1, 1*(gm/l*min) =

+ [C in by liquid flow to section 1, (l/min)*(gm/l)]

- [C out by liquid flow from section1, (l/min)*(gm/l)]

+ [C (in - out) by back flow for section1,(l/min)*(gm/l)]

+ [Rate of generation in sec. 1, (gm/l*min)*(l)]

Figure: 4.3 Material balances (biomass, substrate, product and oxygen) in bottom section.

$$V_b(1-\varepsilon_{gr}) \times \frac{dC}{dt} = QC_N - (1+b)QC_1 + bQC_2 - 0 + R_{C1} V_b(1-\varepsilon_{gr})$$

$$\Rightarrow \frac{dC}{dt} = \frac{Q}{V_b(1-\varepsilon_{gr})}C_N - \frac{(1+b)Q}{V_b(1-\varepsilon_{gr})}C_1 + \frac{bQ}{V_b(1-\varepsilon_{gr})}C_2 + R_{C1}$$

$$\Rightarrow \frac{dC}{dt} = A_1 C_N - B_1 C_1 + D_1 C_2 + R_{C1} \qquad (4.1)$$

Where, $A_1 = Q/V_b(1-\varepsilon_{gr})$, $B_1 = (1+b)Q/V_b(1-\varepsilon_{gr})$ and $D_1 = bQ/V_b(1-\varepsilon_{gr})$

For Dissolved oxygen (Co):

Oxygen balance in bottom section-1 can be written as

Rate of change in Co in sec.1, 1*(gm/l*min) =

+ [Co in by liquid flow to sec.1, (l/min)*(gm/l)]

- [Co in by liquid flow to sec.1, (l/min)*(gm/l)]

+ [Co (in – out) by back flow in sec.1, (l/min)*(gm/l)]

+ [Oxygen addition by MT in sec.1, (min*gm/l)*1]

+ [Rate of generation of oxygen in sec.1, (gm/l*min)*1]

The oxygen transfer rate per unit reactor volume is given by

$$\text{Oxygen absorption rate} = \frac{(\text{flux})(\text{interfacial area})}{\text{reactor liquid volume}} = k_L (Co^* - Co) \times \frac{A}{V}$$
$$= k_L a (Co^* - Co)$$

where, a is the gas – liquid interfacial area per unit volume

$$V_b(1-\varepsilon_{gr}) \times \frac{dCo}{dt} = QCo_N - (1+b)QCo_1 + bQCo_2 - 0$$

$$+ (k_L a)_r (Co_1^* - Co_1) \times V_b(1-\varepsilon_{gr}) + R_{Co1} V_b(1-\varepsilon_{gr})$$

$$\Rightarrow \frac{dCo_1}{dt} = \frac{Q}{V_b(1-\varepsilon_{gr})}Co_N - \frac{(1+b)Q}{V_b(1-\varepsilon_{gr})}Co_1 + \frac{bQ}{V_b(1-\varepsilon_{gr})}Co_2 + (k_L a)_r (Co_1^* - Co_1) + R_{Co1}$$

$$\Rightarrow \frac{dCo_1}{dt} = A_1 Co_N - B_1 Co_1 + D_1 Co_2 + (k_L a)_r (Co_1^* - Co_1) + R_{Co1} \qquad (4.2)$$

4.4.2 RISER SECTION [i = 2, ..., M-1]:

For C = Substrate (S), micro organisms (X) & Product (P):

Material balance in section - i can be written as

Rate of change in C in section i, 1*(gm/l*min) =

+ [C in by liquid flow to sec. i, (l/min)*(gm/l)]

44

- [C out by liquid flow from sec. i, (l/min)*(gm/l)]

+ [C (in – out) by back flow for sec. i, l/min)*(gm/l)]

+ [Rate of generation of C in sec. i, (gm/l*min)*(l)]
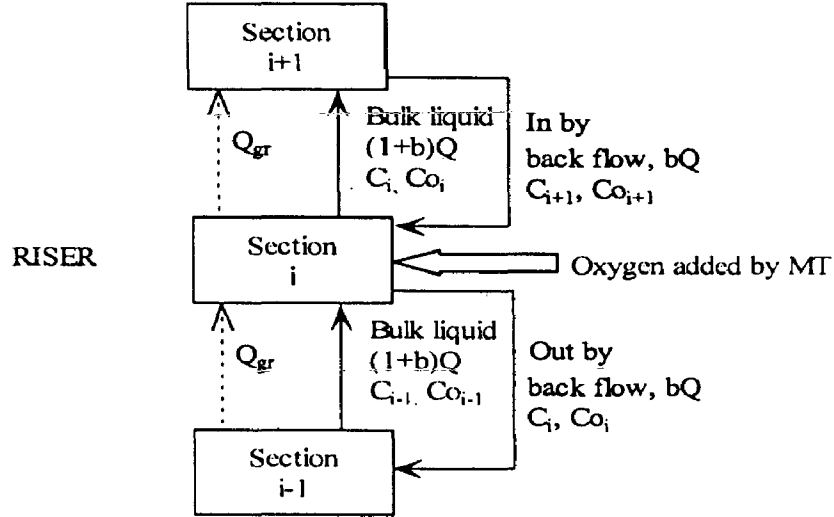
RISER

Figure: 4.4 Material balances (biomass, substrate, product and oxygen) in riser section.

$$\left(\frac{V_r(1-\varepsilon_{gr})}{M-2}\right) \times \frac{dC_i}{dt} = (1+b)QC_{i-1} - (1+b)QC_i + bQC_{i+1} - bQC_i + R_{ci} \times \left(\frac{V_r(1-\varepsilon_{gr})}{M-2}\right)$$

$$\Rightarrow \frac{dC_i}{dt} = \frac{(1+b)Q}{\left(\frac{V_r(1-\varepsilon_{gr})}{M-2}\right)}(C_{i-1} - C_i) + \frac{bQ}{\left(\frac{V_r(1-\varepsilon_{gr})}{M-2}\right)}(C_{i+1} - C_i) + R_{ci}$$

$$\Rightarrow \frac{dC_i}{dt} = A_2(C_{i-1} - C_i) + B_2(C_{i+1} - C_i) + R_{ci} \qquad (4.3)$$

Where, $A_2 = (1+b)Q / \left(\frac{V_r(1-\varepsilon_{gr})}{M-2}\right)$, $B_2 = bQ / \left(\frac{V_r(1-\varepsilon_{gr})}{M-2}\right)$

For Dissolved oxygen (Co):

Oxygen balance in section - i can be written as

Rate of change in Co in section i, l*(gm/l*min) =

+ [Co in by liquid flow to sec. i, (l/min)*(gm/l)]

- [Co in by liquid flow to sec.i, (l/min)*(gm/l)]

+ [Co (in – out) by back flow in sec.i, (l/min)*(gm/l)]

+ [Oxygen addition by MT in sec.i, (min*gm/l)*l]

+ [Rate of generation of oxygen in sec.i, (gm/l*min)*l]

45

$$\left(\frac{V_r(1-\varepsilon_{gr})}{M-2}\right) \times \frac{dCo_i}{dt} = (1+b)QCo_{i-1} - (1+b)QCo_i + bQ(Co_{i+1} - Co_i)$$

$$+ (k_La)_r(Co_i^* - Co_i) \times \left(\frac{V_r(1-\varepsilon_{gr})}{M-2}\right) + R_{Co_i} \times \left(\frac{V_r(1-\varepsilon_{gr})}{M-2}\right)$$

$$\Rightarrow \frac{dCo_i}{dt} = \frac{(1+b)Q}{\left(\dfrac{V_r(1-\varepsilon_{gr})}{M-2}\right)}(Co_{i-1} - Co_i) - \frac{bQ}{\left(\dfrac{V_r(1-\varepsilon_{gr})}{M-2}\right)}(Co_{i+1} - Co_i) + (k_La)_r(Co_i^* - Co_i) + R_{Co_i}$$

$$\Rightarrow \frac{dCo_i}{dt} = A_2(Co_{i-1} - Co_i) - B_2(Co_{i+1} - Co_i) + (k_La)_r(Co_i^* - Co_i) + R_{Co_i} \quad (4.4)$$

4.4.3 TOP SECTION [i =M]:

For C = Substrate (S), micro organisms (X) & Product (P):

Material balance in top section - M can be written as

Rate of change in C in sec.M, I*(gm/l*min) =

    + [C in by liquid flow to sec. M, (l/min)*(gm/l)]

    - [C out by liquid flow from sec. M, (l/min)*(gm/l)]

    + [C (in – out) by back flow for sec. M, l/min)*(gm/l)]

    + [Rate of generation of C in sec. M, (gm/l*min)*(l)]
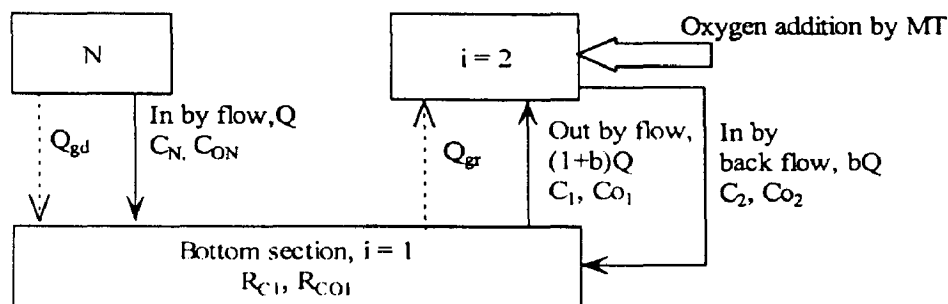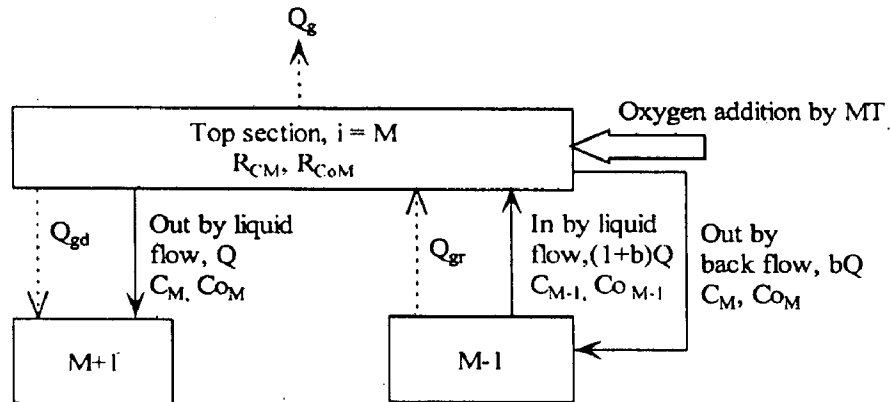

Figure: 4.5 Material balances (biomass, substrate, product and oxygen) in top section.

$$V_t(1-\varepsilon_r) \times \frac{dC_M}{dt} = (1+b)QC_{M-1} - QC_M + bQ(0-C_M) + R_{CM}V_t(1-\varepsilon_{gr})$$

$$V_t(1-\varepsilon_r) \times \frac{dC_M}{dt} = (1+b)C_{M-1} - QC_M - bQC_M + R_{CM} \times V_t(1-\varepsilon_{gr})$$

$$\Rightarrow \frac{dC_M}{dt} = \frac{(1+b)Q}{V_t(1-\varepsilon_{gr})}(C_{M-1}-C_M)+R_{CM}$$

$$\Rightarrow \frac{dC_M}{dt} = A_3(C_{M-1}-C_M)+R_{CM} \qquad (4.5)$$

Where, $A_3 = (1+b)Q/V_t(1-\varepsilon_{gr})$

For C Dissolved oxygen (Co):

Oxygen balance in top section - M can be written as

[Rate of change in Co in section M, 1*(gm/l*min)] =

<div style="text-align:center">

+ [Co in by liquid flow to sec. M, (l/min)*(gm/l)]

- [Co in by liquid flow to sec. M, (l/min)*(gm/l)]

+ [Co (in – out) by back flow in sec. M, (l/min)*(gm/l)]

+ [Oxygen addition by MT in sec. M, (min*gm/l)*l]

+ [Rate of generation of oxygen in sec. M, gm/l*min)*l]

</div>

$$V_t(1-\varepsilon_{gr})\times\frac{dCo_M}{dt} = (1+b)QCo_{M-1} - QCo_M + bQ(0-Co_M)$$
$$+(k_La)_r(Co^*_M-Co_M)\times V_t(1-\varepsilon_{gr})+R_{CoM}V_t(1-\varepsilon_{gr})$$

$$\Rightarrow \frac{dCo_M}{dt} = \frac{(1+b)Q}{V_t(1-\varepsilon_{gr})}(Co_{M-1}-Co_M) + (k_La)_r(Co^*_M-Co_M)+R_{CoM}$$

$$\Rightarrow \frac{dCo_M}{dt} = A_3(Co_{M-1}-Co_M) + (k_La)_r(Co^*_M-Co_M)+R_{CoM} \qquad (4.6)$$

4.4.4 DOWNCOMER [i = M+1, ..., N]:

For C = Substrate (S), micro organisms (X) & Product (P):

Material balance in down comer section - i can be written as

Rate of change in C in section i, 1*(gm/l*min) =

<div style="text-align:center">

+ [C in by liquid flow to sec. i, (l/min)*(gm/l)]

- [C out by liquid flow from sec. i, (l/min)*(gm/l)]

+ [C (in – out) by back flow for sec. i, (l/min)*(gm/l)]

+ [Rate of generation of C in sec. i, (gm/l*min)*l]

</div>

Section
i-1

Q_{gd}

In by bulk liquid flow, Q
C_{i-1}, Co_{i-1}

Section
i
$R_{C\,i}$, $R_{CO\,i}$

Q_{gd}

Out by bulk liquid flow, Q
C_{i+1}, Co_{i+1}
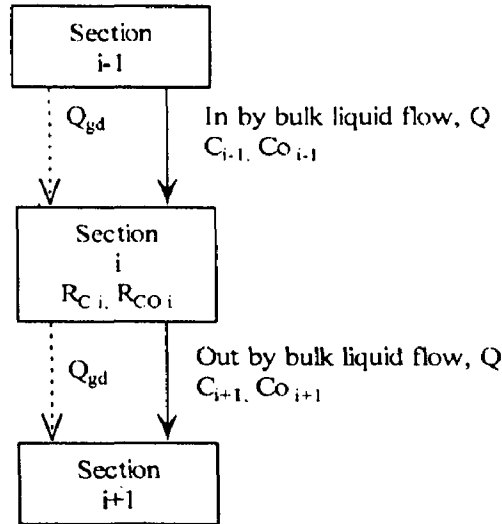
Section
i+1

Figure: 4.6 Material balances (biomass, substrate, product and oxygen) in down comer section.

$$\left(\frac{V_d(1-\varepsilon_{gd})}{N-M}\right) \times \frac{dC_i}{dt} = QC_{i-1} - QC_i + R_{Ci} \times \left(\frac{V_d(1-\varepsilon_{gd})}{N-M}\right)$$

$$\Rightarrow \frac{dC_i}{dt} = \frac{Q}{\left(\frac{V_d(1-\varepsilon_{gd})}{N-M}\right)}(C_{i-1}-C_i) + R_{Ci}$$

$$\Rightarrow \frac{dC_i}{dt} = A_4(C_{i-1}-C_i) + R_{Ci} \qquad (4.7)$$

$$\text{Where, } A_4 = Q / \left(\frac{V_d(1-\varepsilon_{gd})}{N-M}\right)$$

For Dissolved oxygen (Co):

Oxygen balance in down come section - i can be written as

Rate of change in Co in section i, l*(gm/l*min) =

+ [Co in by liquid flow to sec. i, (l/min)*(gm/l)]

- [Co in by liquid flow to sec. i, (l/min)*(gm/l)]

+ [Co (in – out) by back flow in sec. i, (l/min)*(gm/l)]

+ [Oxygen addition by MT in sec. i, (min*gm/l)*l]

+ [Rate of generation of oxygen in sec. i, (gm/l*min)*l]

$$\left(\frac{V_d(1-\varepsilon_{gd})}{N-M}\right) \times \frac{dCo_i}{dt} = QCo_{i-1} - QCo_i + (k_La)_d(Co_i^* - Co_i) \times \left(\frac{V_d(1-\varepsilon_{gd})}{N-M}\right) + R_{Coi} \times \left(\frac{V_d(1-\varepsilon_{gd})}{N-M}\right)$$

$$\Rightarrow \frac{dCo_i}{dt} = \frac{Q}{\left(\frac{V_d(1-\varepsilon_{gd})}{N-M}\right)}(Co_{i-1} - Co_i) + (k_La)_d(Co_i^* - Co_i) + R_{Coi}$$

$$\Rightarrow \frac{dCo_i}{dt} = A_d(Co_{i-1} - Co_i) + (k_La)_d(Co_i^* - Co_i) + R_{Coi} \qquad (4.8)$$

4.4.5 KINETIC EQUATIONS

It was found that a high degree of dependence of biomass growth on carbon source (glucose) do exists Ghose et al. [18]. The dependence of specific growth rate on carbon was assumed to follow the Logistic equation or Contois kinetic model, which considers biomass inhibition and substrate limitation, respectively. The material balances of the biomass, product (gluconic acid) and substrates (glucose and DO) for stages, $i = 1, 2, \ldots, M-1, M, M+1, \ldots, N$ can be written in the following form.

The biomass growth should be directly proportional to X,

$$\text{Biomass growth rate,} \qquad \frac{dX_i}{dt} = rx_i = \mu_i X_i \qquad (4.9)$$

The specific growth rate μ_i is defined by Logistic equation as

$$\mu_i = \mu_m \left(1 - \frac{X_i}{X_m}\right) \qquad (4.10a)$$

and by Contois model as

$$\mu_i = \mu_m \frac{S_i}{(kos\, X_i + S_i)} \frac{Co_i}{(koc\, X_i + Co_i)} \qquad (4.10b)$$

Luedeking - Piret et al. [32] had developed a kinetic equation, which combines growth- and non growth-associated contributions towards product formation for the fermentation of lactic acid. This unstructured model is also used in our work for simulation. The product formation depends upon both, the growth rate dX_i/dt and instantaneous biomass concentration X_i in a linear way, given by

49

Rate of product formation, $\dfrac{dP_i}{dt} = \alpha \dfrac{dX_i}{dt} + \beta X_i$ (4.11)

where, α and β are the Luedeking - Piret equation [32] parameters for growth- and non growth-associated product formation, respectively.

D-glucose is used as a substrate to form cell material and metabolic products as well as for the maintenance of cells. Therefore, substrate consumption can be described by the following equation

Rate of substrate uptake, $\dfrac{dS_i}{dt} = -\left(\dfrac{1}{Y_{X/S}} \dfrac{dX_i}{dt} + \dfrac{1}{Y_{P/S}} \dfrac{dP_i}{dt} \right) - ms\, X_i$ (4.12)

where, $Y_{X/S}$ and $Y_{P/S}$ are the yield coefficients for biomass and product, respectively, and ms is the specific maintenance coefficient.

Substituting equation (4.11) into equation (4.12) yields

$$\dfrac{dS_i}{dt} = -\left(\dfrac{1}{Y_{X/S}} \dfrac{dX_i}{dt} + \dfrac{1}{Y_{P/S}} \left\{ \alpha \dfrac{dX_i}{dt} + \beta X_i \right\} \right) - ms\, X_i$$

$$= -\left(\dfrac{1}{Y_{X/S}} + \dfrac{\alpha}{Y_{P/S}} \right) \dfrac{dX_i}{dt} - \left(\dfrac{\beta}{Y_{P/S}} + ms \right) X_i$$

$$\Rightarrow \dfrac{dS_i}{dt} = -\gamma \dfrac{dX_i}{dt} - \lambda X_i$$ (4.13)

where, γ and λ are the parameters for growth- and non growth-associated substrate consumption, respectively.

The oxygen uptake rate can be described by the sum of oxygen uptake for cell growth, product formation and cell maintenance as per equation

Rate of oxygen uptake, $\dfrac{dCo_i}{dt} = k_L a\, (Co_i^* - Co_i) - ro_i$ (4.14)

Where, $ro_i = \dfrac{1}{Y_{X/O}} \dfrac{dX_i}{dt} + \dfrac{1}{Y_{P/O}} \dfrac{dP_i}{dt} + mo\, X_i$

Substituting value of (ro_i) from equation (4.15) and dP_i/dt from equation (4.11) into equation (4.14) gives
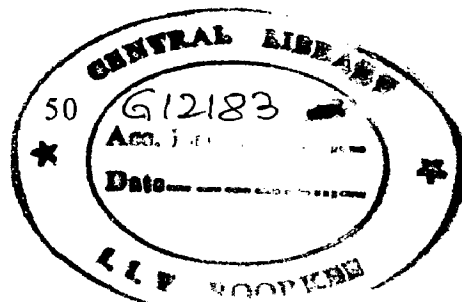
$$\frac{dCo_i}{dt} = k_L a (Co_i^{\bullet} - Co_i) - \left\{ \frac{1}{Y_{X/O}} \frac{dX_i}{dt} + \frac{1}{Y_{P/O}} \left(\alpha \frac{dX_i}{dt} + \beta X_i \right) + moX_i \right\}$$

$$= k_L a (Co_i^{\bullet} - Co_i) - \left(\frac{1}{Y_{X/O}} + \frac{\alpha}{Y_{P/O}} \right) \frac{dX_i}{dt} - \left(\frac{\beta}{Y_{P/O}} + mo \right) X_i$$

$$\Rightarrow \frac{dCo_i}{dt} = k_L a (Co_i^{\bullet} - Co_i) - \eta \frac{dX_i}{dt} - \psi X_i \qquad (4.15)$$

where. η and ψ are the parameters for growth- and non growth-associated oxygen uptake, respectively.

4.5 HYDRODYNAMIC AND MASS TRANSFER CORRELATIONS

Airlift reactor is a reactor in which the fluid dynamics is different in each of the part of the reactor. Mass transfer characteristics and correlations discussed in Chisti et al. [12.13] is also used in our work.

The superficial gas velocity in riser is given by

$$U_{gr} = Q_g / A_r \qquad (4.16)$$

For the axial dispersion coefficient of the liquid-phase (D_{ax}). Towell and Ackerman. given the following equation as cited in [61].

$$D_{ax} = 2.61 (D_r)^{1.5} (U_{gr})^{0.5} \qquad (4.17)$$

The gas hold-up in the riser and the down comer are related to the overall hold up by the analytical relations,

$$\varepsilon_g = \frac{A_r \varepsilon_{gr} + A_j \varepsilon_{gd}}{A_r + A_d} \qquad (4.18)$$

Empirical equation for determining the overall gas hold up can be obtained by

$$\varepsilon_g = 4.334 \times 10^{-3} * \left(\frac{P_G}{V_L} \right)^{0.49} \qquad (4.19)$$

51

Another way to determine overall gas hold up is the experimental method, which is used in our

work.
$$\varepsilon_g = \left(\frac{h_G - h_L}{h_G} \right)$$
(4.20)

The equation necessary for calculation of ε_{gr} or ε_{gd} is given by,

$$\varepsilon_{gd} = 0.89\, \varepsilon_{gr}$$
(4.21)

The liquid velocities in the airlift bioreactor were calculated using the well-known and widely tested model developed by Chisti et al. [13] for airlift devices,

$$U_{Lr} = \left[\frac{2g h_D (\varepsilon_{gr} - \varepsilon_{gd})}{K_B (A_r/A_d)^2 (1/(1-\varepsilon_{gd})^2)} \right]^{0.5}$$
(4.22)

$$\text{where, } K_B = 11.40 * \left(\frac{A_d}{A_b} \right)^{0.79} \text{ and } h_D = \frac{h_L}{(1-\varepsilon_g)}$$
(4.23)

h_D = Height of dispersion

h_L = Height of gas-free liquid

ε_g = overall gas hold up

K_B = Form friction loss coefficient for the bottom section

The overall oxygen transfer coefficient was calculated by the following equation [61],

$$k_L a = 1.27 \times 10^{-4} * \left(\frac{P_G}{V_L} \right)^{0.925} ; \text{ Where } \left(\frac{P_G}{V_L} \right) = \frac{\rho_L g U_{gr}}{(1 + (A_d/A_r))}$$
(4.24)

$(K_L a)_r$ and $(K_L a)_d$ values were selected in such a way that the following two equations were satisfied:

$$k_L a = \frac{(k_L a)_r A_r + (k_L a)_d A_d}{A_r + A_d}$$
(4.25)

$(K_L a)_d - \Psi (K_L a)_r$; The value of Ψ was fixed at 0.8 as recommended by Chisti et al. [13].

The superficial liquid velocity U_{Lr} could be converted to the linear liquid velocity in the riser (Vlr) and the down comer (Vld),

$$V_{lr} = \frac{U_{Lr}}{1 - \varepsilon_{gr}} \quad \text{and} \quad V_{lr}\left(1 - \varepsilon_{gr}\right)A_r = V_{ld}\left(1 - \varepsilon_{gd}\right)A_d \tag{4.26}$$

4.6 BOUNDARY CONDITIONS

Both models are initial value boundary value problems, thus initial values of parameters are necessary for the solution. At time $t = 0$, the initial conditions are

$$X = X_0, \ P = P_0, \ S = S_0, \ Co = Co_0 \tag{4.27}$$

4.7 CONSTITUTIVE RELATIONSHIPS

Equations (4.1) to (4.8) are material balance equations in the different sections of the airlift bioreactors. Equations (4.9), (4.10a), (4.10b), (4.11), (4.13) and (4.15) are equations representing microbial kinetic behavior in each of the stage in the reactor. Equations (4.16) to (4.26) are equations correlating hydrodynamics and mass transfer in the airlift bioreactor.

The difference between the tanks-in-series model and axial dispersion model is that the former utilizes two parameters, the number of tanks in series N and the back flow b, while later contains only one parameter, the axial dispersion coefficient D_{ax}, which characterizes the deviations from ideal flow. The relationship between these two models, can be represented by, as cited in [61]

$$\text{Peclet number, } P_e = N / [b + 0.5] \tag{4.28}$$

$$\text{Where, } P_e = (V_{lr} H_D) / D_{ax} \tag{4.29}$$

$$V_{lr} = \text{linear liquid velocity, m/s}$$

$$H_D = \text{height of dispersion, m}$$

$$\text{If back flow is absent, as in down comer, } N = P_e / 2 \tag{4.30}$$

4.8 INTEGRATED FORM OF KINETIC MODEL

Integrated form of the basic kinetic equations is used to determine the kinetic parameters by non-linear regression using test version of GraphPad V4.03. In the present work, kinetic parameters of logistic equation are determined. Kinetic parameters for Contois model is taken from literature [61] and adjusted for the study of product formation of gluconic acid from glucose under submerged fermentation in airlift bioreactor.

4.8.1 LOGISTIC EQUATION

Logistic equation is given by $\dfrac{dX}{dt} = \mu \, X = \mu_m \left(1 - \dfrac{X}{X_m} \right) X$

Where X_M is the maximum biomass concentration, X is the biomass concentration at any time t. Reasons for selecting above kinetic model are,

(1) It is approved to represents many fermentation processes, e.g. gluconic acid, lactic acid [7,13,40,49].

(2) Easy to obtain kinetic parameters using non-linear regression, which efficiently represent biomass, substrate and product formation.

(3) Prediction to study the effect of changes in X_0, μ_m and S_0 was done reasonably well.

Limitations:

(i) In above equation, the upper limit ($X=X_m$) of biomass concentration represents the lack of a limiting substrate (which is not included in the expression).

(ii) Logistic equation fails when there is sharp rise or decrease in the value of variable w.r.t. time [Pandey et al. (2003)].

(iii) Representation of DO in ALR is poor. The reason may be limitation (i) as above.

Integrating between the initial and final condition, with initial cell concentration X_0 (t = 0), is given by

$$\int_{X_0}^{X} \frac{1}{X(1-(X/X_m))} dX = \mu_m \int_0^t dt$$

Integrating and rearranging the above equation, we get

$$\Rightarrow \int_{X_0}^{X} \left[\frac{1}{X} + \frac{1}{X_m - X} \right] dX = \int_0^t \mu_m \, dt$$

$$\Rightarrow \ln \left[\frac{(X / X_0)}{(X_m - X)/(X_m - X_0)} \right] = \mu_m \, t$$

$$\Rightarrow X = \frac{X_0 X_m e^{\mu_M t}}{\left(X_m - X_0 + X_0 e^{\mu_M t} \right)} \quad OR \quad \frac{X_0 e^{\mu_M t}}{\{1 - (X / X_m) * (1 - e^{\mu_M t})\}} \tag{2.31}$$

Further, Contois model was suggested to present the production behavior for airlift bioreactor [61]. The representation of DO profile in ALR was efficient in the study carried out by Znad et al [61]. In the present work, comparison of these two models is carried out to get better result.

The complete model consists of model equations from (4.1) to (4.26), initial conditions by (4.27) and constitutive relationships from (4.28) to (4.30). A set of model equations is given in section 5.2 of Chapter 5.

MATHEMATICAL MODEL SOLUTION

In this chapter solution technique and its suitability has been discussed. Integrated forms of equations are given which are used to determine kinetic parameters. Parameters including kinetic. design and hydrodynamic are tabulated. Details of ODE solver of MATLAB V6.5 are discussed and were used to predict model behavior. The complete computer program is given in Appendix B.

5.1 DETERMINATION OF KINETIC PARAMETERS

In the present work, two kinetic models namely logistic and contois were tested. Kinetic parameters of logistic equation were determined by fitting the experimental data using non-linear regression (NLR), whereas parameters of contois model were taken from the literature [61].

There are eight kinetic parameters including maximum specific growth rate (μ_m) in four component balance equations in logistic equation. Other parameters are X_0, α, β, γ, λ, η and ψ. The maximum biomass concentration (X_m) was obtained from the experiment was used as input parameter [23]. These kinetic parameters are determined by non-linear regression (NLR) analysis of the experimental data. Integrated forms of the equations (4.9), (4.11), (4.13) and (4.15) were used.

5.1.1 PARAMETERS FOR CELL GROWTH: μ_m at X_0

Integrated form of equation (4.9), which is given by

$$x = x_0\, x_m\, e^{\mu_m t} / (x_m - x_0 + x_0 e^{\mu_m t}) \qquad (5.1)$$

is used for determination of μ_m and X_0 using X_m = 4.502 g/l as an input parameter.

$\Rightarrow \mu_m$ = 0.1335 h^{-1} and X_0 = 0.3080

5.1.2 PARAMETERS FOR PRODUCT FORMATION: α and β

Integrated form of equation (4.11), which can be given as

$$P = P_0 + \alpha \left\{ (x_0 \, x_m \, e^{\mu_m t} / (x_m - x_0 + x_0 e^{\mu_m t})) - x_0 \right\} +$$

$$(\beta \, x_m / \mu_m) * \ln \left\{ 1 - (x_0 / x_m)(1 - e^{\mu_m t}) \right\}$$

$$P = P_0 + \alpha \left\{ x - x_0 \right\} + (\beta \, x_m / \mu_m) * L, \text{ where } L = \ln \left\{ 1 - (x_0 / x_m)(1 - e^{\mu_m t}) \right\} \tag{5.2}$$

Initial conditions are $P_0 = 0.0$ g/l, $X_m = 4.502$ g/l,

$\Rightarrow \alpha = 18.028$ [-] and $\beta = 0.751$ h^{-1}

5.1.3 PARAMETERS FOR SUBSTRATE UTILIZATION: γ and λ

Integrated form of equation (4.13), which can be given as

$$S = S_0 - \gamma \left\{ (x_0 \, x_m \, e^{\mu_m t} / (x_m - x_0 + x_0 e^{\mu_m t})) - x_0 \right\} + (\lambda \, x_m / \mu_m) * \ln \left\{ 1 - (x_0 / x_m)(1 - e^{\mu_m t}) \right\}$$

$$S = S_0 + \gamma \left\{ x - x_0 \right\} + (\lambda \, x_m / \mu_m) * L \tag{5.3}$$

Initial conditions are $S_0 = 200.0$ g/l, $X_m = 4.502$ g/l,

$\Rightarrow \gamma = 13.144$ [-] and $\lambda = 0.604$ h^{-1}

5.1.4 PARAMETERS FOR OXYGEN UTILIZATION: η and ψ

Integrated form of equation (4.15), which can be given as

$$Co = Co^* - \left(\begin{array}{l} \eta \left\{ (x_0 x_m e^{\mu_m t} / (x_m - x_0 + x_0 e^{\mu_m t})) - x_0 \right\} + \\ (\psi \, x_m / \mu_m) * \ln \left\{ 1 - (x_0 / x_m) * (1 - e^{\mu_m t}) \right\} \end{array} \right) / (1 + k_L a t)$$

$$Co = Co^* - (\eta \left\{ x - x_0 \right\} + (\psi \, x_m / \mu_m) * L) / (1 + k_L a t) \tag{5.4}$$

Initial conditions are $Co^* = 0.00651$ g/l, $X_m = 4.502$ g/l and $k_L a = 94.7312$ h^{-1}

$\Rightarrow \eta = 0.58$ [-] and $\psi = 0.103$ h^{-1}

The results of regression analysis is tabulated in table 5.1

5.1.5   ESTIMATION OF $Y_{X/S}$, $Y_{P/S}$ and m_s

Yield coefficients are found from the experimental values. $Y_{X/S}$ is defined as the ration of cell mass produced per mass of limiting substrate utilized, where as $Y_{P/S}$ is defined as the mass of gluconic acid produced per mass of limiting substrate utilized. Thus calculated values of $Y_{X/S}$, $Y_{P/S}$ and m_s are 0.0225 g/g, 0.8778 g/g and 0.2515 g/g.h^{-1}, respectively.

5.2   MODEL EQUATIONS AND PARAMETERS

For the solution of the model, model equations incorporating parameters of different sections of airlift reactor are summarized in this section. These equations are solved in ODE Solver of MATLAB V6.5

5.2.1   MODEL EQUATIONS FOR SOLUTION

Bottom section: [i=1]

$$\frac{dX_1}{dt} = A_1 X_N - B_1 X_1 + D_1 X_2 + \mu_m (1 - X_1 / X_m) X_1$$

$$\frac{dP_1}{dt} = A_1 P_N - B_1 P_1 + D_1 P_2 + \alpha \frac{dX_1}{dt} + \beta X_1$$

$$\frac{dS_1}{dt} = A_1 S_N - B_1 S_1 + D_1 S_2 - \gamma \frac{dX_1}{dt} - \lambda X_1$$

$$\frac{dCo_1}{dt} = A_1 Co_N - B_1 Co_1 + D_1 Co_2 + (k_L a)_r (Co_1^* - Co_1) - \eta \frac{dX_1}{dt} - \psi X_1$$

Riser section: [i = 2, ..., M-1]

$$\frac{dXi}{dt} = A_2 (X_{i-1} - X_i) + B_2 (X_{i+1} - X_i) + \mu_m (1 - X_i / X_m) X_i$$

$$\frac{dP_i}{dt} = A_2 (P_{i-1} - P_i) + B_2 (P_{i+1} - P_i) + \alpha \frac{dX_i}{dt} + \beta X_i$$

$$\frac{dS_i}{dt} = A_2 (S_{i-1} - S_i) + B_2 (S_{i+1} - S_i) - \gamma \frac{dX_i}{dt} - \lambda X_i$$

$$\frac{dCo_i}{dt} = A_2 (Co_{i-1} - Co_i) - B_2 (Co_{i+1} - Co_i) + (k_L a)_r (Co_i^* - Co_i) - \eta \frac{dXi}{dt} - \psi Xi$$

Top section [i=M]

$$\frac{dX_M}{dt} = A_3 (X_{M\text{-}1} - X_M) + \mu_m (1 - X_M / X_m) X_M$$

$$\frac{dP_M}{dt} = A_3 (P_{M\text{-}1} - P_M) + \alpha \frac{dX_M}{dt} + \beta X_M$$

$$\frac{dS_M}{dt} = A_3 (S_{M\text{-}1} - S_M) - \gamma \frac{dX_M}{dt} - \lambda X_M$$

$$\frac{dCo_M}{dt} = A_3 (Co_{M\text{-}1} - Co_M) + (k_L a)_r (Co_M^* - Co_M) - \eta \frac{dX_i}{dt} - \psi X_i$$

Down comer section: [i = M+1, ..., N]

$$\frac{dX_i}{dt} = A_4 (X_{i\text{-}1} - X_i) + \mu_m (1 - X_i / X_m) X_i$$

$$\frac{dPi}{dt} = A_4 (P_{i\text{-}1} - P_i) + \alpha \frac{dX_i}{dt} + \beta X_i$$

$$\frac{dS_i}{dt} = A_4 (S_{i\text{-}1} - S_i) - \gamma \frac{dX_i}{dt} - \lambda X_i$$

$$\frac{dCo_i}{dt} = A_4 (Co_{i\text{-}1} - Co_i) + (k_L a)_d (Co_i^* - Co_i) - \eta \frac{dX_i}{dt} - \psi X_i$$

Where, hydrodynamic constants are defined as

$$A_1 = Q/V_b (1 - \varepsilon_{gr}), \quad B_1 = (1 + b)Q/V_b (1 - \varepsilon_{gr}), \quad D_1 = bQ/V_b (1 - \varepsilon_{gr}),$$
$$A_2 = (1 + b)Q/\{V_r (1 - \varepsilon_{gr})/(M - 2)\}, \quad B_2 = bQ/\{V_r (1 - \varepsilon_{gr})/(M - 2)\},$$
$$A_3 = (1 + b)Q/V_t (1 - \varepsilon_{gr}) \text{ and}$$
$$A_4 = Q/\{V_d (1 - \varepsilon_{gd})/(N\text{-}M)\}$$

5.2.2   KINETIC PARAMETERS

The kinetic parameters of logistic equation were determined by non-linear regression analysis using integrated forms as given by equations (5.1) to (5.4) using GraphPad V4.03 software. The determined parameters are given in the following table 5.1. For the determination of maximum specific growth rate, experimental value of maximum cell mass concentration was used.

Table: 5.1 Kinetic parameters of logistic equation at X_m = 4.502

Sr. No.	Parameter	Unit	Values	Regression coefficient (R^2)	Absolute sum of squares (ASS)
1.	μ_m	h^{-1}	0.1335	0.9940	0.2521
2.	X_0	g/l	0.3080		
3.	α	-	18.028	0.9967	199.2
4.	β	h^{-1}	0.751		
5.	γ	-	13.144	0.9912	333.9
6.	λ	h^{-1}	0.604		
7.	η	-	0.58	0.9339	2.3e-06
8.	ψ	h^{-1}	0.103		

Table: 5.2 Kinetic parameters of contois model [61].

Sr.No.	Parameter	Unit	Values
1.	μ_m	h^{-1}	0.3610
2.	kos	-	21.239
3.	koc	-	0.004134
4.	α	-	4.5865
5.	β	h^{-1}	1.3757
6.	γ	-	3.9868
7.	λ	h^{-1}	0.9660
8.	η	-	1.52
9.	ψ	h^{-1}	0.0808

5.2.3   ESTIMATED DESIGN AND HYDRODYNAMIC PARAMETERS

Following parameters have been estimated from the hydrodynamic and mass transfer correlations for the present size of airlift bioreactor and used in the simulation.

Table: 5.3 Estimated design and hydrodynamic parameters of a 4.5 l ALBR.

Sr.No	Description	Unit	Reactor - 1
1.	Working volume (V)	L	4.5
2.	k_La	h^{-1}	106.4915
3.	Pg/V	W/m^3	362.3637
4.	ε_g	-	0.0770
5.	Q_g	m^3/s	1.3000e-004
6.	Q	m^3/s	3.6003e-004
7.	Ugr	m/s	0.1014
8.	Ulr	m/s	0.2590
9.	HD	m	1.1159
10.	Pe	-	44.0308
11.	N	-	44
12.	M	-	22

5.3 SOLUTION SCHEME ADAPTED

In order to predict the performance of the model, solution of model equations is very essential. The developed mathematical model in Chapter 4 as given in Section 5.2 consists of a set of first order ordinary coupled differential equations. These equations constitute initial value problem (IVP), which can be solved using ODE solvers of MATLAB (version 6.5).

5.3.1 MATLAB ODE SOLVER

In MATLAB V6.5, this class of problem is solved using 'ODE '(Ordinary Differential Equations) solvers. Here to solve our equations 'ode23s' is used.

Brief description of 'ode23s' solver:

ODE23S solve stiff differential equations, low order method.

61

[T. Y] = ODE23S (ODEFUN, TSPAN, Y0) with TSPAN = [T0 TFINAL] integrates the system of differential equations y' = f(t,y) from time T0 to TFINAL with initial conditions Y0. Function ODEFUN (T, Y) must return a column vector corresponding to f(t, y). Each row in the solution array Y corresponds to a time returned in the column vector T. To obtain solutions at specific times T0. T1,...,TFINAL (all increasing or all decreasing). use TSPAN = [T0 T1 ... TFINAL].

[T. Y] = ODE15S (ODEFUN, TSPAN, Y0, OPTIONS) solves as above with default integration properties replaced by values in OPTIONS.

ODE functions of our problem:

tspan=[0 51];

% Initial conditions for Logistic equation

x101 = [0.3080*ones(1,N)];

p10 = zeros(1,N);

s10 = [200*ones(1,N)];

c10 = [0.0065*ones(1,N)];

z101 = [x101 p10 s10 c10];

% Initial conditions for Contois model

x201 = [0.04*ones(1,N)];

p20 = zeros(1,N);

s20 = [200*ones(1,N)];

c20 = [0.0065*ones(1,N)];

z201 = [x201 p20 s20 c20];

% ODE functions

[t11, z11] = ode23s('odealrlogisticli', tspan, z101);

[t21, z21] = ode23s('odecontoisli', tspan, z201);

Theoretical investigation to develop a mathematical model for the production of gluconic acid from glucose in an airlift bioreactor was undertaken. The mathematical model uses logistic equation and contois model to represent concentrations of biomass, gluconic acid, glucose and dissolved oxygen in the reactor. The airlift bioreactor is divided into four sections, namely bottom, riser, top and down comer sections. All these sections were modeled by considering these as tank in series model consisting of 44 stages. The model uses four coupled ordinary differential equations to represent concentration of four variables, namely biomass, product, substrate and DO in each hypothetical stage of the reactor. The complete set of model equations are given in section 5.2.1 of Chapter 5. The set of kinetic and hydrodynamic parameters are given in Table 5.1, 5.2 and 5.3 respectively in Chapter 5. The reaction mechanism is provided in section 1.1 of Chapter 1.

The model has been validated with the experimental data of Znad et al. [61]. In the present Chapter the validated model was then used to predict the variation of output parameters with input parameters. Variation of initial cell mass concentration (X_0) and overall gas hold-up (ε) as shown in Table 6.1 was used to predict the fermentation behavior in an airlift bioreactor.

Table 6.1 Parameters and its selected variation range for model predictions.

Sr. No.	Parameter	Range of Parameter	Model Used
1.	Initial biomass concentration	0.308 ± 0.2032 g/l (~ 66 % variation from mean value)	Logistic equation
2.	Gas hold-up	0.077 ± 0.02 (26 % variation from mean value)	Contois model

6.1 ANALYSIS OF EXPERIMENTAL DATA

The experimental data for concentrations of biomass, product, substrate and dissolved oxygen as given in Appendix A has been taken from Znad et al. [61]. The operating conditions have been mentioned in Tables 2.3 and 6.2. The above mentioned parameters have been plotted as a function of time in a batch operation period of 51 h. The profiles are shown in figures 6.1 through 6.4, respectively to develop in-depth understanding of the process.

6.1.1 VARIATION OF BIOMASS CONCENTRATION WITH TIME

Figure 6.1 shows the variation of biomass concentration (X) with batch time available for the growth of microorganisms in the gluconic acid fermentation by *A. niger* at the constant operating conditions (30 °C temperature and 6.0 pH). From the plot, following facts are observed:

❑ After *seeding* a liquid medium with an *inoculum* of living cells into the reactor, only air is added to the culture for its growth. Four different phases of the growth cycle are observed. These are (i) lag phase, (ii) exponential phase, (iii) deceleration phase and (iv) stationary phase.

❑ The first phase is lag-phase, which varies up to 4 h period. In this phase practically there is no apparent growth of biomass. In this phase a metabolic turnover takes place, which indicate that the cells are in process of adapting to the environmental conditions and that new growth will eventually begin.

❑ In the exponential phase, which varies from 4 to 25 h period, microbial cell growth proceeds at the maximum possible rate. During this period, nutrients are in excess and growth inhibitors are absent. This provides an ideal environmental condition for the growth micro-organisms. The strain started to form gluconic acid and therefore cell growth and gluconic acid production took place simultaneously. However, in batch fermentations exponential growth is of limited duration and as nutrient conditions change, growth rate decreases.

64
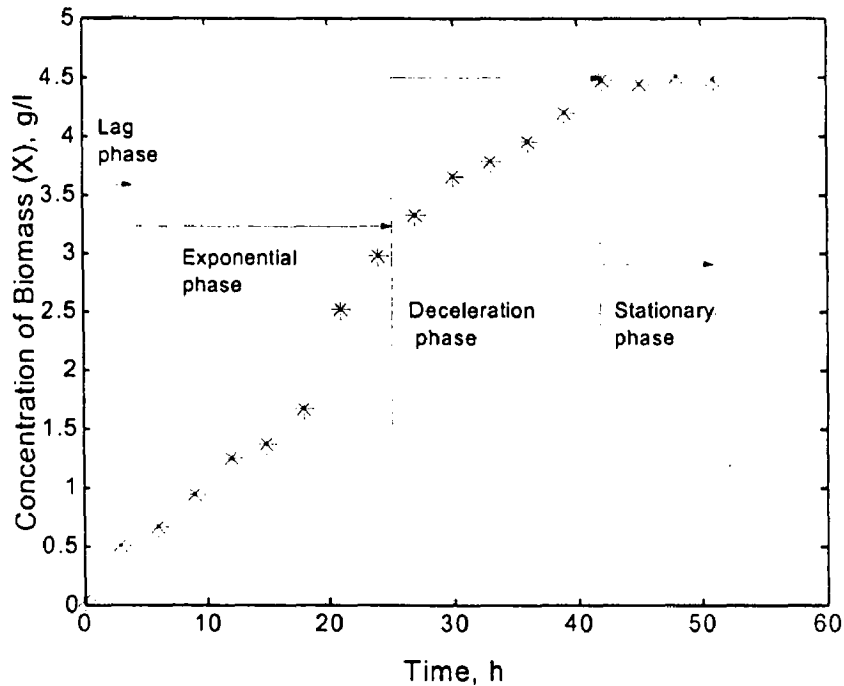
Figure: 6.1 Concentration of biomass as a function of time.

- ☐ The third phase is deceleration phase, which ranges from 25 to 42 h. Limited nutrients and changing environmental conditions in the system leads to decelerate the growth of cells entering into the deceleration phase, which ranges from 25 to 42 h.

- ☐ In the fourth stationary phase, which varies from 42 to 51 h period the cell mass growth becomes stable and in this time the cell production and cell death rate becomes equal. Once the limiting substrate become scarce, the overall growth can no longer be obtained because of nutrient exhaustion resulting into the death phase.

- ☐ For the determination of maximum specific growth rate (μ_m) and initial biomass concentration (X_0), the experimental value of maximum cell mass (Xm) was taken as 4.502 g/l from the stationary phase.

- ☐ The final phase of the cycle is the death phase when growth rate has ceased. The death phase was not conducted for the batch and thus it is not considered in the present work.

6.1.2 VARIATION OF GLUCONIC ACID CONCENTRATION WITH TIME

Figure 6.2 is plotted to show the variation of gluconic acid concentration with batch time at constant operating conditions as mentioned in Table 2.3. From this figure, following facts are evident:

❑ Once the cells start growing, the micro-organisms start to hydrolyze gluconolactone to form gluconic acid and hence concentration of GA increases linearly with batch time.
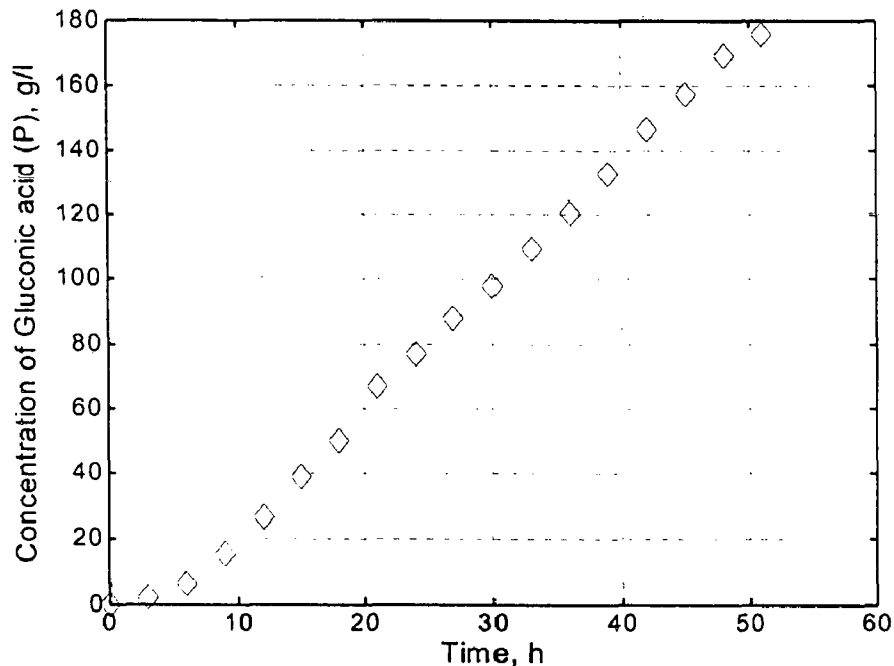
Figure: 6.2 Concentration of gluconic acid as a function of time.

❑ The hydrogen peroxide produced during the process is decomposed to provide oxygen, which is again utilized during the reaction. As shown in the figure, initially the gluconic acid formation is very less up to a period of bout 4 to 5 h period, but as soon as the cells grow, the product is formed at a constant rate after 10 h indicated by the constant slop of the plot. The GA formation continues till the biomass is present. The enzymes that are present in the A.niger catalyze this process. The biological process is affected by the adverse conditions such as exhaustion of nutrients, inhibition effect or extreme operating conditions.

66

❏   This process continues until the cells produce the product catalyzed by enzymes present or is influenced by the adverse conditions such as exhaustion of nutrients, inhibition effect or extreme operating conditions.

6.1.3   VARIATION OF GLUCOSE CONCENTRATION WITH TIME

Figure 6.3 is plotted to show the variation of glucose concentration with time. From the figure, following facts are evident:

❏   Growth of microorganisms starts as soon as they adapted themselves to the environmental conditions. They initially in the lag phase utilize the glucose slowly, which increase rapidly in the exponential phase as can be seen from the figure 6.3.

❏   The rate of glucose consumption is less in the first 10 hr. However, the consumption rate is maintained after 10 h. This may be attributed to the constant rate of GA production as can be seen from the figure 6.2.
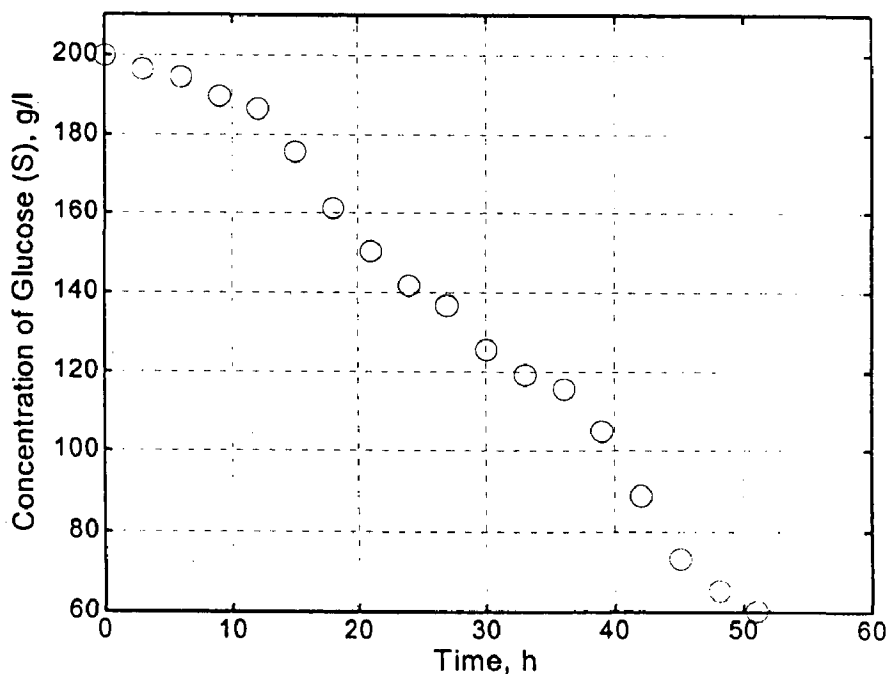

Figure: 6.3 Concentration of glucose as a function of time.

❏   Glucose consumption result in the formation of biomass and subsequently to the formation of GA. In the stationary phase, the rate of concentration consumption fall beyond 42 h and

67

90 g/l of glucose as can be seen from the figure 6.3. After the stationary phase, the biological process enters in to death phase in which rate of cell death is higher than rate of new cell formation resulted in quick fall in GA formation.

6.1.4   VARIATION OF DISSOLVED OXYGEN CONCENTRATION WITH TIME

Figure 6.4 is plotted to show the variation of dissolved oxygen concentration with time. From the figure, following facts are evident.

□   Saturated DO concentration at air supply rate of 7.8 lpm and gas hold-up is 0.00651 g/l in an ALBR. This value rapidly reduces to 0.0028 g/l in the first 15 h duration of batch time. During this period, the oxygen requirement is maximum because GA formation starts according to the reaction (1.1) of Chapter 1, which can be seen from figure 6.2. The oxygen requirement during this duration is accomplished by dissolved oxygen.
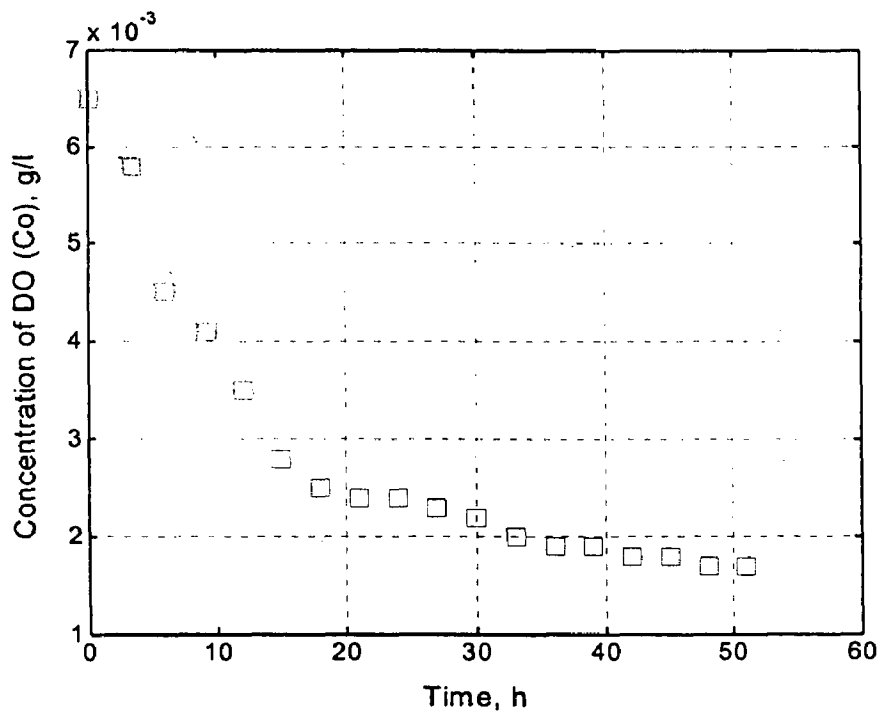

Figure: 6.4 Concentration of dissolved oxygen as a function of time.

□   Beyond 15 h of duration, the H_2O_2 decomposition become prominent and so then the concentration of DO fall slowly to 0.0018 at 42 h.

68

❏   In the stationary phase, the DO concentration is almost stationary between 0.0018 g/l to

0.0017. The consumption is balanced by air supply and H_2O_2 decomposition although the

GA is produced which consumes DO and glucose at constant rate as can be seen from

figures 6.2 and 6.3.

6.2   VALIDATION OF MODELS

The model has been validated by experimental data given in Appendix A. This

experimental data is obtained at the operating conditions given in Table 2.3 of Chapter 2.

Logistic equation and contois model were tested to represent the concentration profiles of

biomass, gluconic acid, substrate and dissolved oxygen with batch time as shown in figures 6.5

to 6.8. Model predictions are compared with experimental data for their relative deviations as

shown in figures 6.9 through 6.12.

6.2.1   EXPERIMENTAL AND PREDICTED BIOMASS CONCENTRATION

Figure 6.5 shows the comparison between model predictions and experimental data [61]

for biomass concentration in an ALBR. From the figure, following facts can be observed:

❏   Prediction of biomass concentration by logistic equation is very good except for the first 2

to 4 h of batch time. During this period predicted value is 0.308 g/l whereas the

experimental value is 0.04 g/l. This discrepancy has also been observed by [23] for

prediction of biomass concentration using the logistic model.

❏   The contois model under predicts the biomass concentration in part A of figure 6.5.

However, the prediction is good for in the batch period from 15 h to 42 h. Further, it over

predicts beyond 42 h indicated by B region of figure 6.5. This is in contrast to observations

made by Mayani et al. [62] during their study of gluconic acid production in stirred

bioreactor. This may be attributed to the fact that hydrodynamic behavior of stirred and

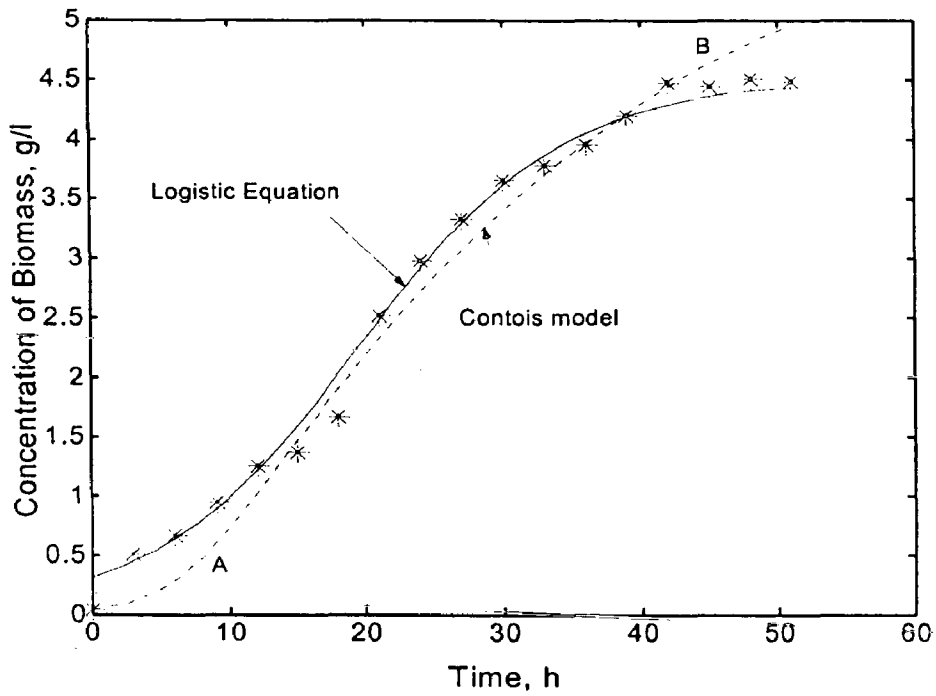airlift bioreactors are not similar.

69

Figure: 6.5 Cell biomass concentration profile represented by logistic equation and

contois model.
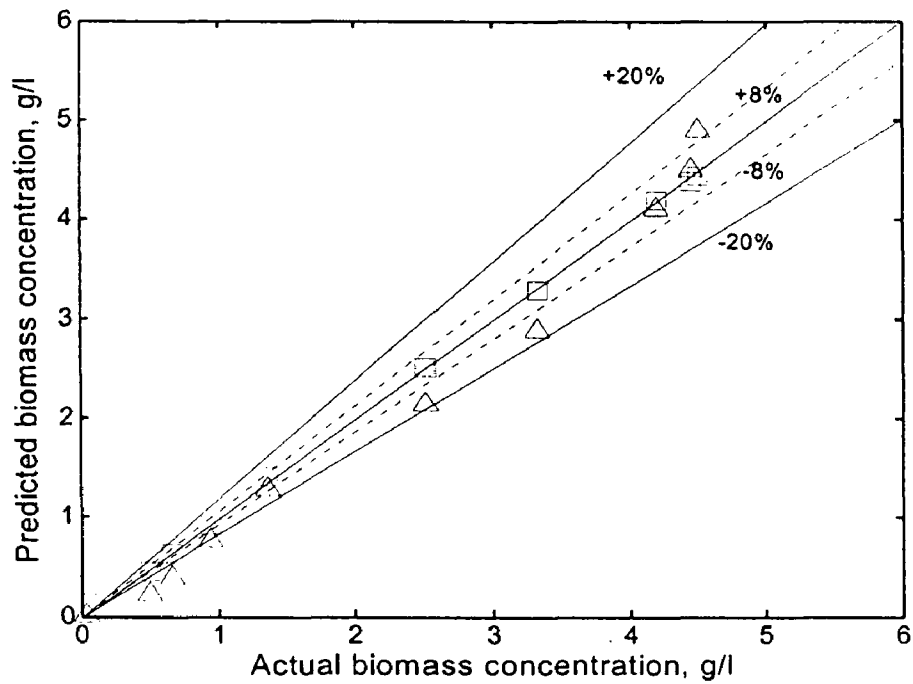
Figure: 6.6 Relative deviations of predicted values from experimental data for biomass

concentration.

70

◻   Thus, for the prediction of biomass concentration, the logistic equation is more preferable for the prediction of biomass in the ALBR.

◻   Figure 6.6 is drawn to show the error band, in which the model predicts the experimental values. From the figure it is clear that the logistic and contois model predicts time dependent biomass concentration with $\pm$ 8% and $\pm$ 20% errors respectively.

6.2.2   EXPERIMENTAL AND PREDICTED GLUCONIC ACID CONCENTRATION

Figure 6.7 shows the comparison of model predictions with experimental data [61] for gluconic acid concentration in an ALBR. From the figure, following facts can be observed:

◻   Logistic equation: The figures 6.7 & 6.8 show that the representation of gluconic acid concentration by logistic equation in an ALBR is very good through out the batch period.
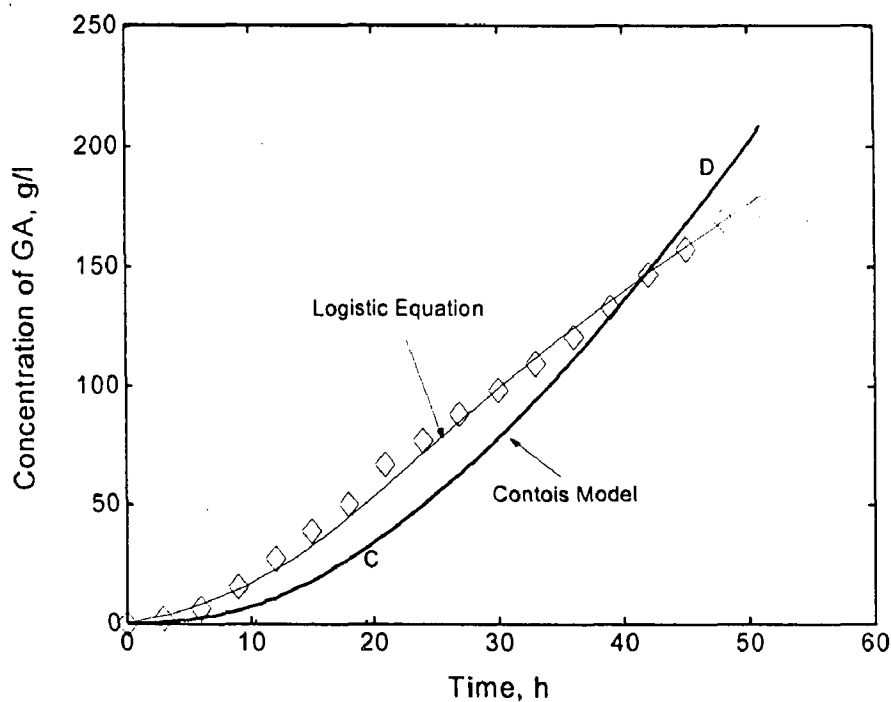
Figure: 6.7 Gluconic acid concentration profile represented by logistic equation and contois model.

◻   Contois model: The contois model is not in agreement with the experimental data in the exponential as well as in the stationary phase. The slow formation of GA according to this

model, as indicated by part C in the figure 6.7, is less from 4 h to 42 h of batch period. The model is also over predicting in the last phase as indicated by D in the figure 6.7.

❑ Thus, for the prediction of the gluconic acid concentration in an ALBR, the logistic equation is more accurate.

❑ Figure 6.8 is drawn to show the error band, in which the model predicts the experimental values. From the figure it is clear that the logistic and contois model predicts time dependent biomass concentration with ± 9% and ± 16% errors respectively.

Figure: 6.8 Relative deviations of predicted values from experimental data for the gluconic acid concentration.

6.2.3 EXPERIMENTAL AND PREDICTED GLUCOSE CONCENTRATION

Figure 6.9 shows the comparison between model predictions and experimental data [61] for gluconic acid concentration in an ALBR. From the figure, following facts can be observed:

❑ Logistic equation: The figures 6.9 & 6.10 show that the representation of glucose concentration in an ALBR can be accurately predicted by the logistic equation.

□ Contois model: The model over predicts the glucose concentration in the ALBR in the period from 4 h to 42 h as indicated by E part of the figure 6.9.
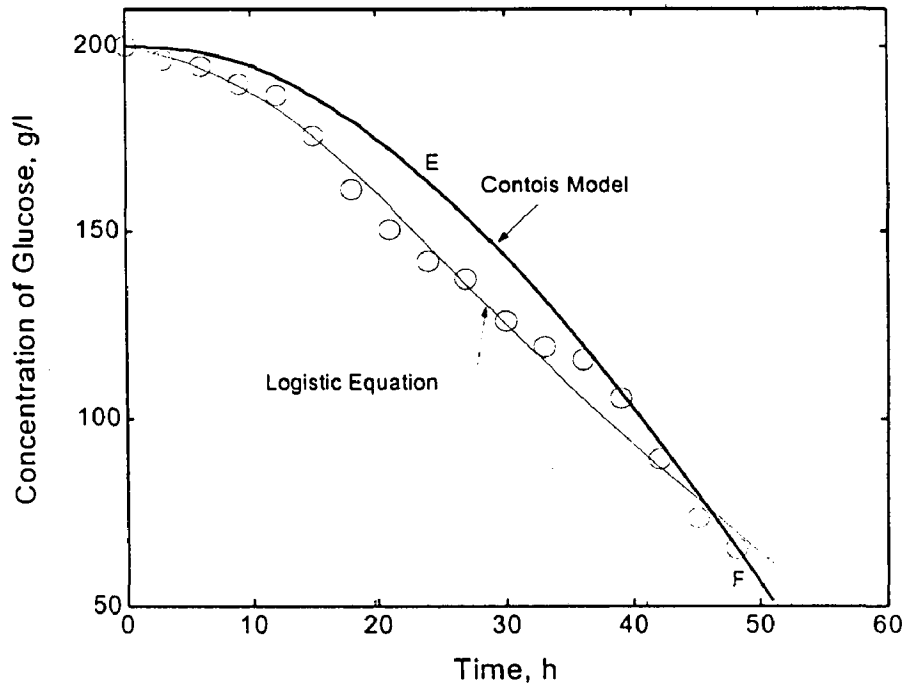
Figure: 6.9 Glucose concentration profile represented by logistic equation and contois model.
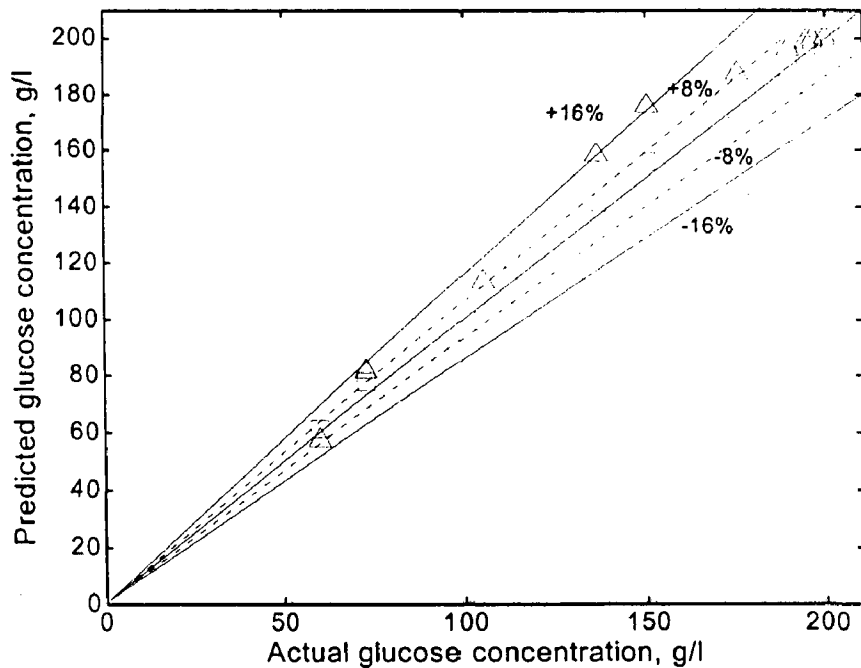
Figure: 6.10 Relative deviations of predicted values from experimental data for glucose concentration.

□ The prediction for the variations of glucose concentration is exactly opposite to that predicted for gluconic acid concentration. This may be due to the complex form as shown in the equation (2.12), in which glucose concentration is the dominating term. The effect of hydrodynamic constants in the model equations is also contributs to this behavior.

□ Thus, the prediction of glucose concentration in an ALBR is better by logistic equation when compared to that of contois model.

□ Figure 6.10 is drawn to show the error band, in which the model predicts the experimental values. From the figure it is clear that the logistic and contois model predicts time dependent biomass concentration with $\pm$ 8% and $\pm$ 16% errors respectively.
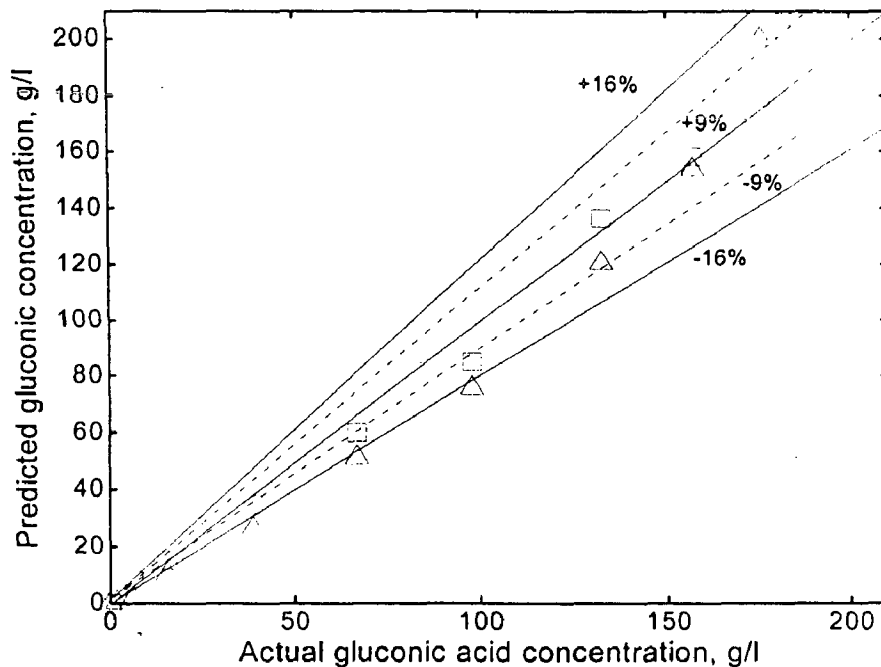
6.2.4 EXPERIMENTAL AND PREDICTED D.O. CONCENTRATION

Figure 6.11 shows the comparison of model predictions with experimental data [61] for dissolved oxygen concentration in an ALBR. From the figure, following facts can be observed:
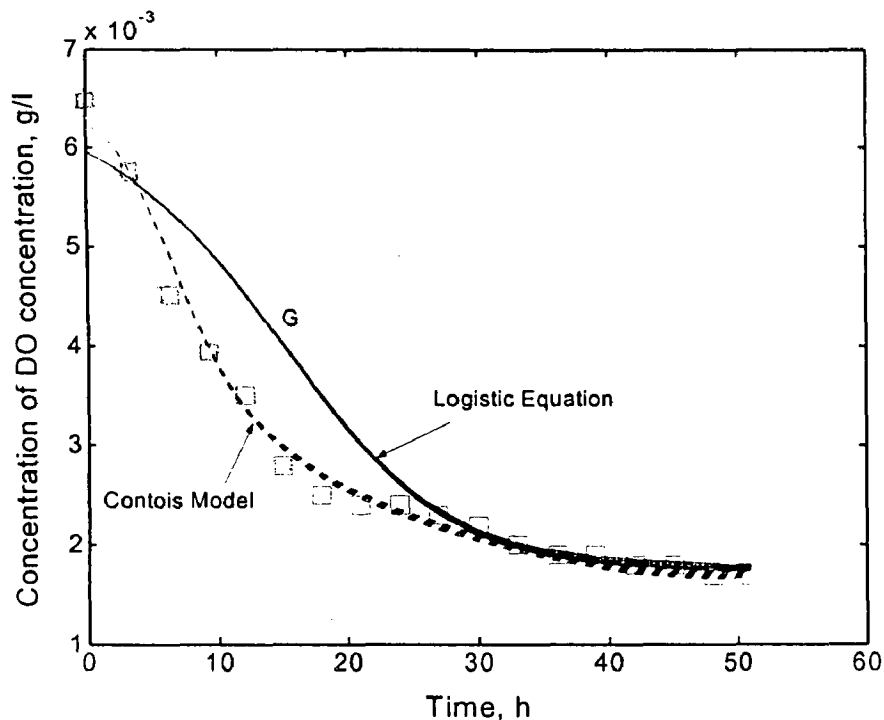
Figure: 6.11 Dissolved oxygen concentration profile represented by logistic equation and contois model.

□ Logistic equation: Figure 6.11 shows that logistic model fails to represent the DO concentration in the ALBR. The large deviation in predicted values from actual values are shown in the figure 6.11 indicated by G in the case of logistic equation. The reason for

such a behavior is that the model equation does not account for DO concentration. This equation is independent of dissolved oxygen concentration.

❑ Contois model: The prediction by contois model is very good since it accounts for the DO concentration through the entire range of batch time. This behavior indicates that the contois model is better for the study of DO concentration within the ALBR.
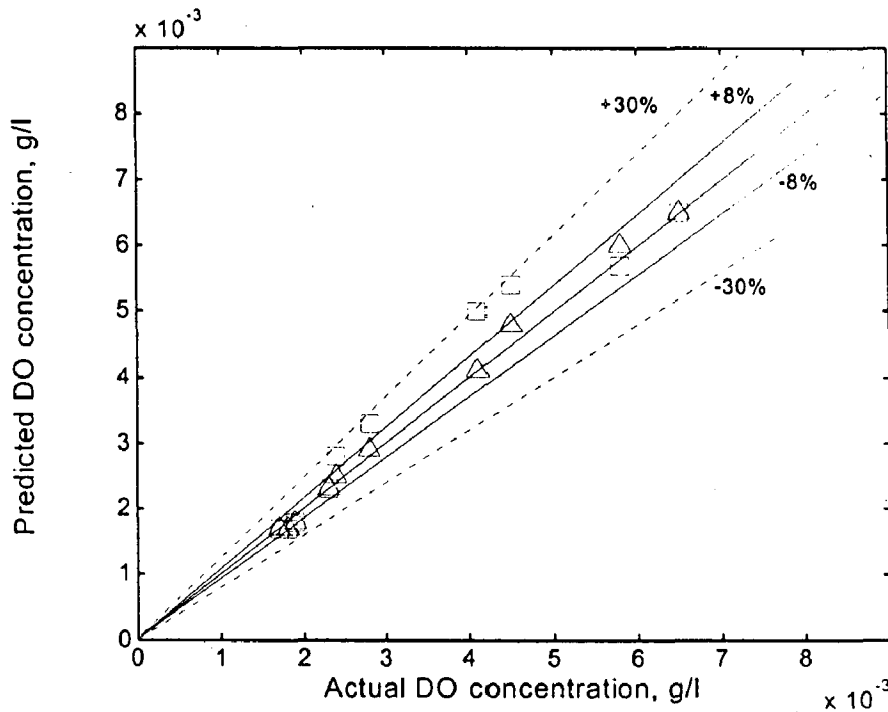
Figure: 6.12 Relative deviations of predicted values from experimental data for DO concentration.

❑ Figure 6.12 is drawn to show the error band, in which the model predicts the experimental values. From the figure it is clear that the logistic and contois model predicts time dependent biomass concentration with ± 30% and ± 8% errors respectively..

6.3 EFFECT OF VARIATION OF PARAMETERS BASED ON MODEL PREDICTIONS

It was found that initial cell mass, gas hold-up, airflow rate and mass transfer significantly influence the fermentation in an airlift bioreactor. In this section, the effects of two important parameters have been investigated. The effect of variation of operating parameters as given in Table 6.1 presented in this section to predict the behavior of the biological process in an ALBR.

The airflow rate and overall gas hold up can be related using equation (4.24) of Chapter 4 and equation (25) by [61]. The new equation is given by (6.1), which can be used to convert airflow rate to overall gas hold up and vice versa.

$$Q_g = \frac{(Ar + Ad)}{\rho_L g} \left(\frac{\varepsilon_g}{4.334 \times 10^{-3}} \right)^{2.004} \tag{6.1}$$

Logistic equation is used to predict the effect of variation in time dependent biomass, gluconic acid and glucose concentrations. Contois model is used to predict the effect of gas hold up on the time dependent concentration. The profiles obtained from the model simulation are shown in the figures from 6.13 through 6.16.

6.3.1 EFFECT OF INITIAL CELL MASS CONCENTRATION (X_0)

Different initial biomass values using logistic equation with 66 % variation of the mean value ($X_0 = 0.308 \pm 0.2032$) are tested and simulated results are shown in figure 6.13 through 6.15.
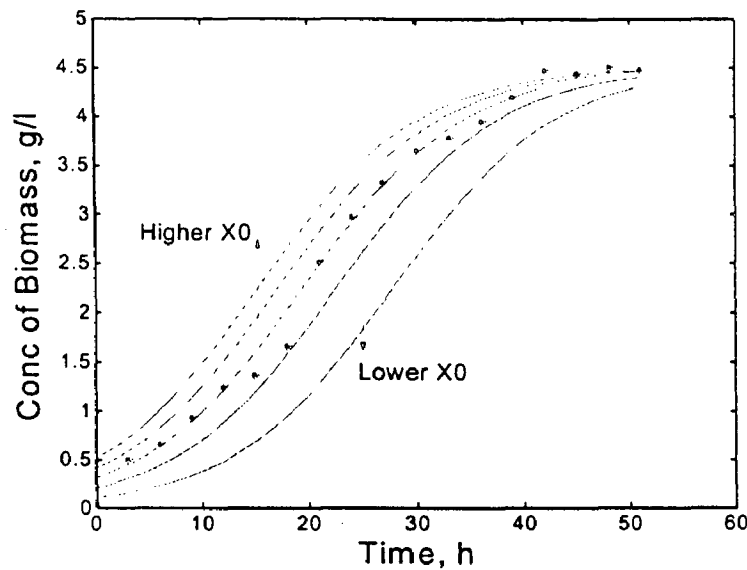
Figure: 6.13 Effect of change in initial cell mass on biomass growth by logistic equation.

□ Higher initial cell concentration results in rapid growth of biomass, and subsequently immediate formation of product and reduces the batch time considerably.
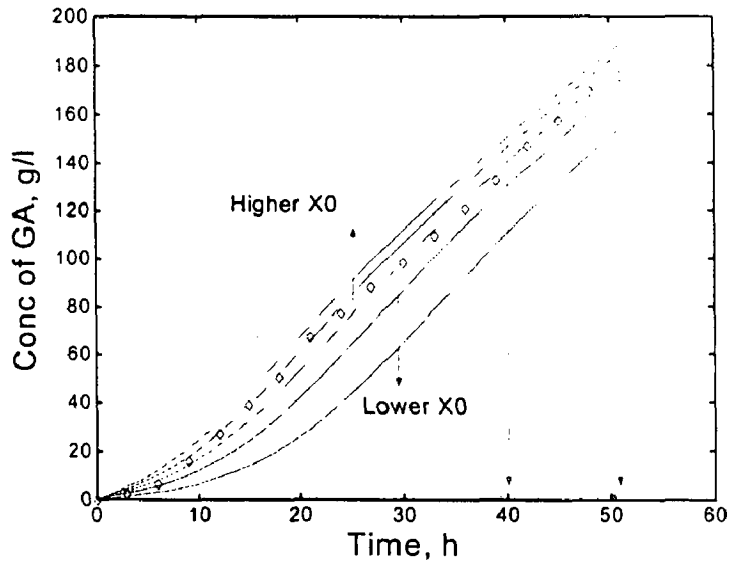
Figure: 6.14 Effect of change in the initial biomass concentration on gluconic acid production by logistic equation.
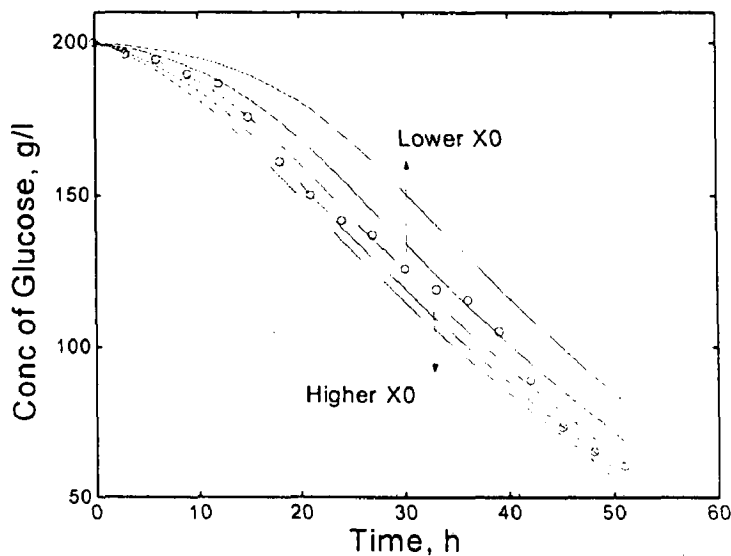
Figure: 6.15 Effect of change in change in initial cell mass on glucose consumption by logistic equation.

❑ As seen from figure 6.14, the gluconic acid formation of 151.0 g/l is achieved in 42 h instead of 51 h if the X_0 is increased from 0.1048 g/l to 0.5112 g/l.

❑ As expected, the glucose concentration falls rapidly when higher initial cell mass concentration is used as can be seen from figure 6.15. The profiles are almost parallel after

30 h of batch time, indicating that the higher cell mass reduces the batch time to for the same yield of gluconic acid.

6.3.2   EFFECT OF AIRFLOW RATE (Qg)

Contois model is tested for various values of airflow rates. The airflow rate values considered are 4.269, 5.9021, 7.8, 9.962, 12.3892, corresponds to overall gas hold-up of 0.057, 0.067, 0.077, 0.087 and 0.097, which are equivalent to 20 % variation around the mean airflow rate value. Figures 6.17 to 6.20 show the typical profiles of change in airflow rates.

As can be seen from the figure 6.16, the higher value of flow rate maintains high gas hold up and high DO concentration in an airlift reactor. High value of DO concentration generates higher cell mass and thus, higher gluconic acid formation takes place at the 51 h of fermentation. Further, it is noted that airflow rate with in terms of finely divided bubbles in the reactor, increases the surface area between the gas and liquid phase. As a result of this, high DO is available for the cells to convert glucose into gluconic acid as can be seen from the reaction (1.4) of Chapter 1.
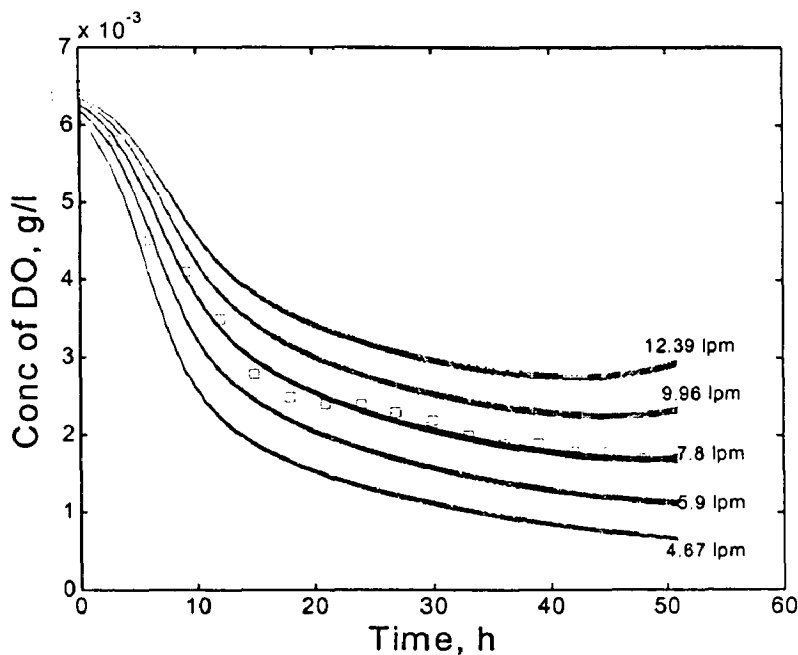
Figure: 6.16 Effect of change in gas hold up on dissolved oxygen concentration in reactor by contois model.

7.1 CONCLUSIONS

Gluconic acid produced from glucose using *Aspergillus niger* is an aerobic fermentation having two step reaction. The biotransformation represents a simple dehydrogenation reaction without involvement of complex metabolic cell pathways, which can be presented by a mathematical model. A mathematical model, which incorporates two kinetic models, describes a complete bioprocess of gluconic acid production in batch in an airlift bioreactor (ALBR). The predictions of the present model match excellently with the experimental data. From the results shown in Chapter 6, following salient conclusions can be drawn:

1. The comparison of both kinetic models, namely logistic equation and contois model revealed that the logistic mode represents the time dependent concentrations of biomass, gluconic acid and glucose very effectively, but fails to predict the dissolved oxygen concentration. On the other hand, the contois model predicts the time dependent dissolved oxygen concentration correctly but predicts the time dependent biomass, gluconic acid and glucose concentrations poorly.

2. The result show that the initial cell mass concentration (X_0) and overall gas hold – up (ε) significantly affect the gluconic acid production in an airlift bioreactor. Higher is the initial cell mass concentration, lower is the fermentation time and vice versa.

3. There is a great effect of initial cell mass and gas hold up in airlift reactor. Higher the cell mass concentration at the start of the batch reduces the fermentation time considerably.

4. High gas hold-up present in the reactor enhances the gluconic acid formation.

5. A multi-kinetic models constituted with logistic and contois model has provided better prediction of the overall bioprocess of gluconic acid production in comparison to single kinetic such as logistic or contois.

7.2 RECOMMENDATIONS FOR FUTURE WORK

Following future works are recommended based on the study carried out in the present work.

❏ The performance of the present mathematical model can be improved by incorporating the effect of pH, temperature and inhibition of product in the basic kinetic model.

❏ The airlift bioreactor developed as a part of the present work may be used for further investigation and model development.

REFERENCES

1. Aiba, S., Shoda, M., Nagatani, M., Kinetics of product inhibition in alcohol fermentation. *Biotechnology and Bioengineering*, 10 (1968) pp 845-864.

2. Adler, I., Deckwer, W.D., Schugerl, K., Performance of tower loop bioreactors—II. Model calculations for substrate limited growth, Chem. Eng. Sci. 37 (1982) 417–424.

3. Andre, G., Robinson, C.W., Moo-Young, M., New criteria for application of the well-mixed model to gas–liquid mass transfer studies, Chem. Eng. Sci. 38 (1983) 1845–1854.

4. Andrews, J. F., A mathematical model for the continuous culture of microorganisms utilizing inhibitory substrates, Biotechnol. Bioeng., 10 (1968), In Bailley & Ollis, Biochemical Engineering Fundamentals, 2nd Ed., 1986 pp 455

5. Badino Jr, A.C., Gouveia, E.R., Hakka, C.O., The geometry and operational conditions on gas hold-up, liquid circulation and mass transfer in an airlift reactor, Brazilian Jr. Chem. Eng., Vol. 20, No.04, 2004, pp 363-374

6. Baker, D.L., Sarett, B.L., Enzymatic process for producing gluconic acid, U.S.Patent No. 2651592, Sept. 8, 1953.

7. Bailley, J.E., Ollis, D.F., Biochemical Engineering Fundamentals, 2nd Ed., McGraw Hill Intl., 1986, pp 403-424

8. Bao, J., Furumoto, K., Fukunaga, K., Nakao, K., A kinetic study on air oxidation of glucose catalysed by immobilized glucose oxidase for production of calcium gluconate, Biochem. Eng. Jr., 8, 2001, pp 91-102

9. Blom, R.H., Pfeifer, V.F., Moyer, A.J., Traufler, D.H., Convay, H.F., Crocker, C.K., Farison, R.E., Hannibal, D.V., Sodium gluconate production: Fermentation with *Aspergillus niger*, Ind. Eng. Chem., Vol. 44, No.2 (1952) pp 435-440

10. Cabral, J., Mota, M, Tramper, J., *Multiphase bioreactor design*, 2001, Taylor & Francis, London

11. Chisti, M.Y., Moo-Young, M., Airlift reactors: characteristics, application and desing considerations. Chem. Eng. Commun., 60 (1987) 195-242

12. Chisti, Y., Choi, K.H., Moo-Young, M., Comparative evaluation of hydrodynamic and gas-liquid mass transfer characteristics in bubble column and airlift slurry reactors, The

Chem. Eng. Jr. **62** (1996) 223-229

13. Chisti, Y., Jauregui-Haza, U.J., Oxygen transfer and mixing in mechanically agitated airlift bioreactors, Biochem. Eng. Jr. **10** (2002) 143-153

14. Das, A., Kundu, P.N., Microbial production of gluconic acid, Jr. Sci. Ind. Res., **46**, 1987, pp 307-331

15. Dirkx, J.M.H., van der Baan, H.S., The oxidation of glucose with platinum on carbon as catalyst, Jr. Catalysis, **67**, 1981, pp 1-13

16. Erickson, LE., Lee, S.S., Fan, LT., Modelling and analysis of tower fermentation processes-I. Steady state performance, J. Appl. Chem. Biotechnol. **22** (1972) 199–214.

17. Galindez-Mayer, J., Sanchez-Teja, O., Cristiani-Urbina, E., Ruiz-Ordaz, N., A novel split-cylinder airlift reactor for fed-batch cultures, Biopro. & Biosys. Engg. **22** (2001) 171-177

18. Ghose, T. K., *Bioprocess Computations in Biotechnology*, Vol. **1**, 1990, Ellis Horwood Ltd., England, pp 302-328.

19. Ghose T., K., Gosh, P., Kinetic analysis of gluconic acid production by *P. avails*. J. Appl. Chem. Biotechnol., **26** (1976) 768-777

20. Gutierrez-Rojas, M., Favella-Torres, E., Cordova-Lopez, J., Garcia-Rivero, M., Kinetics of *A .niger* during submerged, agar surface and solid state fermentations, Process Biochem., **33** (1998) 103-107

21. Heinrichs, A., Harmeier, W., Membrane enclosed alginate beads containing *Gluconobacter* cells and molecular dispersed catalase, Biotechnol. Lett., **8** (1986) pp 567–572

22. Ho, C.S., Erickson, LE., Fan, LT., Modeling and simulation of oxygen transfer in airlift fermentors, Biotechnol. Bioeng. **14** (1977) 1503– 1522

23. Jian-Zhong, L., Weng, L., Zhang, Q., Xu, H., Ji, L., A mathematical model for gluconic acid fermentation by *Aspergillus niger*, Biochem. Eng. Jr., **14** (2003) 137-141

24. Kawase, Y., Kanai, T., Uzumaki, Y. Simulation of airlift bioreactors: steady-state performance of continuous culture processes, Comp. Chem. Eng. **20** (1996) 1089–1099

25. Klein, J., Rosenberg, M., Markos, J., Dolgos, O., Kroslak, M., Kristofikova, L., Biochem. Eng. Jr., **1** (2002) 3568

26. Kristiansen,B., Mcneil, B., The design of a tubular loop reactor for scale-up and scale-

down of fermentation processes, In: Intl. Conference on Bioreactors and Biotransformetions, 1987 edn. Moody, G.W., Baker, P.B., Scotland, UK

27. Kulkarni, B.D., Sankalp, N.V., Optimization of fermentation conditions for gluconic acid production using *Aspergillus niger* immobilized on cellulose microfibrils, Process Biochemistry, 37 (2002) 1343-1350

28. Kulkarni, B.D., Cheena, J.J.S., Sankalp, N.V., Tambe, S.S., Genetic programming assisted stochastic optimization strategies for optimization of glucose to gluconic acid fermentation, Biotechnol. Prog., 18 (2002) 1356-1365

29. Laan, C., Pronk, W., Franssen, M., Veeger, C., Use of bioelectrochemical cell for synthesis of biochemicals, Enzyme Microb. Technol., 6 (1984) 165-168

30. Lantero, O.J., Shetty, J. K., Process for the preparation of gluconic acid and gluconic acid produced thereby, **U.S.Patent** No. 0077062A1, April 22, 2004

31. Levenspiel, O., The Monod equation. A revisit and a generalization to product inhibition situations. Biotech. & Bioeng., 22 (1980) 1671-1687

32. Leudeking, R., Piret, E.L., A kinetic study of the lactic acid fermentation: batch process at controlled pH, Jr. Biochem. Microbiol. Technol. Eng., 4 (1959) 231-241

33. Lu, W.J., Hwang, S.J., Chang, C.M., Liquid velocity and gas hold up in 3 phase internal loop airlift reactors with low density particles, Chem. Eng. Sci., 50, 1995, pp 1301-1310

34. Luttman, R., Thoma, M., Buchholz, H., Schugerl, K., Model development, parameter identification and simulation of SCP production processes in air lift tower reactor with external loop-I, Comp. Chem. Eng. 7 (1983) 43–50.

35. Luttman, R., Thoma, M., Buchholz, H., Schugerl, K., Model development, parameter identification, and simulation of SCP production processes in air lift tower reactor with external loop-II, Comp. Chem. Eng. 7 (1983) 51–63.

36. Markos, J., Klein, J., Rosenberg, M., Dolgos, O., Kroslak, M., Kristofikova, L., Biotransformation of glucose to gluconic acid by Aspergillus niger-study of mass transfer in an airlift reactor, Biochem. Eng. Jr., 10 (2002) 197-205

37. Milsom, P.E., Meers, J.L., Gluconic and itaconic acids, in: Moo-Young, M., *Comprehensive Biotechnology*, Vol. 3, 1985, Pergaman Press, NY, pp 681-689

38. Merchuk, J.C., In: Biotechnology, 2nd Ed., K. Schuger (ed.), VCH, Weinheim, 1993

39. Merchuk, J.C., Stein, Y., Mateles, R.T., Distributed parameter model of an airlift fermenter, Biotechnol. Bioeng. **22** (1980) 1189–1211.

40. Mitchell, D.A., von Meien, O.F., Krieger, N., Dalsenter, D.H., A review of recent developments in modeling of microbial growth kinetics and intraparticle phenomena in SSF, Biochem Eng Jr., **17** (2004) 15-26

41. Nakao, K., Kiefner, A., Furumoto, K., Harada, T., Production of gluconic acid with immobilized glucose oxidase in airlift reactors, Chem. Eng. Sci., Vol 52 (1997) Nos. 21-22, pp. 4127-4133

42. Oosterhuis, N.M.G., Groesbeek, N.M., Olivier, A.P.C., Kossen, N.W.F., Scale-down aspects of the gluconic acid production, Biotechnol. Lett., **5** (1983) 141–146.

43. Pigache, S., Trystram, G., Dhoms, P., Oxygen transfer modeling and simulation for an industrial continuous airlift fermentor, Biotechnol. Bioeng. **39** (1992) 923–931.

44. Prokop, A., Erickson, L.E., Fernandez, J., Humphrey, A.E., Design and physical characteristics of a multistage, continuous tower, Biotechnol. Bioeng. **11** (1969) 945–966.

45. Ratledge, C., Kristiansen, B., *Basic Biotechnology*, 2nd Edn., 2001, Cambridge Press, UK, pp 173-186, 315-317.

46. Rao, D.S., Panda, T., Comprehensive analysis of calcium gluconate and sodium gluconate techniques for the production of gluconic acid by *A. niger*, Bioprocess Eng., **8** (1993) 203-207

47. Schmidell, W., Badino Jr, A.C., Facciotti, M.C.R., Volumetric oxygen transfer coefficient (k_La) in batch cultivations involving non-Newtonian broths, Biochem. Eng. Jr. **8** (2001) 111-119

48. Singh, O.V., Production of gluconic acid from alternative economic sources, Ph.D. Thesis, Indian Institute of Technology, Roorkee, 2000

49. Stanbury, P., Whiteker, A, Principles of Fermentation Technology, 1984, Pergamon Press, New York

50. Sun, Y., Li, Y.L., Bai, S., Modeling of continuous L(+)-lactic acid production with Immobilized R. oryzae in an airlift bioreactor, Biochem. Eng. Jr. **3** (1999) 87-90

51. Thibault, J., Halsall-Whitney, H, Taylor, D., Multicriteria optimization of gluconic acid production using net flow, Bioprocess Biosyst. Eng., **25** (2003) 299-307

52. Tobajas, M., Garcia-Calvo, E., Comparison of experimental methods for determination of

the volumetric mass transfer coefficient in fermentation processes, Heat & Mass Transfer, 36 (2000) 201-207

53. Trager, M., Quazi, G.N., Onken, U., Chopra, C.L., Jr. of Ferm. Bioeng., 68 (1989) pp 112

54. Tripathi, C.K.M., Rastogi, S., Bihari, V., Basu, S.K., Production of calcium gluconate by fermentation, Ind. Jr. Exp. Biology, 37 (1999) 731-733

55. Tseng. M.C., Wayman, M., Kinetics of yeast growth, inhibition-threshold substrate concentrations, Canadian Journal of Microbiology, 21 (1975) 994-1003

56. Turner, J.R., Mills, P.L., Comparison of axial dispersion and mixing cell models for design and simulation of Fischer-Tropsch slurry bubble column reactors, Chem. Eng.Sci., 45 (1990) 2317-2324

57. Verlaan, P., Tramper, J., Hydrodynamics, axial dispersion and gas-liquid oxygen transfer in an airlift-loop bioreactor with three-phase flow; In Bioreactor and Biotransformation, Moody, G.W., Baker, P.B., Elsevier Appl. Sci., (1987) 350-373

58. Velizarov, S., Beschokov, V., Biotransformation of glucose to gluconic acid by *Gluconobacto oxydans*: substrate and product inhibition situations, Proc. Biochemistry, 33, No. 5, (1998) pp 527-534

59. Wen, C.Y., Fan, L.T., Models for flow systems and chemical reactors, Marcel Dekker, New York, 1975.

60. Znad, H, Markos, J., Bales, V., Production of gluconic acid from glucose by A. niger: growth and non growth conditions, Process Biochemistry, 39 (2004) 1341-1345

61. Znad, H, Markos, J., Bales, V., Kawase, Y., Modeling and simulations of airlift bioreactors, Biochem. Eng. Jr., 21 (2004) 73-81

62. Mayani, M.K, Mohanty, B., Singh, R.P., Modeling of a bioprocess of Gluconic acid Production from D-Glucose, BIOHORIZON 2005, March 11-12 (2005), Indian Institute of Technology - New Delhi, India

EXPERIMENTAL DATA

Table: B1 Experimental data of bioprocess for gluconic acid production Znad et al [61].

(32 °C temperature, 6.0 pH, 15.36 lpm of airflow rate in a 10.5 l airlift bioreactor)

Sr. No.	Time (hour)	Biomass Concentration (g/l)	Glucose Concentration (g/l)	Gluconic acid Concentration (g/l)	DO Concentration (g/l)
	tp	xp	sp	pp	cp
1.	0	0.040	0	200	0.0065
2.	3	0.503	1.96	196.302	0.0058
3.	6	0.662	6.23	194.66	0.0045
4.	9	0.939	15.4	189.789	0.0041
5.	12	1.247	26.68	186.532	0.0035
6.	15	1.366	38.686	175.746	0.0028
7.	18	1.661	49.975	161.194	0.0025
8.	21	2.511	66.91	150.405	0.0024
9.	24	2.973	76.788	141.771	0.0024
10.	27	3.324	88.078	136.9	0.0023
11.	30	3.656	97.956	125.576	0.0022
12.	33	3.786	109.245	119.092	0.002
13.	36	3.952	120.535	113.681	0.0019
14.	39	4.192	132.53	105.274	0.0019
15.	42	4.469	146.642	88.88	0.0018
16.	45	4.44	157.226	73.252	0.0018
17.	48	4.502	169.22	65.155	0.0017
18.	51	4.488	175.57	60.284	0.0017

COMPUTER PROGRAMS

PROGRAM 1:

```
clear all;
% SIMULATION OF GLUCONIC ACID PRODUCTION FROM GLUCOSE IN AN ALBR
% Mukesh Mayani, M.Tech (CAPPD)
% MODEL VALIDATION-LOGISTIC EQUATION AND CONTOIS MODEL
% Function program to simulate various models using ode solver - ode23s


global mum xm ksc koc ceqm x10 p10 s10 c10 z10 x20 p20 s20 c20 z20 x30 p30 s30 c30 z30
A1 B1 C1 A2 B2 A3 A4 Q NL ML N M;
global dto Dr Ddi Ddo HL Hr Hd Hb Ds Hs Vt k rhol Q_lpm epsg b;
global g Ar Ad Ab At Vb Vr Vd V Qg Q epsgr epsgd Ugr Ulr Dax HD Kb PgpV kla klar klad
vlr vld Pe;
N=44;
M=22;


tspan=[0 51];


% Initial conditions for Logistic equation
x101 = [0.3080*ones(1,N)];
p10 = zeros(1,N);
s10 = [200*ones(1,N)];
c10 = [0.0065*ones(1,N)];
z101 = [x101 p10 s10 c10];


% Initial conditions for Contois model
x201 = [0.04*ones(1,N)];
p20 = zeros(1,N);
s20 = [200*ones(1,N)];
c20 = [0.0065*ones(1,N)];
z201 = [x201 p20 s20 c20];


[t11, z11] = ode23s('odealrlogistic1i', tspan, z101);
disp('hello... Logistic equation simulated. Wait for plots.......!')
```

```matlab
[t21, z21] = ode23s('odecontois1i', tspan, z201);
disp('hello... Contois model simulated. Wait for plots......!');


tp=[0;3;6;9;12;15;18;21;24;27;30;33;36;39;42;45;48;51];
% Exp data of Biomass
xp=[0.04;0.5030;0.6620;0.9390;1.2470;1.3660;1.6610;2.5110;2.9730;3.3240;3.6560;3.7860;3.9
520;4.1920;4.4690;4.4400;4.5020;4.4880];
% Exp data for Product (Gluconic acid)
pp=[0.000;1.960;6.230;15.400;26.680;38.686;49.975;66.910;76.788;88.078;97.956;109.245;12
0.535;132.530;146.642;157.226;169.220;175.570];
% Exp data for Substrate(Glucose)
sp=[200.000;196.302;194.660;189.789;186.532;175.746;161.194;150.405;141.771;136.900;125
.576;119.092;115.681;105.274;88.880;73.252;65.155;60.284];
% Exp data for DO
cp=[0.0065;0.0058;0.0045;0.0041;0.0035;0.0028;0.0025;0.0024;0.0024;0.0023;0.0022;0.0020;0
.0019;0.0019;0.0018;0.0018;0.0017;0.0017];


% PLOTS
% Logistic equation
plot(t11,z11(:,(1:N)),'b',t21,z21(:,(1:N)),'r:',tp,xp,'k*');
xlabel('Time, h');
ylabel('Conc of Biomass, g/l');
title('Model Prediction - Time vs Conc of Biomass');
figure;


plot(t11,z11(:,(N+1:2*N)),'b',t21,z21(:,(N+1:2*N)),'b:',tp,pp,'kd');
xlabel('Time, h');
ylabel('Conc of GA, g/l');
title('Model Prediction - Time vs Conc of Product');
figure;


plot(t11,z11(:,(2*N+1:3*N)),'b',t21,z21(:,(2*N+1:3*N)),'r:',tp,sp,'ko');
xlabel('Time, h');
ylabel('Conc of Glucose, g/l');
title('Model Prediction - Time vs Conc of Substrate');
figure;
```

88

```matlab
plot(t11,z11(:,(3*N+1:4*N)),'b',t21,z21(:,(3*N+1:4*N)),'r:',tp,cp,'ks');
xlabel('Time, h');
ylabel('Conc of DO, g/l');
title('Model Predictions - Time vs Conc of DO');
```

PROGRAM 2:
```matlab
% ESTIMATION OF HYDRODYNAMIC PARAMETERS OF AIRLIFT REACTOR (4.5 L)
function [A1, B1, C1, klar,A2, B2, A3, A4, klad] = HYDDYN1i();

% Variable declaration
global dto Dr Ddi Ddo HL Hr Hd Hb Ds Hs Vt k rhol Q_lpm epsg b A1 A2 A3 A4 B1 B2 C1;
global g Ar Ad Ab At Vb Vr Vd V Qg Q epsgr epsgd Ugr Ulr Dax HD Kb PgpV kla klar klad
vlr vld Pe NL ML N M;
% Units of dto(sparger tube outer dia) Dr Ddi Ddo HL Hr Hd Hb Ds(separator dia) Hs(Sep.
height) are in m
% Volumes Vt Vr Vb V are in m3, rhol in kg/m3, g in m/s2, Areas in m2,Gas flow(Q_lpm) in
lpm,Qg in m3/s
% Q(Liquid circulation)in m3/s, Superficial gas and liquid vel.(Ugr Ulr) in m/s,
% Axial dispersion coefficient(Dax)in m2/s, PgpV in power/m3, MTCs(kla klar klad) in 1/h,
% Liquid linear velocities in m/s, k is vertical height of expansion joint in m,


% DATA INPUT
g=9.81; b=0.5; rhol=1215;Q_lpm=7.8;epsg=0.077;
dto=0.0115; Dr=0.042; Ddi=0.0506; Ddo=0.0725; HL=1.03; Hr=1.0; Hd=1.032; Hb=0.03;
Ds=0.2; Hs=0.18;k=0.06375;
Vt=0.0009;
% C/S areas
Ar=(pi/4)*(Dr^2-dto^2);
Ad=(pi/4)*(Ddo^2-Ddi^2);
Ab=pi*Dr*Hb;
At=(pi/4)*(Ds^2);
% Volumes of different sections
Vr=(pi/4)*(Dr^2-dto^2)*Hr;
Vb=(pi/4)*(Ddo^2)*Hb;
Vd=(pi/4)*(Ddo^2-Ddi^2)*Hd;
%Vt=(At-(pi/4)*Ddo^2)*(Hs + 0.7*k);
V=Vr+Vd+Vb+Vt;
```

%Superficial gas velocity & Dispersion coefficient

Qg=Q_lpm/(1000*60); %m3/s

Ugr=Qg/Ar; %m/s

Dax=2.61*(Dr^1.5)*(Ugr^0.5); %m2/s

%Gas hold up in riser and downcomer

epsgr=epsg*(Ar+Ad)/(Ar+0.89*Ad);

epsgd=0.89*epsgr; %Znad et al.[61]

% OR

%epsgd=0.988*epsgr-0.016; %Chisti & Moo-Young [10]

%Liquid velocity

HD=HL/(1-epsg);

Kb=11.4*(Ad/Ab)^0.79;

Ulr=(2*g*HD*(epsgr-epsgd)/(Kb*(Ar/Ad)^2*(1/(1-epsgd))^2))^0.5;

% Overall MTC

PgpV=(epsg/0.004334)^2.004; %From gas hold up

%OR

%PgpV=rhol*g*Ugr/(1+(Ad/Ar));

kla=3600*(1.27*10^(-4)*(PgpV)^0.925); % 1/h

%MTC in riser and downcomer

klar=kla*(Ar+Ad)/(Ar+0.8*Ad); %1/h

klad=0.8*klar; % 1/h

% Linear liquid velocity

vlr=Ulr/(1-epsgr);

vld=(vlr*Ar*(1-epsgr))/(Ad*(1-epsgd));

Q1=vlr*Ar;

Q2=vld*Ad;

Q=(Q1+Q2)/2;

%To determine no of stages in sections

Pe=vlr*HD/Dax;

.NL=Pe*(b+0.5);

%N=ceil(NL);

ML=NL-(Pe/2);

%M=ceil(ML);

% Value of Hydrodynamic Constants

A1=3600*Q/(Vb*(1-epsgr));

```matlab
B1=(1+b)*3600*Q/(Vb*(1-epsgr));
C1=b*3600*Q/(Vb*(1-epsgr));


A2=(1+b)*3600*Q*(M-2)/(Vr*(1-epsgr));
B2=b*3600*Q*(M-2)/(Vr*(1-epsgr));


A3=(1+b)*3600*Q/(Vt*(1-epsgr));


A4=3600*Q*(N-M)/(Vd*(1-epsgd));
```

PROGRAM 3:

```matlab
% Modeling of a Bioprocess for Gluconic acid production
% Mukesh Mayani, M.Tech (CAPPD)
% Logistic Equation Programme_ALR (4.5 L)


function zprime = odealrlogistic1i(t, z);
global N M xm ceqm zprime mum alpha beta gamma lemda eta psi ceqm;


% Call HYDDYN1i function for hydrodynamic parameters
[A1, B1, C1, klar, A2, B2, A3, A4, klad] = HYDDYN1i;


%Logistic equation parameters (Non-linear Regression)
mum=0.1335;
xm = 4.502;
alpha=18.028;
beta = 0.751;
gamma=13.144;
lemda = 0.604;
eta=0.58;
psi=0.103;
ceqm = 0.00651;


zprime= zeros(4*N,size(z,2));
% for biomass x
i=1;
zprime(i) = A1*z(N)-B1*z(i)+C1*z(i+1)+ mum*(z(i)*(1-(z(i)/xm)));
i=2:M-1;
```

91

```
zprime(i) = A2*(z(i-1)-z(i))+ B2*(z(i+1)-z(i))+ mum*(z(i).*(1-(z(i)/xm)));
i=M;
zprime(i) = A3*(z(i-1)-z(i))+ mum*(z(i)*(1-(z(i)/xm)));
i=M+1:N;
zprime(i) = A4*(z(i-1)-z(i))+ mum*(z(i).*(1-(z(i)/xm)));


% for product p
i=N+1;
zprime(i) = A1*z(2*N)-B1*z(i)+C1*z(i+1)+ alpha*zprime(i-N)+beta*z(i-N);%%%
i=N+2:N+M-1;
zprime(i) = A2*(z(i-1)-z(i))+ B2*(z(i+1)-z(i))+alpha*zprime(i-N)+beta*z(i-N);
i=N+M;
zprime(i) = A3*(z(i-1)-z(i))+ alpha*zprime(i-N)+beta*z(i-N);
i=N+M+1:2*N;
zprime(i) = A4*(z(i-1)-z(i))+alpha*zprime(i-N)+beta*z(i-N);


% for substrate s
i=2*N+1;
zprime(i) =A1*z(3*N)-B1*z(i)+C1*z(i+1)-gamma*zprime(i-2*N)-lemda*z(i-2*N);
i=2*N+2:2*N+M-1;
zprime(i) = A2*(z(i-1)-z(i))+ B2*(z(i+1)-z(i))-gamma*zprime(i-2*N)-lemda*z(i-2*N);
i=2*N+M;
zprime(i) = A3*(z(i-1)-z(i))-gamma*zprime(i-2*N)-lemda*z(i-2*N);
i=2*N+M+1:3*N;
zprime(i) = A4*(z(i-1)-z(i))-gamma*zprime(i-2*N)-lemda*z(i-2*N);


% for DO c
i=3*N+1;
zprime(i) = A1*z(4*N)-B1*z(i)+C1*z(i+1)+klar*ceqm-klar*z(i)-eta*zprime(i-3*N)-psi*z(i-
3*N);
i=3*N+2:3*N+M-1;
zprime(i) = A2*(z(i-1)-z(i))+ B2*(z(i+1)-z(i))+klar*ceqm-klar*z(i)-eta*zprime(i-3*N)-psi*z(i-
3*N);
i=3*N+M;
zprime(i) = A3*(z(i-1)-z(i))+klar*ceqm-klar*z(i)-eta*zprime(i-3*N)-psi*z(i-3*N);
i=3*N+M+1:4*N;
zprime(i) = A4*(z(i-1)-z(i))+klad*ceqm-klad*z(i)-eta*zprime(i-3*N)-psi*z(i-3*N);
```

PROGRAM 4:

% Modeling of a Bioprocess for Gluconic acid Production
% Mukesh Mayani, M.Tech (CAPPD)
% Contois model Program_ALR (4.5 L)

```
function zprime = odecontois1i(t, z);
global ksc koc N M;

% Call HYDDYN1i function for hydrodynamic parameters
[A1, B1, C1, klar, A2, B2, A3, A4, klad] = HYDDYN1i;

% Contois model (4.5 L)
mum=0.3610;
ksc=21.239;
koc=0.004134;
alpha=4.5865;
beta=1.3757;
gamma=3.9868;
lemda=0.9560;
eta=1.52;
psi=0.0808;
ceqm=0.00651;
zprime= zeros(4*N,size(z,2));

% for biomass x
i=1;
zprime(i) = A1*z(N)-B1*z(i)+C1*z(i+1)+
mum*(z(i+2*N).*z(i+3*N).*z(i)./((ksc*z(i)+z(i+2*N)).*(koc*z(i)+z(i+3*N))));
i=2:M-1;
zprime(i) = A2*(z(i-1)-z(i))+ B2*(z(i+1)-z(i))+
mum*(z(i+2*N).*z(i+3*N).*z(i)./((ksc*z(i)+z(i+2*N)).*(koc*z(i)+z(i+3*N))));
i=M;
zprime(i) = A3*(z(i-1)-z(i))+
mum*(z(i+2*N).*z(i+3*N).*z(i)./((ksc*z(i)+z(i+2*N)).*(koc*z(i)+z(i+3*N))));
i=M+1:N;
```

```matlab
zprime(i) = A4*(z(i-1)-z(i))+
mum*(z(i+2*N).*z(i+3*N).*z(i)./((ksc*z(i)+z(i+2*N)).*(koc*z(i)+z(i+3*N)))));

% for product p
i=N+1;
zprime(i) = A1*z(2*N)-B1*z(i)+C1*z(i+1)+ alpha*zprime(i-N)+beta*z(i-N);
i=N+2:N+M-1;
zprime(i) = A2*(z(i-1)-z(i))+ B2*(z(i+1)-z(i))+alpha*zprime(i-N)+beta*z(i-N);
i=N+M;
zprime(i) = A3*(z(i-1)-z(i))+ alpha*zprime(i-N)+beta*z(i-N);
i=N+M+1:2*N;
zprime(i) = A4*(z(i-1)-z(i))+alpha*zprime(i-N)+beta*z(i-N);

%for substrate s
i=2*N+1;
zprime(i) =A1*z(3*N)-B1*z(i)+C1*z(i+1)-gamma*zprime(i-2*N)-lemda*z(i-2*N);
i=2*N+2:2*N+M-1;
zprime(i) = A2*(z(i-1)-z(i))+ B2*(z(i+1)-z(i))-gamma*zprime(i-2*N)-lemda*z(i-2*N);
i=2*N+M;
zprime(i) = A3*(z(i-1)-z(i))-gamma*zprime(i-2*N)-lemda*z(i-2*N);
i=2*N+M+1:3*N;
zprime(i) = A4*(z(i-1)-z(i))-gamma*zprime(i-2*N)-lemda*z(i-2*N);

% for  DO c
i=3*N+1;
zprime(i) = A1*z(4*N)-B1*z(i)+C1*z(i+1)+klar*ceqm-klar*z(i)-eta*zprime(i-3*N)-psi*z(i-3*N);
i=3*N+2:3*N+M-1;
zprime(i) = A2*(z(i-1)-z(i))+ B2*(z(i+1)-z(i))+klar*ceqm-klar*z(i)-eta*zprime(i-3*N)-psi*z(i-3*N);
i=3*N+M;
zprime(i) = A3*(z(i-1)-z(i))+klar*ceqm-klar*z(i)-eta*zprime(i-3*N)-psi*z(i-3*N);
i=3*N+M+1:4*N;
zprime(i) = A4*(z(i-1)-z(i))+klad*ceqm-klad*z(i)-eta*zprime(i-3*N)-psi*z(i-3*N);
```